N65 10375
(ACCESSION NUMBER) (THRU)
176 1
(PAGES) (CODE)
CR-59440 27
(NASA CR OR TMX OR AD NUMBER) (CATEGORY)
FACILITY FORM 602

FINAL REPORT

DESIGN ASPECTS OF EXPLOSIVE MIXTURES IN A VEHICLE INTERSTAGE

CONTRACT NO. NAS 8-5390

Prepared for

NATIONAL AERONAUTICS AND SPACE ADMINISTRATION
GEORGE C. MARSHALL SPACE FLIGHT CENTER
HUNTSVILLE, ALABAMA

JULY 13, 1964

CASE 65651

OTS PRICE
XEROX $ 5.00 FS
MICROFILM $ 1.25 mf.

Arthur D. Little, Inc.

FINAL REPORT

ON

DESIGN ASPECTS OF EXPLOSIVE MIXTURES IN A VEHICLE INTERSTAGE

CONTRACT NO. NAS 8-5390

CONTROL NO. TP 3-84014 (1F)

PREPARED FOR

NATIONAL AERONAUTICS AND SPACE ADMINISTRATION

GEORGE C. MARSHALL SPACE FLIGHT CENTER

HUNTSVILLE, ALABAMA

BY

D. S. ALLAN, E. K. BASTRESS, J. M. BONNEVILLE

I. W. DINGWELL AND A. E. GERMELES

DIVISION 500

ARTHUR D. LITTLE, INC.

CAMBRIDGE, MASSACHUSETTS

JULY 13, 1964

65651

ACKNOWLEDGEMENT:

In addition to the authors listed on the title page, we wish to acknowledge the significant contributions made by Dr. S. R. Brinkley of Combustion and Explosives Research, Inc., and by Dr. K. Smith, Associate Professor of Chemical Engineering at the Massachusetts Institute of Technology.

TABLE OF CONTENTS

I. INTRODUCTION

II. SUMMARY

- A. Explosions in a Vehicle Interstage
- B. Effects of Explosions on Interstage Structures
- C. Explosion Hazards During Flight
- D. Methods of Preventing and Controlling Explosions

III. CHARACTER OF EXPLOSIONS

- A. Introduction
- B. Gas Phase Reactions
- C. Condensed Phase Reactions

IV. OCCURRENCE OF EXPLOSIONS IN AN INTERSTAGE

- A. Leakage of Hydrogen, Oxygen and Air
- B. Mixing
- C. Ignition Sources
- D. Maximum Allowable Leakage Rates

V. STRUCTURAL CONSIDERATIONS

- A. Aerodynamic Loads
- B. Stresses in Interstage Structural Elements
- C. Typical Interstage Components
- D. Minimum Mass of Detonable Mixture

VI. METHODS OF PREVENTION AND CONTROL OF EXPLOSIONS

A. System Requirements for Inert Purging

B. Aerodynamic Purging

C. Interstage Venting Requirements

D. Compartmenting

E. Hardening

F. Preventing Accumulation of Condensed Phase Mixtures

G. Intentional Ignition Sources

H. Weight Comparison of Control Techniques

VII. RECOMMENDATIONS FOR ADDITIONAL WORK

A. The Impulsive Loading of Detonation Waves--Analytical

B. The Impulsive Loading of Detonation Waves--Experimental

C. Response of Structures to Detonations

D. Transition from Deflagration to Detonation

E. Venting

F. Purging

G. Condensed Phase Reactions

REFERENCES

APPENDIX A--Gas Dynamics of Spherical Detonation

APPENDIX B--Effect of a Detonation Wave at Normal Incidence on a Rigid Wall

APPENDIX C--Calculation of Maximum Dynamic Bending Stresses

APPENDIX D--Comparison of Results With Some Possible Exact Solutions

APPENDIX E--Numerical Derivation of Maximum Allowable Radius of Stoichiometric Mixture

APPENDIX F--Sample Calculations

LIST OF FIGURES

1. General Configuration of Interstage
2. Ambient Pressure as a Function of Time after Launch for a Typical Vehicle
3. Burning Velocities of Mixtures of Hydrogen, Oxygen and Nitrogen
4. Average Flame Front Velocity
5. Flammability Limits
6. Effects of Diluents on Quenching Distance
7. Pressure Limits for Deflagration
8. Minimum Ignition Energies (Sparks)
9. Emperically Established Relationship for Induction Distance
10. Detonation Limits
11. Effect of Temperature on Predicted Limits
12. Effect of Pressure on Predicted Limits
13. Normalized Gas Properties Behind a Spherical Detonation Front
14. Approximate Variation of Wall Pressure with Time after Impact
15. Dynamic Stresses Due to Sustained Launch Acceleration
16. Stresses Required to Cause Failure During Launch
17. Middle Interstage
18. Upper Stage
19. After Skirt Panel S-II Interstage
20. Ambient Pressure History for S-IV B/S-II Interstage
21. Base Heat Shield Panel
22. LH_2 or LOX Fuel Lines

23. Mass of Detonable Mixture Allowed

24. Diluent Injection Rates

25. Tank Weights for Compressed Gas Storage

26. Weight of Gas Storage System for Purging Hydrogen and Oxygen

27. Flight Velocity of a Typical Vehicle

28. Typical Vehicle Fuel Concentration--Aerodynamic Purging

LIST OF TABLES

I. Detonation Wave Characteristics for Mixtures of Hydrogen, Oxygen and Nitrogen

II. Effect of Additives on Minimum Ignition Energy Required to Detonate Mixtures of Hydrogen and Oxygen

III. Detonation Induction Distances, Hydrogen-Oxygen Mixtures

IV. Detonation Induction Distances of Hydrogen-Oxygen-Diluent Mixtures

V. Maximum Allowable Leakage Rates S-IC/S-II Interstage

VI. Values of the Parameter α and β for Rectangular Plates

VII. Physical Properties of Purging Fluids

VIII. Specific Strength of Tank Materials

IX. Ratio of Tank Weight to Fluid Weight

I. INTRODUCTION

The objective of this study program is to establish design techniques for the prevention and control of explosive mixtures of hydrogen and oxygen (or air) within a vehicle interstage. The period from propellant loading until stage separation is to be evaluated for an interstage of the general configuration given in Figure 1.

In conducting this study, the limiting conditions for explosive reactions within the vehicle were established and the characteristics of explosions as they affect the structural integrity of the interstage were derived. The response of various typical structures to explosive forces were evaluated and the critical periods in flight were determined. The principal methods of prevention and control considered in this program included aerodynamic and inert purging techniques, venting, compartmenting and hardening of structural components.

The criteria that have been developed will enable the vehicle designer to achieve a system that will perform with the lowest probability of occurrence of a destructive explosion that is consistent with the limitations of current knowledge. Because the methods for elimination or control of explosions must necessarily be defined by the characteristics of the vehicle to which they are to be applied, recommendations as to specific techniques are left to the design engineer.

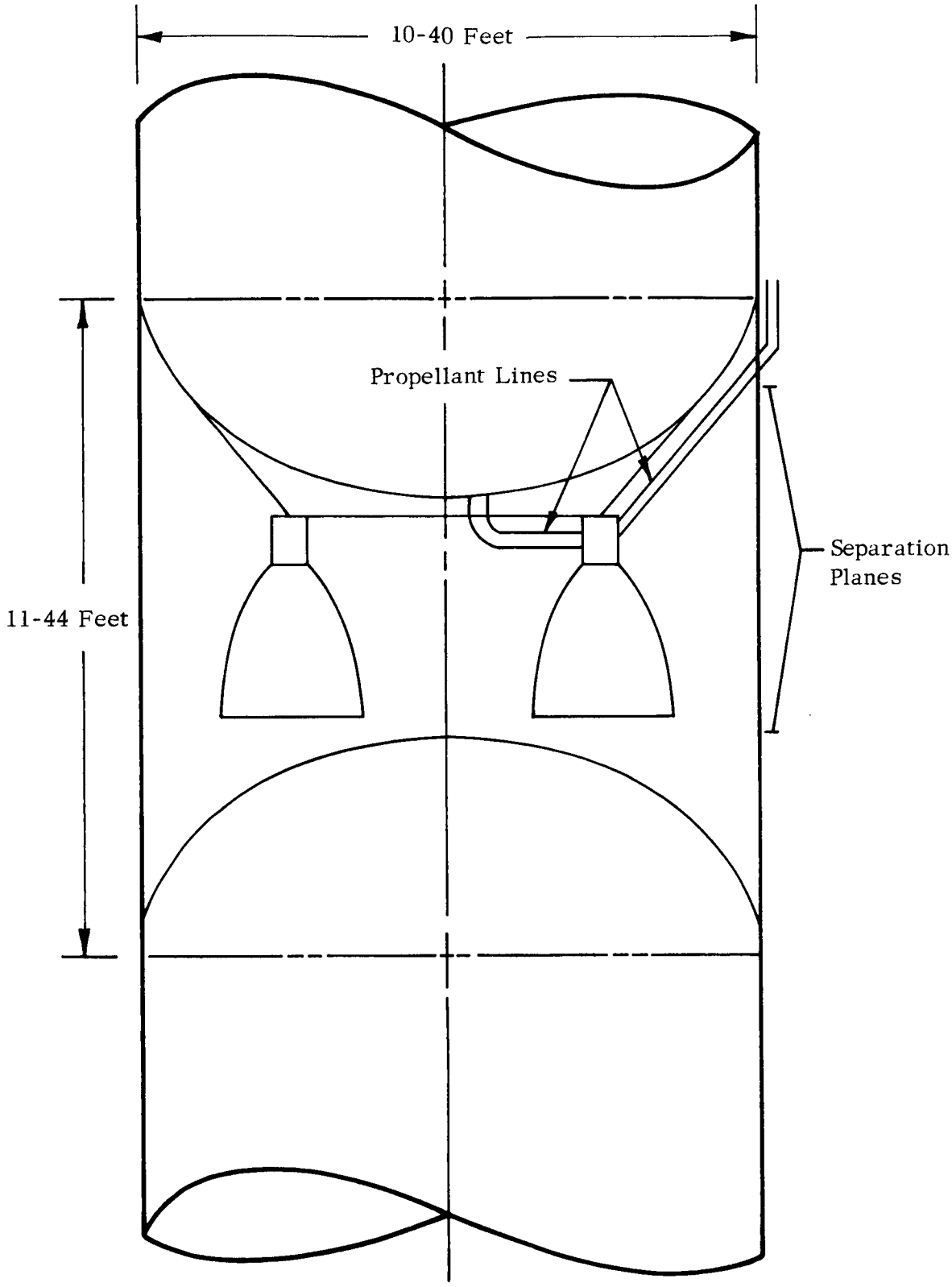

FIGURE 1 GENERAL CONFIGURATION OF INTERSTAGE

II. SUMMARY

A. Explosions in a Vehicle Interstage

Explosions that are the object of this study are characterized by an increase in gas pressure caused by the release of chemical energy during the reaction of hydrogen and oxygen (or air). The occurrence of the chemical reaction and the rate of rise, magnitude and duration of the pressures produced will determine whether destructive forces are created. These factors have been examined in detail to establish criteria for the prevention and control of interstage explosions.

This study has been primarily concerned with relatively low (accidental) leakage rates since practical measures for the prevention and control of explosions do not appear feasible for large releases of the vehicle propellants in flight. While the vehicle is on the launch pad and during the early stages in flight, it is expected that surfaces within the interstage will have sufficient heat capacity to vaporize the escaping fluids. Gas phase mixtures will form. Later in flight, the interior surfaces may be cooled by prolonged leakage and condensed phase mixtures may be created.

Gas phase reactions have been of primary interest since at the lower altitudes, they are quite readily initiated. With gas phase mixtures, it has been concluded that accidental ignition will result, initially, in the occurrence of a flame front (deflagration) that travels through the unreacted mixture at less than the speed of sound. After some distance of travel, the combustion wave may increase in

intensity and a transition to detonation may take place. The detonation will be characterized by a combined reaction and shock front that propagates through the mixture at many times the speed of sound. At present, there is insufficient information to allow one to predict the occurrence of a detonation.

If only deflagration occurs, the maximum pressures produced will be of the order of eight times ambient and may subsist for a significant interval of time. The peak pressure in a detonation wave will be of the order of 18 times ambient and will occur for only a short interval. The effects of both types of explosions will depend upon the total quantity of material reacted.

B. Effects of Explosions on Interstage Structures

The forces applied to interstage structures resulting from the relatively slow rising pressures produced by deflagrations will act as static loads. The ability of structures to withstand these forces are simply calculated.

In the case of detonation, the rapidly acting forces create dynamic loads. The response of the structure is a function of the impulsive force of the pressure wave as well as its natural period, physical properties, dimensions and restraint. The evaluation of the effect of detonations on structures has required that the pressure wave gas dynamics be evaluated in detail in order to specify the impulsive characteristics imposed on the structure. Considerable effort was spent during this study in deriving self-similar solutions for freely expanding and reflected, spherical detonation waves.

General relationships were then established for the response of various types of interstage structures. Calculations were made as to the quantity of detonable material required to cause failure of structural components at various ambient pressures. The characteristics of the S-IC/S-II interstage of the Saturn vehicle were used to provide quantitative examples.

C. Explosions Hazards during Flight

The probable rate of leakage of propellants into the interstage is difficult, if not impossible, to define. An indication of the maximum leakage rate that may be possible can be found, however, by assuming that a major failure of a transfer line, fitting or other component allows full discharge of the propellants from the engine chill down circulation system that is in operation prior to stage separation. Under these conditions, the maximum leakage rate of liquid hydrogen would be of the order of 1.2 lbs/sec for systems using the RL-10 or J-2 engines and 1.5 lb/sec of liquid oxygen (for the RL-10).

The most critical hazards from explosions in the interstage are believed to exist after launch. The current practice of providing an active inert purge and monitoring the interstage atmosphere appears to be adequate prior to lift off.

After launch, it is expected that gas phase reactions could not be initiated at altitudes where the ambient pressure exceeds 0.15 psia. The interval of time from launch until this altitude is reached is of the order of 120 seconds for a typical vehicle.

For explosions caused by gas phase deflagrations, destructive pressures would not be expected to occur when the ambient pressure is somewhat greater than 0.15 psia, however. For the S-IC/S-II stage of Saturn, the limiting ambient pressure would be of the order of 0.3 psia and the flight time would be approximately 110 seconds.

The quantity of reactable mixture necessary to cause destructive gas phase detonation increases with altitude. Since (for a constant leak rate) the quantity of material will accumulate with time after launch, the maximum allowable leakage rate is found to depend upon the conditions that occur at some 35 seconds after launch. For the Saturn S-IC/S-II interstage maximum allowable leakage rate for hydrogen and oxygen is 23 cc/min (6.4×10^{-5} lb/sec) and 12 cc/min (5×10^{-4} lb/sec) of liquid, respectively.

During the flight interval from 110 seconds until stage separation, the hazard from the explosion of condensed phase mixtures will predominate. The worst condition will occur when the condensed forms of the fuel or oxidant are allowed to collect on a surface or in a cavity. Detonation pressures of the order of hundreds of thousands of pounds per square inch resulting from a condensed phase reaction will be destructive even when only small quantities react. In most cases, the maximum allowable leakage rates derived for gas phase detonations may not allow significant quantities of the condensed phase to accumulate in a single cavity within the interstage.

The critical periods for the different explosion hazards that may occur during the flight of a typical vehicle are given in Figure 2.

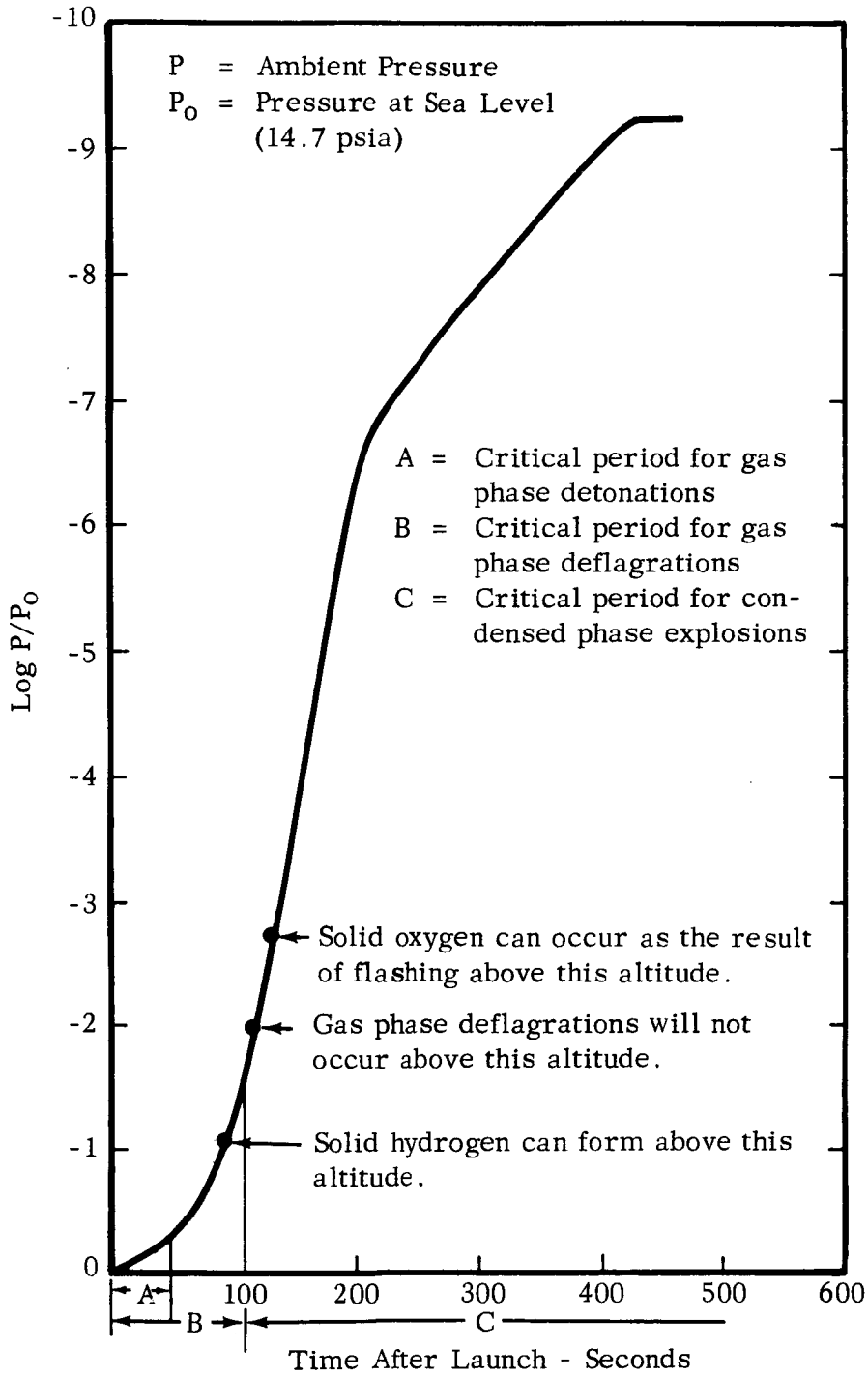

FIGURE 2 AMBIENT PRESSURE AS A FUNCTION OF TIME AFTER LAUNCH FOR A TYPICAL VEHICLE

D. Methods of Preventing and Controlling Explosions

The most positive method of reducing the probability of occurrence of a destructive explosion involves active purging during flight. When good mixing is achieved, the weight of the purging system is high. If a system relying on controlled streaming of the inert gas to keep escaping fuel and oxidant separated, lower weights may be used. In any case, experimentation would be required to determine the degree of effectiveness achieved. For an ideal, well-stirred, inert purging system using nitrogen, it is estimated that flow rates of the order of 17 lb/sec would be required for a hydrogen leak rate of about 0.05 lb/sec. Approximately 2.5 lb/sec of helium would be required for the same leak rate. Storage tank weights for 100 second purges would be a minimum of 1200 and 800 lbs for nitrogen and helium respectively.

Aerodynamic purging that provides good mixing may be capable of keeping hydrogen concentrations below the flammable limit for much higher leakage rates (e.g. approaching chill down recirculation rates of the order of one lb/sec). Aerodynamic purging can increase the hazard of an explosion occurring, however, when hydrogen leak rates exceed those for which the purge system is designed.

Increased venting of the interstage may reduce the probability of occurrence and severity of gas phase detonations. To be effective, however, the vent area may have to be as large as 40 percent of the interstage skirt surface area. During the early stages of flight, an increase in vent size may allow air to enter the system and may upset the balance of forces across the skirt. Increasing the

vent area later in flight would help to reduce the effect and probability of occurrence of both gas and condensed phase explosions.

Compartmenting of the interstage volume to reduce the quantity of reactable material that will accumulate will have little practical utility unless very small compartments are placed around the suspected points of leakage. This, in effect, would be a modification to reduce leakage rates and is beyond the scope of this work.

The elimination of small cavities that are quickly cooled and would serve as collection points for the condensed phases may help to reduce the probability of occurrence of destructive condensed phase explosions.

Modifications in design of interstage structures so that they will survive explosions of greater intensity may be accomplished with many of the internal components. It has been estimated, however, that the interstage skirt is currently the weakest component. The strengthening of the skirt to take higher loadings most likely would create undesirably large increases in weight.

III. CHARACTER OF EXPLOSIONS

A. Introduction

The development and evaluation of concepts for the prevention and control of explosions has required a detailed analysis of the character of the hydrogen and oxygen (or air) reactions that may accidentally occur in an interstage. This review is concerned with a description of the combustion processes, and pertinent factors that govern their occurrence and character. Both gaseous and condensed phase mixtures have been considered.

B. Gas Phase Reactions

1. Deflagration

a. Combustion of Hydrogen and Oxygen

The hydrogen-oxygen reaction has been the subject of intensive study by many investigators, is reasonably well understood, and described in detail in the literature.[1]

The principle reactions that enter into the combustion process have been established as:

$$OH + H_2 \longrightarrow H_2O + H \qquad \text{I}$$

$$H + O_2 \longrightarrow OH + O \qquad \text{II}$$

$$O + H_2 \longrightarrow OH + H \qquad \text{III}$$

This is a chain branching process for there are two OH ions produced for each molecule of water formed. The two OH radicals can react with H_2 to form two more molecules of water along with more H ions. This process, when repeated, results in a large multiplication of the products with time.

The controlling reaction is generally believed to be the second of those given. Whether combustion will take place or not depends upon the rate of generation of H ions for participating in this reaction relative to their removal by other processes (e.g. recombination at the wall). At normal temperatures and pressures, the source of dissociated molecules (OH and H) is not great enough relative to their removal and the over-all reaction does not take place. Mixtures of hydrogen and oxygen at normal temperatures and pressures do not react spontaneously (they are not hypergolic). A source of external energy

is required to cause the necessary rate of dissociation. Ignition sources are generally in the form of heat as exemplified by sparks, flames and high temperature surfaces.

Although a premixed hydrogen-oxygen system can react spontaneously in an explosive manner when the pressure and temperature of the mixture exceeds certain limiting values, it would not be expected to occur in the interstage of a launch vehicle. Temperatures above 700°F throughout the mixture would be required. The hazardous reactions that might take place in the interstage would be those that are initiated locally by an external heat source. A combustion zone would then propagate through the mixture at a rate defined by the heat transfer from the product of combustion to the reactants and the mass diffusion of hydrogen ions, or by compression from a strong shock as in a detonation.

Because of the chain-branching mechanism, the rate of propagation (flame speed) is much higher than for many other combustion processes (i.e. hydrocarbons). Less energy is required to initiate combustion and much smaller flame traps are required to stop propagation.

The occurrence of combustion in premixed (or mixing stream of) hydrogen and oxygen depends upon an external source of ignition and the condition being suitable for the propagation of the flame.

The temperatures and pressures produced when hydrogen and oxygen burn without loss of heat to the enclosure are given in Reference [1].

b. Propagation of Hydrogen-Oxygen (or Air) Flames

The limitations and characteristics of flames propagating in a premixed hydrogen-oxygen (or air) system are defined by the initial pressure and temperature, the mixture composition and factors relating to the dimensions and geometry of the containing vessel. In the evaluation of interstage hazards, the rate of energy release and the limiting conditions for propagation are of most interest since they will determine the occurrence and severity of an explosion and may indicate methods of prevention or control.

(1) Propagation Velocity

The velocity of propagation of laminar flames at ambient conditions is given for different mixture ratios of hydrogen and oxygen (or air) in Figure 3. Since the propagation of hydrogen flames becomes turbulent after a relatively short distance of travel in a premixed system, the apparent velocity will generally be much greater than that established for laminar flow. As discussed later, turbulence can lead to the transition to detonation.

There is insufficient knowledge to allow the prediction of the velocity of propagation for the turbulent case. In general, however, the velocity increases with the distance that the flame front travels as the result of the generation of turbulence by several mechanisms, all of which may contribute significantly in any given case. For a flame propagating in a channel, turbulence is generated as a result of wall friction as for any flow with a greater than critical Reynolds number in a channel or pipe. Obstructions in the confining vessel may contribute importantly to the generation of turbulence. Even in the absence of

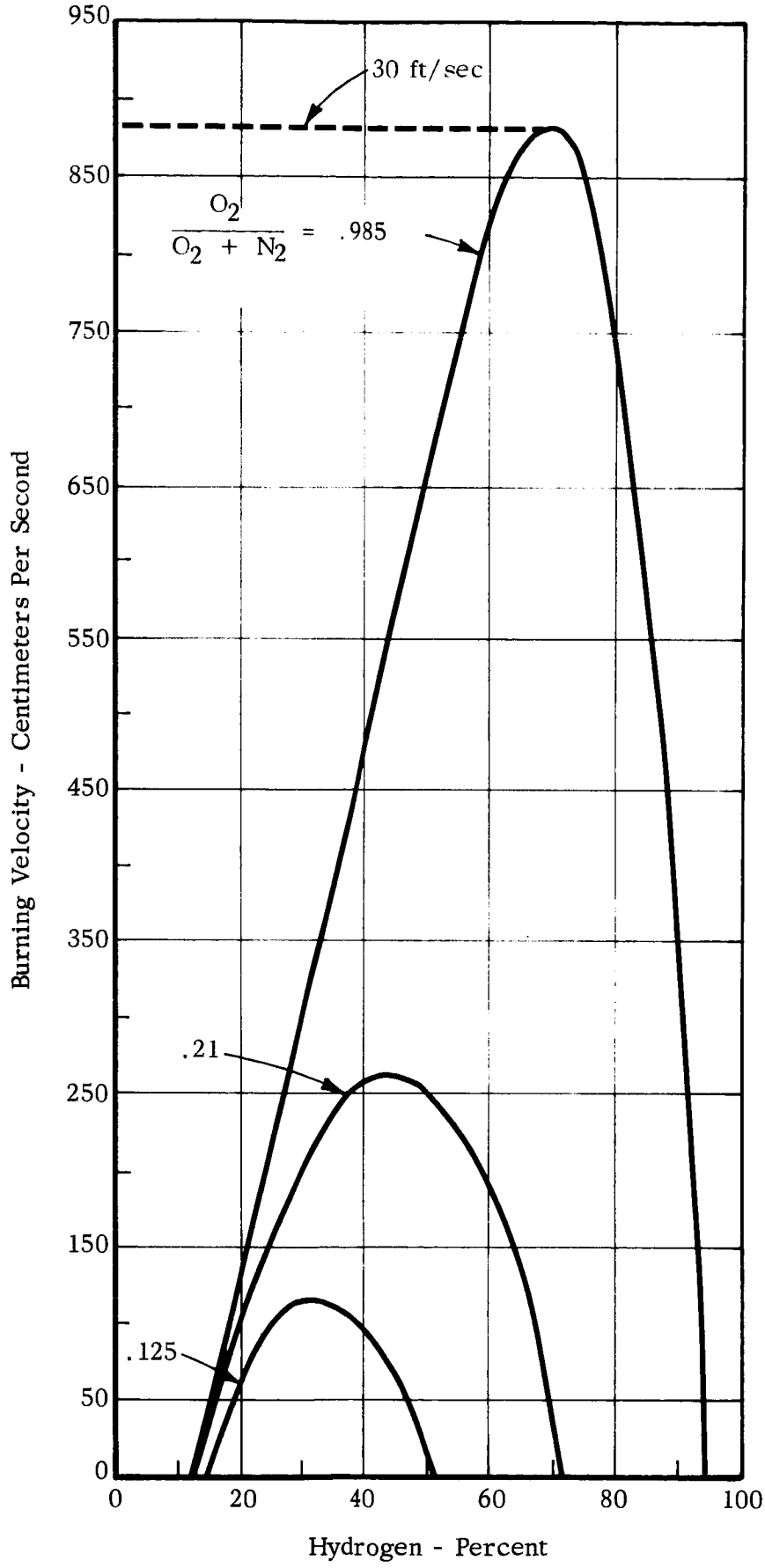

FIGURE 3 BURNING VELOCITIES OF MIXTURES OF HYDROGEN, OXYGEN AND NITROGEN (AT ROOM TEMPERATURE AND SEA LEVEL PRESSURE) (REF. 1)

such geometrical effects, the propagating flame is itself a strong generator of turbulence. Turbulent burning velocities may exceed the laminar velocity of the mixture by a factor of 10 or more.

Measurements of propagation velocities have been made under different test conditions. Those made at reduced pressures by Convair[2] are of particular interest to the interstage hazard study. In this work average propagation velocities were measured during the combustion of hydrogen and oxygen in a cylinder approximately 2 feet in diameter and 20 feet long. Combustion was initiated at one end of the tube and the time for the combustion front to travel between points at 5 feet and 17.5 feet from the ignition end was measured. The average velocity was then computed from this data and is reproduced in Figure 4. It may be seen that the average flame velocity decreases with pressure, and in general, as the mixture ratio departs from stoichiometric.

(2) Composition Limits

When diluents are added to stoichiometric mixtures in the form of excess fuel, oxidant, or inert gas in sufficient quantity the combustion process cannot be propagated. Although the flammability limits depend upon the experimental method by which they are derived, the commonly accepted values for several diluent mixtures are given in Figure 5 for normal temperature and pressure conditions. The limits will tend to be narrower at reduced pressures and possibly at reduced temperatures. Little experimental data is available as to these effects, however.

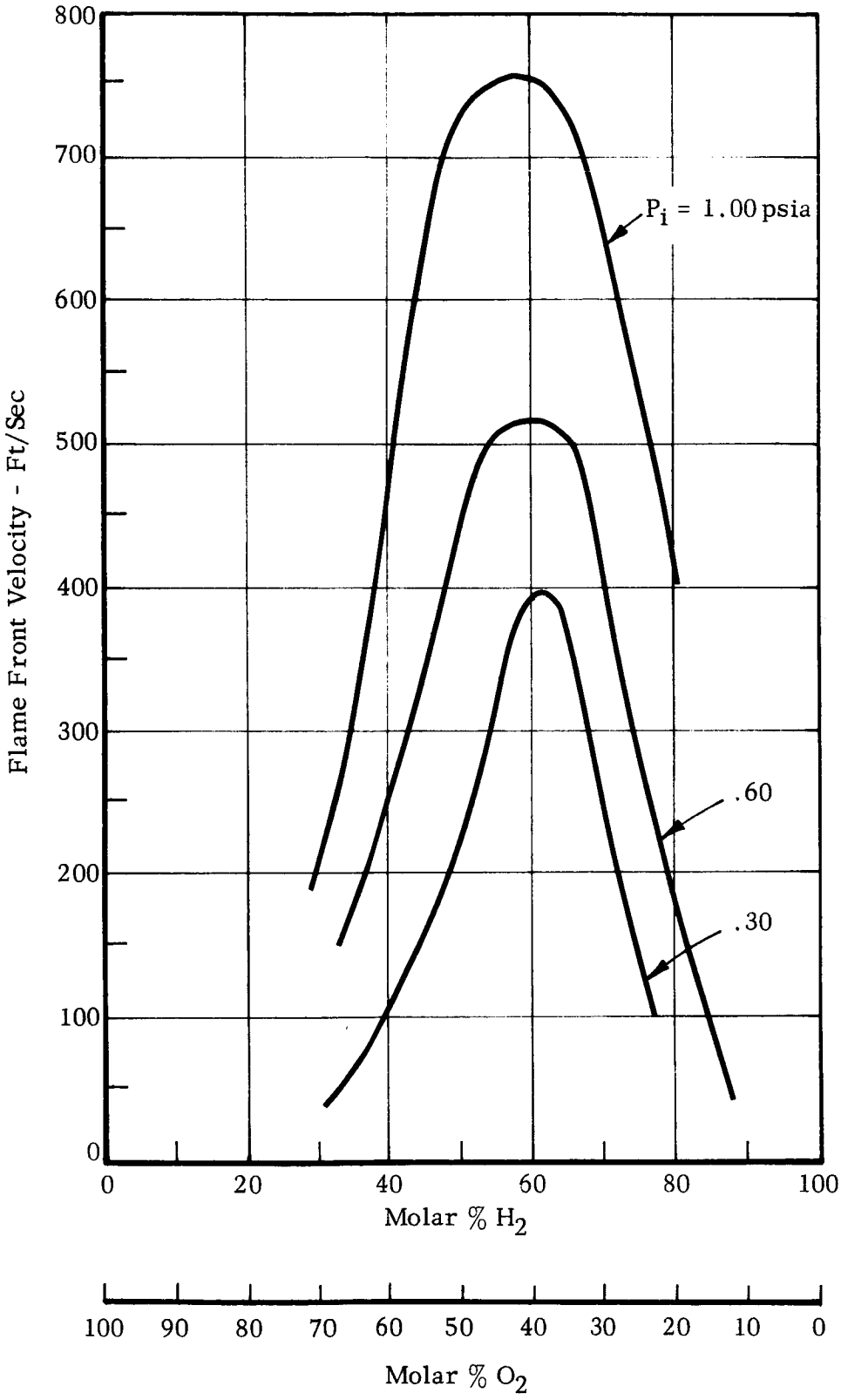

FIGURE 4 AVERAGE FLAME FRONT VELOCITY (REF.2)

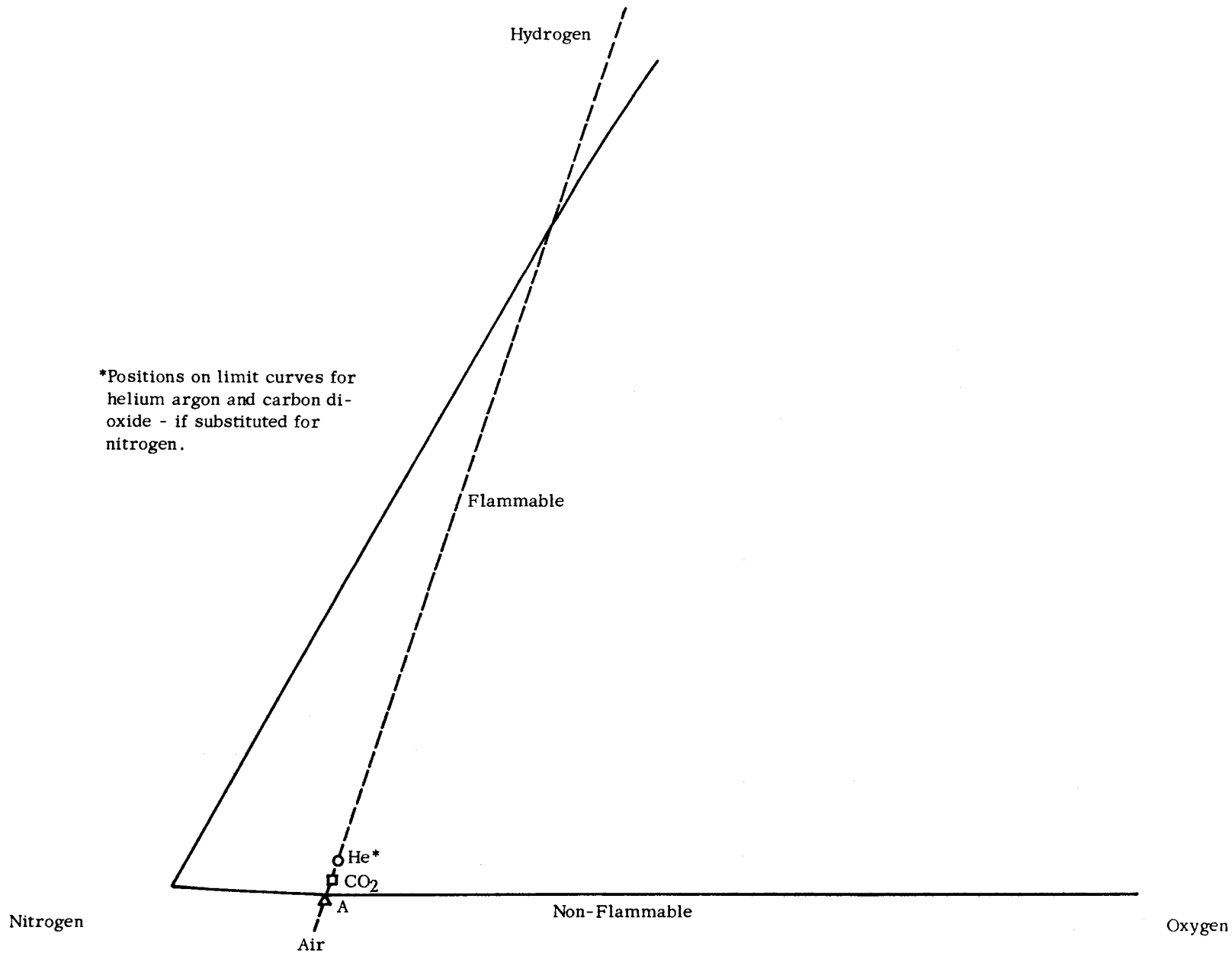

FIGURE 5 FLAMMABILITY LIMITS FOR MIXTURES OF H_2-O_2-N_2 AT NORMAL TEMPERATURES AND PRESSURES

(3) Inhibitors

A comprehensive screening of other gases as to their ability to chemically inhibit hydrogen-air reactions has been made by Monsanto.[3] The laminar flame speed was used as the criterion for the effectiveness of the compounds investigated. It was found that some hydrocarbons and halogenated compounds were the most effective. When 6.6% methane by volume was added to a mixture of 42 percent hydrogen and 58 percent oxygen, the normal flame speed was reduced from 274 cm/sec to 25 cm/sec. Only 3.3 percent of ethyl chloride was required to produce the same effect.

The effectiveness of these compounds in practice would be limited, however, by the fact that they will condense at temperatures well above the boiling point of hydrogen and they are capable of reacting with oxygen in themselves.

(4) Quenching

Heat losses from the flame to the walls in narrow channels can be sufficient to prevent propagation of the flame. The minimum width of the channel that will allow the flame to propagate is referred to as the quenching distance. This principle forms the basis of flame arrestors used prevalently with other gaseous systems (e.g. methane and air).

A classical example of the use of flame arrestors is their application in miners' lamps where a flame was used as the light source. A wire screen was placed around the flame to prevent general conflagration of combustible mixtures of methane and air that can occur in the mines. If a combustible mixture penetrated the screen, it would be ignited by the flame. The flame front would not be propagated through the screen,

however, since the dimensions of the perforations were smaller than the quenching distance for this gaseous mixture.

The quenching distance for a quiescent stoichiometric mixture of hydrogen and oxygen at ambient temperature and pressure is of the order of 0.0075 inches. If flow of the reactants occurs along with the combustion process the quenching distance may be reduced. The very small values for hydrogen limits the practical utility of flame traps. Quenching distances for other mixture ratios of hydrogen, oxygen and diluents are given in Figure 6.

Although there is little data on the effect of pressure and temperature on quenching distance, it is generally believed that it is inversely proportional to pressure and may not vary greatly with temperature. Because of the small quenching distance of hydrogen and oxygen at sea level pressure, however, very low pressures would be necessary before it becomes equivalent to the dimensions of free channels within the interstage.

(5) Pressure and Temperature Limits

At very low ambient pressures the governing thermal and diffusion process can no longer sustain combustion and flames cannot be propagated. Experiments conducted by Convair [2] provide data as to the limiting pressure for the deflagration of hydrogen and oxygen mixtures. As previously described, the reactants were contained in a cylinder approximately 2 feet in diameter and 20 feet long. The initiators, placed close to one end of the chamber, consisted of an electrical spark whose energy was estimated to be of the order of 8 joules, a hot wire at an

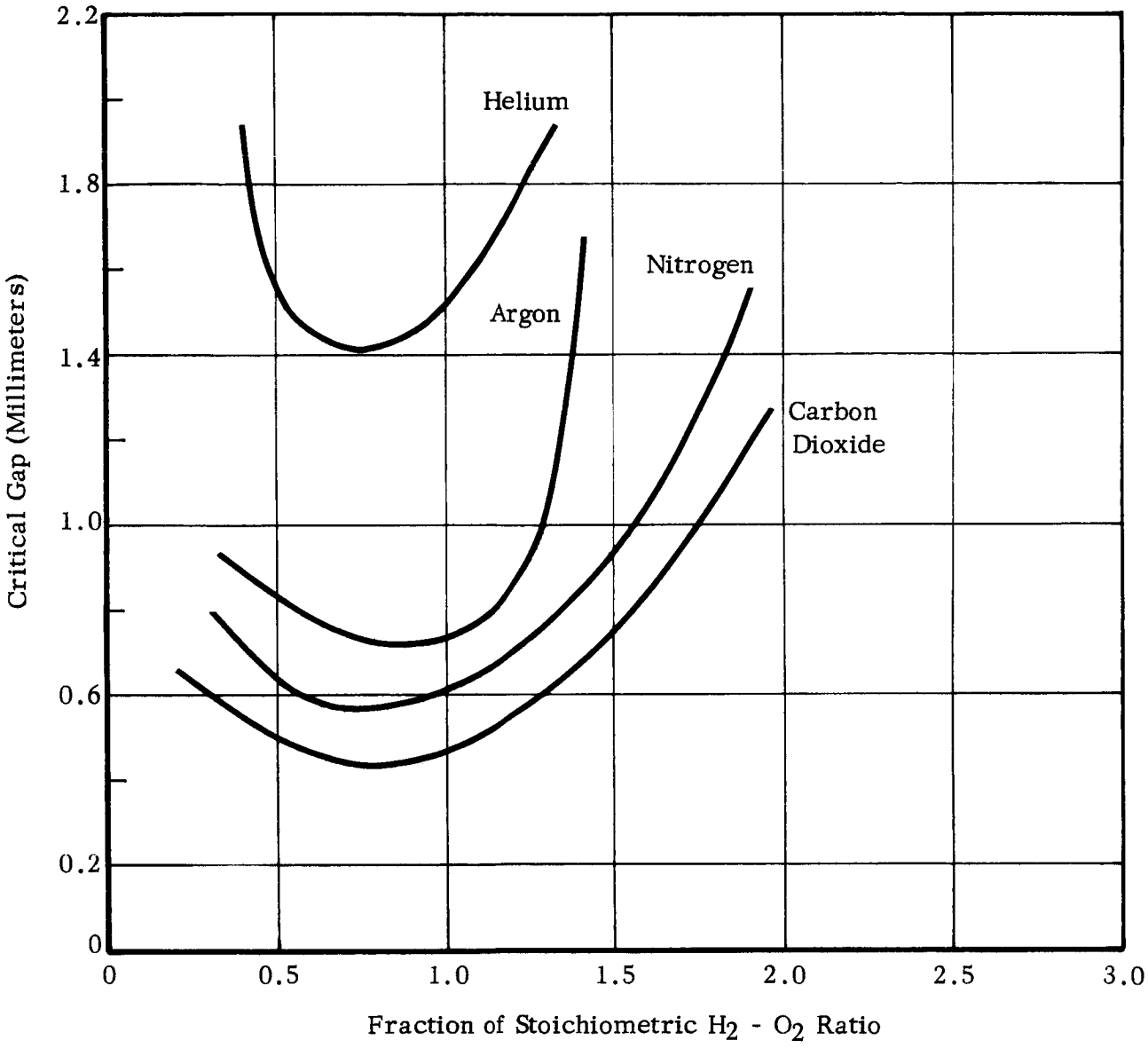

FIGURE 6 EFFECTS OF DILUENTS ON THE QUENCHING DISTANCE OF STOICHIOMETRIC MIXTURE OF HYDROGEN AND OXYGEN (REF. 1)

estimated temperature of 2400°F and a hot surface (.57 in.^{2}) at a temperature of 1000°F.

Although there was some variation in the limiting pressure with ignition source, the lowest limiting value (0.15 psia with hot surfaces) would appear to be adequate for design purposes. The effect of composition on limiting pressures for these experiments is given in Figure 7.

Ambient temperature will have only a slight effect on these limits. Estimates have been made by assuming that there is a limiting flame temperature below which deflagration will not occur. As the temperature is reduced, the concentration limits are narrowed slightly, however, the limit for the stoichiometric mixture remains unchanged.

c. Initiation of Hydrogen-Oxygen (or Air) Flames

The reaction of hydrogen and oxygen within an interstage requires a thermal source of initiation. This source must supply sufficient energy to raise the temperature in some small volume of the mixture to a level where the rate of production of heat and chain carriers by chemical reaction is greater than the rate at which heat and chain carriers are lost to the surroundings by heat conduction and diffusion, respectively. The critical amount of energy just sufficient for this purpose is called the minimum ignition energy. Since the ignition process evidently depends on the volume of gas heated, by the source, and upon the rate of heat transfer from the source to this volume, the minimum energy for initiation depends on the nature of the source, e.g. whether a hot surface, electrical spark, etc.

The minimum energy of electrical sparks required for initiation has been examined in some detail.(1) The minimum spark energies

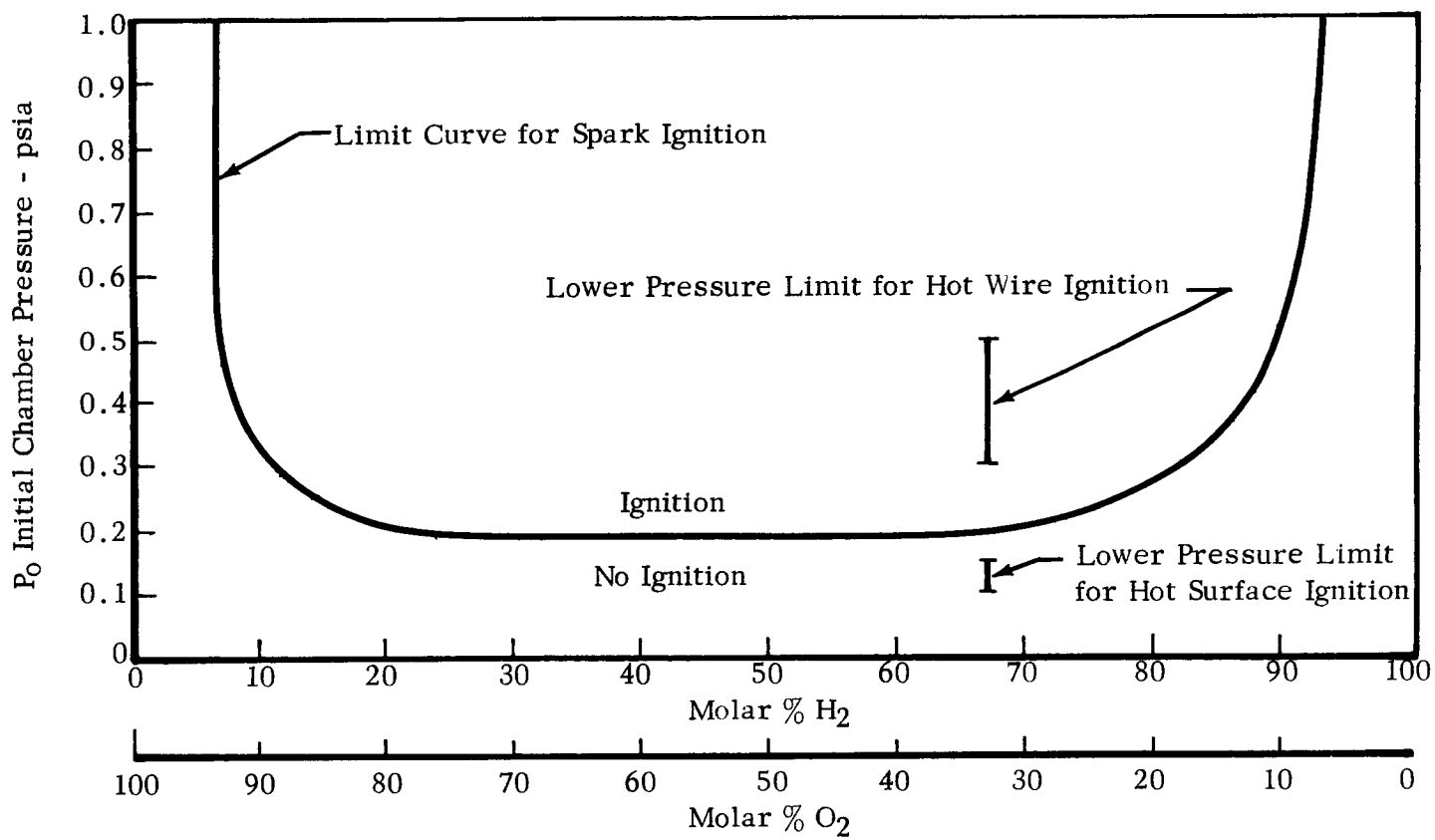

FIGURE 7 PRESSURE LIMITS FOR DEFLAGRATION (REF. 2)

for mixtures of hydrogen, oxygen and diluents at standard temperatures and pressures are given in Figure 8. It would be expected that the minimum energy for a stoichiometric hydrogen-oxygen mixture would be lower than any of the values given. It has been theoretically estimated to be between 10^{-3} and 10^{-4} millijoules. If the rate of energy release is much slower (e.g. hot wires) than that produced by electrical sparks, the minimum energy requirements are increased.

2. Detonation

a. Description of Detonation Waves

A detonation is a shock wave that is sustained by the energy released from the exothermal reaction of a combustible mixture. It is, in fact, formally and theoretically equivalent to a shock wave followed by a deflagration wave. A detonation differs from a flame (deflagration) in several respects. The unique propagation velocity of the latter is governed by the rate at which heat and active particles are transmitted by conduction and diffusion into the unburned mixture. The reaction occurring in a deflagration wave is thus initiated by transport processes. A deflagration wave is always sub-sonic with respect to the unburned mixture. In contrast, a detonation wave is always supersonic with respect to the unburned mixture. Its propagation velocity is usually orders of magnitude greater than that of a deflagration wave. Because of the high speed of the propagation, it can be shown that transport processes such as diffusion and heat conduction exert a negligible effect on the propagation of the wave. The chemical reaction is initiated in the shock front as the result of the shock heating of the unburned mixture. A further consequence of these characteristics is that the unique

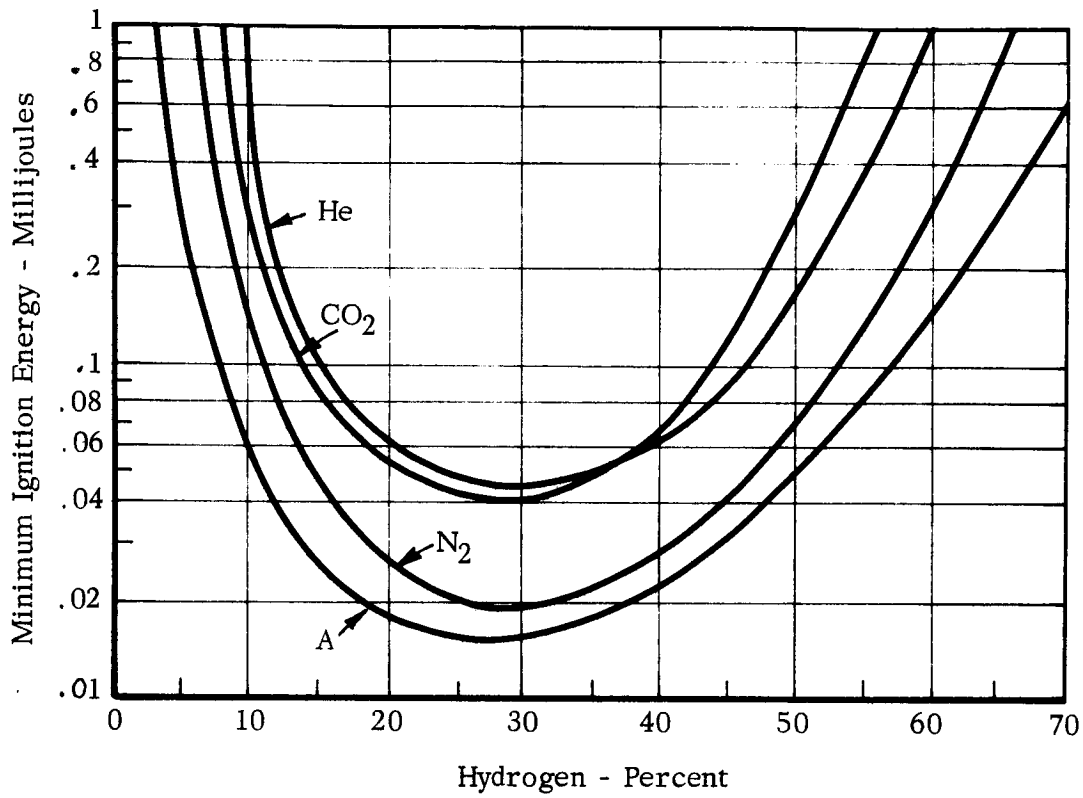

FIGURE 8 MINIMUM IGNITION ENERGIES (SPARKS) (FOR HYDROGEN-OXYGEN-INERT GAS MIXTURES AT ATMOSPHERIC PRESSURE O_2/O_2 + INERT GAS = 0.21) (REF. 1)

velocity of propagation of a detonation wave is determined by aero-thermodynamic considerations alone. The main properties of a detonation wave are described with sufficient accuracy by a simple theory in which it is assumed that the reaction zone following the shock wave is infinitely thin. Descriptions of detonation waves, the fundamental relations that govern their character and computations for the hydrogen-oxygen system may be found in references [1, 4, 5, 6, 7, 8, 9].

In order for a detonation to occur, the reactants must be mixed at the time of initiation and a shock wave of sufficient strength to initiate the chemical reaction must be established. This can be accomplished either by an appropriate igniter or as the result of a process in which a deflagration wave undergoes a transition to detonation. After transients associated with the initiation process have died away, the detonation velocity will either become constant and remain constant or the wave will die out. A mixture is said to be detonable if it can sustain a detonation wave of constant velocity. The pressure of a detonation wave of constant velocity also remains constant. The thickness of the wave (pressure-time integral) increases, however, as it progresses through the reactive mixture, the duration of the wave being proportional to the distance of travel. The pressure and velocity are usually assumed to be the same for both plane and spherical detonations in mixtures of the same composition and at the same ambient conditions.

The properties of the detonation wave at the wave front can be calculated by means of the elementary theory involving Rankine-Hugoniot expressions for the conservation of mass, momentum and energy across

the discontinuity reaction front together with an equation of state for the reaction products and the Chapman-Jouguet stability condition. This condition consists of the statement that the stable detonation velocity is that for which the velocity of the reaction products is sonic, as measured by an observer moving with the detonation front. Values for different hydrogen-oxygen-nitrogen mixtures at various initial pressures and temperatures are given in Table I.

The normalized gas properties behind a spherical detonation front are given in the next section of this report.

b. Initiation of Detonation

The probability of occurrence of gas phase detonations and techniques of preventing them can be significantly related to the initiation process. The initiation of a detonation in a mixture of hydrogen and oxygen within an interstage compartment requires the establishment of a shock wave of amplitude sufficient to initiate a chemical reaction in the unreacted combustible mixture. In principle, this can be accomplished in one of two ways--either as the result of the introduction of external energy or through the conversion of energy released by the deflagration of the reactants themselves. More fundamentally, it is desirable to distinguish between initiations effected by the transmission of a shock wave into the medium from some exterior agency from those effected by a thermal source of energy. The first type are exemplified by explosive boosters such as blasting caps; the second by thermal sources such as electric sparks, hot wires, hot surfaces, etc. In all cases in which initiation is effected by a thermal

TABLE I

DETONATION WAVE CHARACTERISTICS FOR MIXTURES OF HYDROGEN OXYGEN AND NITROGEN

(Ref. 9)

Mixture	P_1 atm	T_1 °K	P/P_1	T/T_1	U_D m/sec
$2H_2 + O_2$	0.01	200	24.22	14.92	2632
	0.10		26.28	16.67	2751
	1.00		28.48	18.73	2875
	10.00		30.71	21.07	2996
	100.00		32.78	23.53	3102
$2H_2 + O_2$	0.01	400	15.96	7.25	2560
	0.10		17.33	8.09	2681
	1.00		18.82	9.09	2809
	10.00		20.35	10.25	2937
	100.00		21.79	11.51	3055
$(2H_2 + O_2) + 1\ N_2$	1	291	17.37	11.58	2407
$(2H_2 + O_2) + 3\ N_2$	1	291	15.63	10.32	2055
$(2H_2 + O_2) + 5\ N_2$	1	291	14.39	9.23	1822

P_1, T_1 Initial pressure and temperature respectively

P, T Detonation pressure and temperature

U_D Detonation velocity

source, the initial condition is the establishment of a deflagration wave followed by a transition from deflagration to detonation. If the thermal source is an intense one, providing a large excess of energy over that necessary for the establishment of a deflagration wave, the transition may occur almost instantaneously with a very short induction time. If, however, the thermal source is just sufficient to establish a deflagration wave, a transition to detonation may occur after a relatively long induction time as the result of the effects of essentially aerodynamic processes.

(1) Initiation by External Sources

Experiments that have been related to ignition by external means have involved the investigation of both plane detonation waves in shock tube equipment and spherical waves generated by centrally igniting the reactant mixture within a container whose radius is usually larger than that of the normal shock tube.

Experiments by Zeldovich[10] in which plane detonation waves were initiated in shock tubes established that 4.1 joules of spark energy (calculated to have been transferred to a shock wave) were necessary to produce an instantaneous detonation of a stoichiometric mixture of hydrogen and oxygen in a shock tube of 30 mm in diameter. This was compared to a minimum of 7.2 joules of liberated energy from a lead nitride explosive found to be required for initiation of the same mixture. It is to be noted that the minimum energies measured in these experiments are much greater than the minimum energies necessary for flame initiation.

Shock tube experiments performed by Fay[11], Berets[12], and Steinberg[13] involved the use of shocks generated in a secondary gas to initiate detonation. In these experiments, an interface was formed between the hydrogen-oxygen mixture and another gas. Detonation of the hydrogen-oxygen mixture was observed as it was exposed to shocks of differing intensities emanating from the secondary gas. The data was analyzed principally in terms of the minimum shock temperature that resulted in instantaneous detonation. It was found, for example, that a shock wave temperature as low as 130° C could initiate detonation.

Experiments at reduced initial pressures are reported by Richmond[14]. It was found that, with the equipment used, detonations could not be initiated by a spark when the initial pressure of a stoichiometric mixture of hydrogen and oxygen was below 1/4 of an atmosphere. A shock wave generated in a secondary gas could initiate detonations (in $2H_2 + O_2$) at 1/10 of an atmosphere and below. With stoichiometric hydrogen and air mixtures detonations could not be initiated by electrical sparks at initial pressures less than 1/2 an atmosphere.

Experiments with the initiation of spherical detonations in hydrogen-oxygen mixtures have been reported by Arthur D. Little, Inc., [15, 16], Atlantic Research, Inc.,[17] and by Zeldovich[10] and Litchfield[18]. In the experiments at Arthur D. Little, Inc., the ignition sources were placed at the center of hydrogen-oxygen mixtures held within 100 feet^3 balloons. Electrical sparks, 6 grain S-68 squibs, and #6 blasting caps were used as ignition sources. Stoichiometric mixtures detonated in all cases. It was found, however, that the

limits of detonability (as defined by the ratio of hydrogen to oxygen) decreased as the energy level of the different ignition sources decreased. With spark ignition, the detonation limits were 35 and 86 percent hydrogen by volume whereas with squib initiation, the limits were of the order of 30 to 87 percent. The detonation limits with the blasting cap initiator appeared to approach those generally given as the standard detonation limits (15 to 90%).

In experiments performed by the Atlantic Research Corporation to determine the effect of various additives on the ability to initiate detonation in hydrogen-oxygen mixtures (H_2/O_2 = 62/38) it was found that 10.8 joules of electrical energy in an exploding bridge wire was necessary to produce a spherical detonation when no additives were present. This compared well with another investigator but is not necessarily consistent with that established by Zeldovich. Estimates made by Zeldovich indicated that the energy in the shock wave required to initiate a spherical detonation was of the order of 40 joules.

Tests were also made to investigate the initiation of spherical detonations by a plane detonation wave emitted from a small tube into a much larger container. With a stoichiometric mixture of hydrogen and oxgyen in both the tube and container, it was found that there was a minimum diameter of tube which would cause detonation in the larger container. This was established to be 19 mm.

When other materials are added to mixtures of hydrogen and oxygen, the energy required to initiate a detonation may decrease. The results of a search for additives that would significantly inhibit detonation of hydrogen and oxygen in this manner is reported by the Atlantic Research Corporation[17]. The amount of energy (released by an exploding bridge wire) that was required to cause a spherical detonation to occur was measured for various mixtures of hydrogen, oxygen and additives. Some of the results of these tests are given in Table II. Hydrocarbons were effective inhibitors as was methyl chloride. The compound producing the greatest effect was pentacarbonyl iron. In general, it appears that additives that inhibit detonation also suppress deflagrations. The exceptions to this are ethylene and some halogen compounds which appear to sensitize rather than inhibit detonations.

The investigation of the effect of powdered additives has been very limited. Preliminary results [17, 19] indicate that they may be quite inefficient in inhibiting the detonation of hydrogen and oxygen.

(2) Transition from Deflagration to Detonation

In many accidents, the source of ignition will not be sufficiently energetic to cause the immediate occurrence of detonation. The mixture will react and a flame front will propagate through the unburned material. The subsequent transition of the flame to a detonation will depend upon the mixture ratio, the geometry of its confinement and the initial temperature and pressure.

TABLE II

EFFECT OF ADDITIVES ON MINIMUM IGNITION ENERGY REQUIRED TO DETONATION MIXTURES OF HYDROGEN AND OXYGEN Ref. (17)

Additive	Minimum Ignition Energy (joules)		
Parts per 100 (1)	1.5	2.0	4.0
Control			
Nitrogen (2)	13.5	14.5	18
Inhibitors			
Methane	16.5	17.5	37.5
Propane	12	14	30.5
Butane	14.5	17.5	---
Propylene	30	38	---
Isobutene	46	---	---
Trans-Butene-2	30	38	---
Methyl Chloride	16	18	28.5
Carbon Monoxide	17	21.5	---
Pentacarbonyl Iron	44	---	---
Sensitizers			
Carbon Tetrachloride	6.5	6	5.5
Chloroform	5	4.75	4.5
Chlorine	---	4	---
Ethylene	9	9.25	10.5

(1) Parts per 100 of a mixture of $H_2:O_2$ of 62:38

(2) With no additives, the minimum ignition energy was 10.8 joules.

The transition to detonation of detonable gas mixtures contained within tubes of relatively small diameter has been examined and qualitatively described by a number of investigators[20, 21, 22, 23, 24]. The combustion process is observed as the flame front propagates in a tube containing a uniform mixture of the reactants that are ignited by a relatively weak initiator at a point near the closed end of the tube. (Initiation at the open end will not result in detonation).

The acceleration of a flame, which may initially be propagating at its laminar burning velocity, and its ultimate transition to detonation is the result of a number of different events which may be occurring simultaneously. It is to be noted that a shock wave is always generated in advance of a deflagration wave propagating through a combustible mixture. This shock wave is generated by the flame which is, in this respect, similar to a piston. If the flame velocity is low, the shock wave will be of low amplitude and will travel at a velocity that is many times greater than the flame velocity. The amplitude of the precursor shock increases as the velocity of the deflagration wave increases. If the precursor shock is reflected from a wall and if the reflected wave then interacts with the deflagration wave, the propagation velocity of the latter will be increased as a result of this interaction. As the flame front propagates, it generates turbulence and the turbulence thus generated may strongly increase the velocity of the flame front. These two mechanisms, operating either together or singly, depending upon the circumstances, together provide a strong mechanism for the acceleration of the flame.

Ultimately, one of two events may occur. The precursor shock may become sufficiently intense to initiate reaction in the shock front. If this occurs, the resulting flow is, by definition, a detonation and, after transients have subsided, a stable detonation results. Alternatively, the level of turbulence in the flame front may become so great that the flame brush approximates a stirred reactor. In this event, the unburned mixture contained in the highly turbulent flame brush will undergo a volume explosion, generating a strong pressure wave and leading to the establishment of a detonation wave. The distance of travel of the flame prior to transition depends upon the nature of the ultimate event and is strongly influenced both by the nature of the combustible mixture and by the geometry of its container.

The distance over which the deflagration wave must travel before the occurrence of detonation has been the subject of many experiments. An empirical correlation of the variables that influence this induction distance has been made by Bollinger[25] using the following relationship.

$$K = Re_b \frac{S_u}{a_b} \frac{T_c}{T_b} \qquad (1)$$

where Re_b = Reynolds number based on the unburned gas conditions

S_u = burning velocity of the mixture

a_b = speed of sound in the unburned gas mixture

T_c = temperature in the combustion wave

T_b = temperature of the unburned gas

The experimentally correlated relationship between the function K and induction distance is given in Figure 9. Experimental values used in deriving the plot are given in Table III. The influence of diluents on the induction distance for stoichiometric mixtures of hydrogen and oxygen (established by Bollinger) are given in Table IV.

The induction distances defined by detonation tube experiments can only be applied in a limited way, however, to the prediction of effects produced in actual accident situations. Explosions that may occur in an interstage would more likely involve reactants that are both not well mixed nor quiescent and which would be confined by a complex structure rather than a simple cylinder. The effect of these differences have been investigated in some instances and considered in a qualitative way in others.

Tests with larger diameter detonation tubes have established, for example, that induction distances increase with the diameter of the confining vessel[25]. No data is available on induction distances for the extreme case of a centrally ignited spherical flame front, however. The presence of obstructions in the path of the flame has been shown to influence induction distances [26, 27, 28]. Experiments have shown and theory suggests that a significant decrease in induction distance can result when the obstruction tends to increase turbulence.

In actual accidents, the location of ignition source relative to the mixed reactants will also be important to transition. Ignition at, or close to, a vent may result in no detonation while ignition in a confined area may increase the probability of its occurrence considerably.

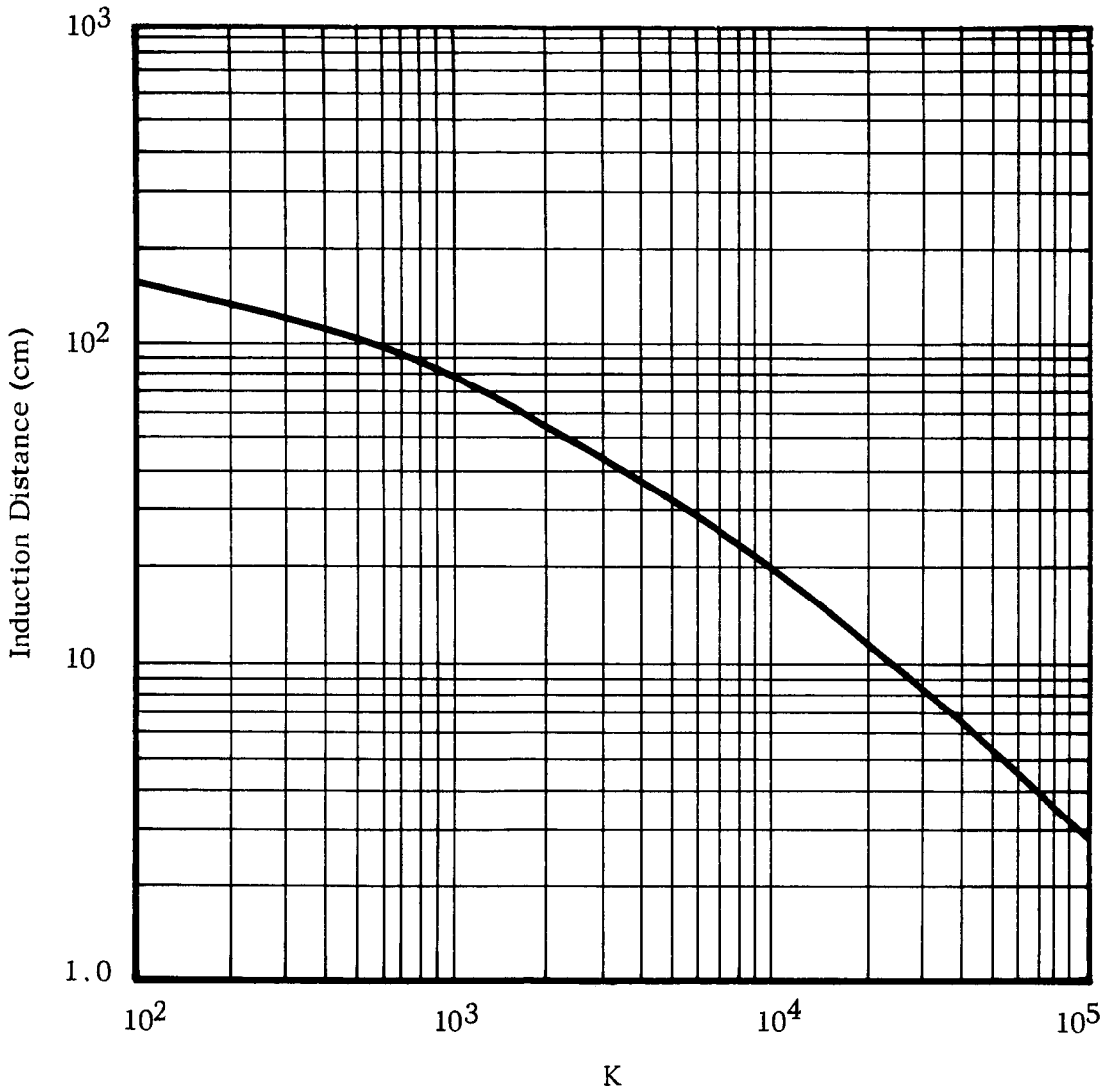

FIGURE 9 EMPIRICALLY ESTABLISHED RELATIONSHIP FOR INDUCTION DISTANCE (REF 25)

TABLE III

DETONATION INDUCTION DISTANCES HYDROGEN-OXYGEN MIXTURES Ref. (25)

Initial Temp. degree	Initial Pressure atm.	Mol percent hydrogen in mixture (induction distance, cm)										
		30	35	40	50	60	65.7	66.7	70	75	80	85
		Based on maximum propagation rates										
100F	1	150	A	102	66	61	72	A	91	95	156	A
100F	5	85	69	41	20	16	A	19	20	A	53	118
100F	10	B	80	36	13.5	13	A	12	13	A	45	A
100F	25	A	A	C	5	5	A	2.5	4	A	31	A
200C	1	B	B	120	76	89	A	98	98	125	B	A
200C	10	A	B	90	15	12	A	13	78	B	A	A
		Based on average propagation rates										
100F	1	150	A	104	74	64	100	A	120	125	194	A
100F	5	100	74	46	21	19	A	20	21	A	54	124
100F	10	B	106	46	22	14	A	13	23	A	47	A
100F	25	A	A	C	3	5	A	3	6.5	A	35	A
200C	1	B	B	140	98	95	A	100	112	132	B	A
200C	10	A	B	126	17	15	A	26	100	B	A	A

A - no data taken B - did not detonate C - data unrelatable

TABLE IV

DETONATION INDUCTION DISTANCES OF HYDROGEN-OXYGEN-DILUENT MIXTURES Ref. (25)

Molar Quantity of Diluent Added	Initial Press = 1 atm. Induction Distance cm. (1)	(2)	Initial Press = 5 atm. Induction Distance cm. (1)	(2)
1/2 N_2	228	234	116	121
N_2	---	---	244	255
1/4 He	185	193	63	76
1/2 He	228	240	108	115
He	---	---	210	218
1/2 Ar	178	180	40	48
Ar	240	244	108	118
1/4 CO_2	239	242	111	120
1/2 CO_2	---	---	159	302

Initial Temperature = 40°C

(1) Induction distance determined for maximum propagation rates of flame in mixture.

(2) Induction distance determined from average propagation rates of flame in mixture.

Because of the large number of combinations of variables and lack of data, no simple criteria have been established that will predict whether transition will take place or not, in a given accident situation. Induction distances, however, might be used in some instances as a relative indication of the degree of improvement achieved in attempts to reduce interstage explosive hazards.

c. Detonation Limits

The ability of a hydrogen-oxygen mixture to sustain a detonation once it has been exposed to a shock wave whose strength is equal to or greater than that defined by the Chapman-Jouget hypothesis is in itself a basic measure of detonability. The limiting compositions of hydrogen and oxygen both with and without additives has been examined both analytically and experimentally from this standpoint.

It was assumed by Belles,[29], for example, that a detonation wave will not be sustained unless the enthalpy increase in the shocked state, corresponding to the critical Mach number, is less than the heat of combustion. That is, if the energy release from the chemical reaction is not great enough relative to the energy requirements of the shock wave, the detonation will die out. It was found that using this assumption as a basis, computations of the limits of detonability of hydrogen and oxygen,and hydrogen and air at normal temperatures and pressures agreed with experimental values to within 2.5 percent.

Other work has been based on a constant temperature criterion for predicting detonation limits [30, 31]. It was assumed that a limiting minimum temperature behind the shock wave (of the critical Mach number) was a necessary condition for the detonation to be sustained. An

improved correlation between predicted and experimental values was obtained on the basis of this hypothesis.

Experiments were also made by Gordon [30] to define the detonation limits of hydrogen-oxygen and additives. This, along with the other data taken from the references noted, is summarized in Figure 10.

The effect of initial pressure and temperature on the detonation limits has also been considered by the above investigators. The effect estimated by Belles is shown in Figures 11 and 12 where it is predicted that the limits become wider as the pressure is reduced and as the temperature is increased.

There is little experimental data, however, on limiting pressures and temperatures beyond which detonation will not occur. Currently, experiments are being conducted at the University of California, Berkeley [32] to obtain this kind of information. The detonation testing is being carried out in relatively large vessels (cylinders - 2 feet in diameter, 20 feet long) using primacord as an initiator. The character of the shock wave is observed as it progresses down the length of the vessel. Published data on the tests conducted to date indicate that equimolar quantities of hydrogen and oxygen at an initial temperature of 65 to 75°F will detonate at initial pressures of less than 10 mm Hg (0.02 psia) but will not sustain a detonation wave at initial pressures less than 0.1 mm Hg (0.002 psia).

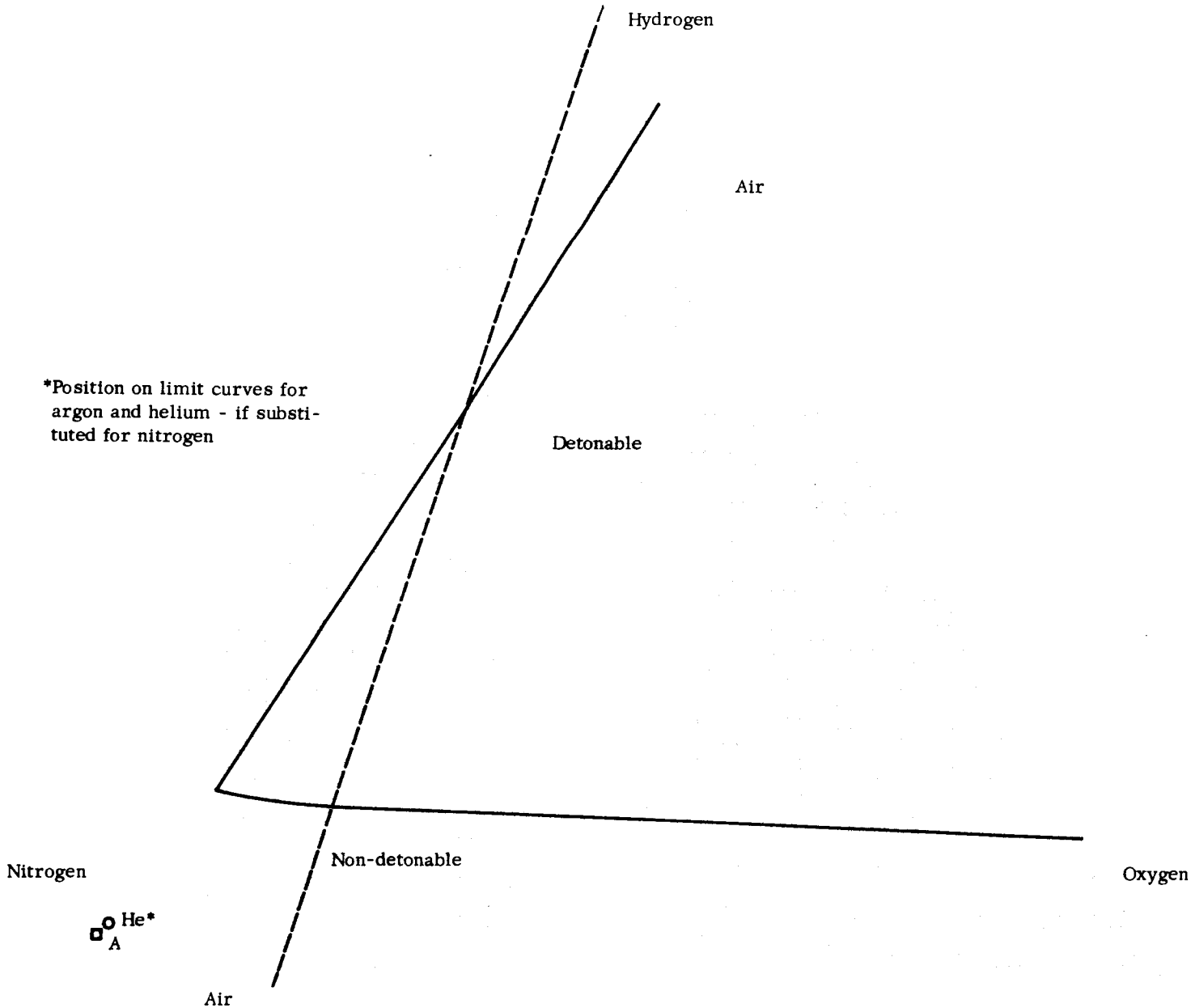

FIGURE 10 DETONATION LIMITS FOR MIXTURES OF H_2-O_2-N_2 AT NORMAL TEMPERATURES AND PRESSURES

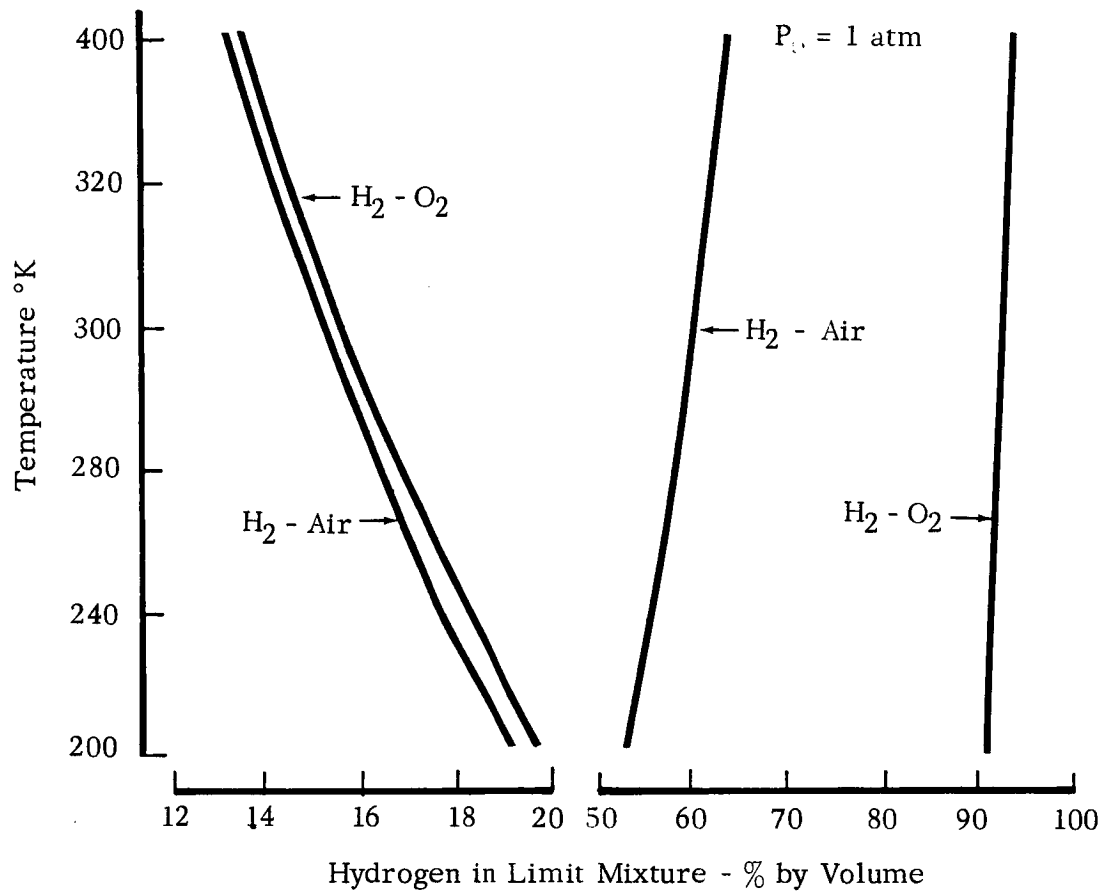

FIGURE 11 EFFECT OF TEMPERATURE ON PREDICTED LIMITS (REF 29)

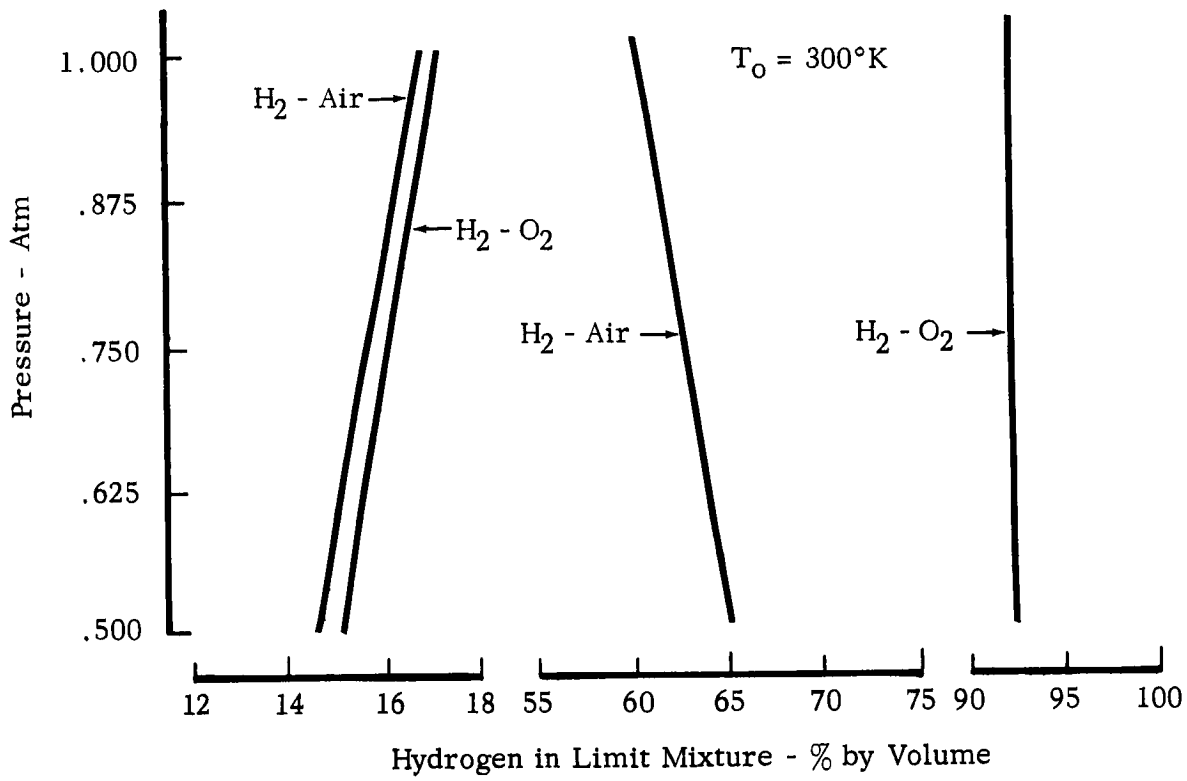

FIGURE 12 EFFECT OF PRESSURE ON PREDICTED LIMITS (REF 29)

In other tests in this program, it was found that pressures much higher than the predicted detonation values occurred during transition from deflagration to detonation. This provides further confirmation of a phenomenon pointed out by other investigators.

Tests performed by Convair [2] in the 2 X 20 foot cylinder at pressures below one psia with the ignition sources previously described apparently did not result in the occurrence of detonation. However, there were no restrictions within the chamber, as there would be within an interstage, that would promote turbulence with the subsequent transition to detonation. The pressure limit for the occurrence of detonation within an interstage remains to be established by experiment.

3. Character of Spherical Detonations and Forces Produced

a. General

Although high peak pressures (of the order of 18 times ambient) are produced in gas phase detonations, the duration of the pressure wave for small quantities reacted and at reduced ambient pressures may not be sufficient to cause damage. In order to establish the limiting effects of detonations on structural elements in the interstage, the character of gas phase detonations in terms of pressure as a function of time have been derived as a part of this study. Both the case of a freely expanding spherical detonation wave and a wave reflected from a rigid wall have been examined.

b. Spherical Detonation

Spherical detonations were selected for study rather than detonations propagated in cylindrical form or as plane waves, since they may be more representative of the wave forms generated within an interstage. They will also produce pressure loadings that are generally as severe as those achieved by other wave front configurations when the total distance that the detonation wave has traveled is the same.

In this work self-similar solutions, equivalent to those of Taylor, [33] have been used to define the detonation wave properties. They have been derived using the following assumptions:

(1) The detonation velocity of a spherically expanding detonation wave is constant and equal to the detonation velocity of a wave propagating through the same mixture in one dimension, as in a pipe.

(2) The reaction zone thickness δ, within the wave is sufficiently small relative to the radius R, of the spherical wave so that it may be neglected ($\delta / R \ll 1$).

(3) The burned products behind the Chapman-Jouget point can be considered to be frozen in composition.

(4) The undisturbed gas is at uniform pressure, density and composition.

The self-similar solutions are based on the assumption that

$$V/D,\ p\ (\rho_1 D^2),\ \mathcal{R}\ T/D^2 \text{ and } \rho / \rho_1$$

are unique functions of the parameter

$$\lambda = \frac{r}{R_o} = \frac{r}{Dt} \qquad (2)$$

where V = particle velocity

D = velocity

ρ = density

ρ_1 = density of undisturbed gas ahead of the detonation front

$\mathcal{R}$ = gas constant

T = absolute temperature

r = local radius from point of ignition

R_o = instantaneous shock front radius

t = time from initiation of detonation

From the assumption that the solutions are self-similar, it follows that the amount of gas having a given velocity will increase as the detonation wave propagates, i.e., as R increases. Similar statements can be made regarding the amount of gas having a given static pressure, dynamic pressure, temperature, etc. Therefore, a structural element will experience a greater impulse, the further away it is from the point of initiation of detonation. Thus, the worst case for an element is that in which detonation was initiated at the furthest point within the interstage volume, and was propagated, unimpeded by other objects, to the element.

The simplifying feature in self-similar flow with spherical detonation, is that all flow properties are functions only of the dimensionless radius r/R_o. This functional relationship is maintained while the detonation wave travels outward unimpeded. The gas properties at the detonation front (behind the Neumann Spike) depend, as does the relationship just referred to, on the nature of the reactions. But

once the reacting mixture is defined, the gas properties can be determined at any location and time once the following two quantities are specified: (1) the distance r of the point in question from the center of initiation of the detonation, and (2) the time since initiation; this time, together with the detonation velocity, determines the distance R_o of the wave front from the center of initiation. The ratio of quantities (1) and (2) is the independent variable $\lambda = r/R_o$ in the unique functional relationship existing in a self-similar flow pattern.

The variables in the self-similar relation for a stoichiometric mixture of hydrogen and oxygen have been calculated (see Appendix A). The variations of reactant velocity, pressure and density with λ are shown in Figure 13. For $\lambda < 0.5$, the pressure and density are uniform and the gas is at rest (V = 0). Now as time evolves, the point $\lambda = 0.5$ represents a sphere of increasing radius ($r = 0.5\ R_o$ and $R_o = Dt$, so $r = 0.5\ Dt$, where D is the detonation velocity). This means that the process leaves behind it a spherical region of gas at rest.

The gas properties are shown in Figure 13 normalized with respect to their respective values at $\lambda = 1$, the Chapman-Jouguet point at the detonation wave front. The properties at the wave front are also shown.

c. Forces Acting on Thin Structural Elements

The results of the self-similar solution for a freely expanding spherical wave have been utilized to predict the forces that would act on thin structural elements within an interstage. The effect of the

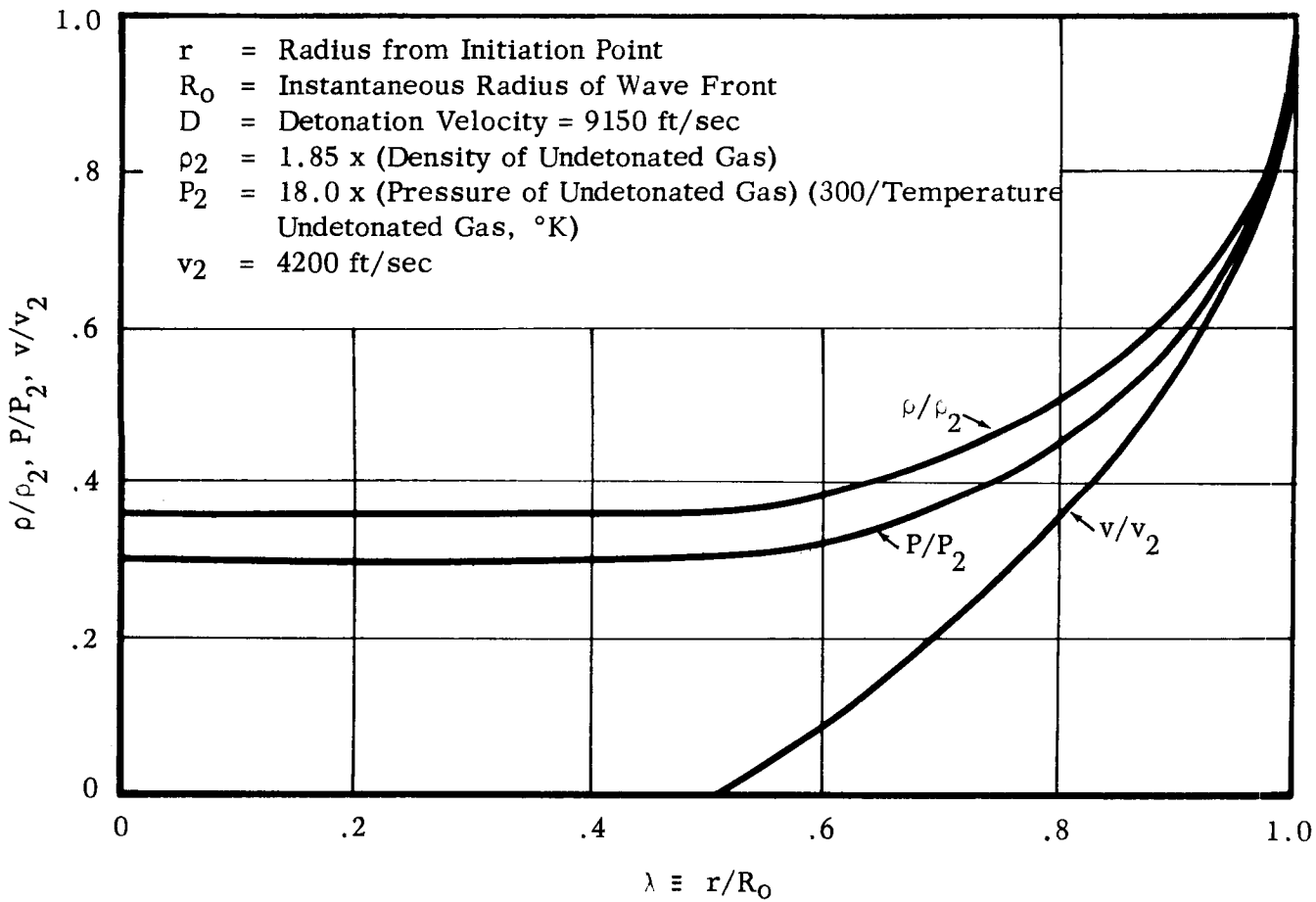

FIGURE 13 NORMALIZED GAS PROPERTIES BEHIND A SPHERICAL DETONATION FRONT - STOICHIOMETRIC H_2-O_2 MIXTURE

detonation wave on a thin, pencil-like element is predominantly one of wind drag, due to the gas velocity associated with the passing wave. The initial pressure differential acting on the element as the front passes by it, will not act long enough to cause damage. The drag force F may be expressed as

$$F = C_D A \frac{\rho v^2}{2} \qquad (3)$$

where C_D = drag coefficient

A = cross-section of the element in the plane of the wave front

ρ = gas density

v = gas velocity

The passing of the wave is, of course, very rapid and the element experiences an impulsive, rather than a steady, loading. One is, therefore, interested in

$$I = \int F dt = \frac{1}{2} C_D A \int \rho v^2 \, dt \qquad (4)$$

This can be re-written as

$$I = \frac{1}{2} C_D A \rho_o v_o^2 \int \left(\frac{\rho}{\rho_o}\right) \left(\frac{v}{v_o}\right)^2 dt \qquad (5)$$

Another characteristic of thin structures is that their presence does not alter the general behavior of the wave, except locally. Therefore, a knowledge of the particle velocity due to the passage of the wave at the location of an element is sufficient for the calculation of the dynamic drag on that element. But the particle velocity and its

variation with time is known at any radius from the point of ignition. Therefore, the effect of a spherical detonation wave on a thin structural element can be calculated.

Since

$$\lambda = \frac{r}{Dt}$$

$$dt = \frac{r}{D} \frac{d\lambda}{\lambda^2} \qquad (6)$$

In the differentiation process, r, the location of the structural element, is considered fixed. We re-write equation (4) as:

$$I = \frac{1}{2} C_D A \rho_o v_o^2 \frac{r}{D} \int_0^1 f(\lambda) \, d\lambda \qquad (7)$$

where

$$f(\lambda) = \frac{1}{\lambda^2} \frac{\rho(\lambda)}{\rho_o} \left[\frac{v(\lambda)}{v_o}\right]^2 \qquad (8)$$

and the subscript "o" refers to conditions at the detonation front.

The function f (λ) can be evaluated from the graphs of Figure 13, and the integration can be performed numerically. We have done so; the result is:

$$\frac{I}{C_D A} = 4.06 \, r \, \rho_1 \quad \text{lb-sec/ft}^2 \qquad (9)$$

where I = lb-sec

A = ft^2

r = distance from the center of initiation to the element, ft

ρ_1 = density of the undetonated mixture, lb/ft^3.

d. Forces Acting on a Rigid Wall

The damage to a wall or other large surface in the interstage is caused by the pressure acting normal to it. The distribution of gas properties behind a detonation front at the instant the front reaches a wall is known provided the point of ignition is located. The pressure generated at the wall at the time of impact and at all times thereafter must be calculated. This pressure-time history will depend on the thickness of the wall and the properties of its material. However, since a perfectly rigid wall will experience the greatest pressures, it has been used in this analysis in order to provide a conservative estimate of the forces that may occur.

Since the initial conditions just before impact are known, it is possible to calculate the subsequent variation in pressure at the wall. The treatment of this problem is not specifically reported in the literature, the cases most commonly treated being those of unsupported shock waves incident on a rigid wall. However, the method for treating this problem is available and is applied here to the case of a detonation wave.

Consider a stoichiometric H_2 - O_2 mixture of detonable concentration, initially at rest in a rigid-walled spherical vessel and let a detonation wave be initiated at the center of the vessel. The detonation wave will propagate outward toward the container wall, will reach it and be reflected from it into the burned products. The pressure experienced at the wall will have a maximum at the instant of impact of the wave front and will thereafter decrease rapidly with time. The duration is such

($< 10^{-3}$) that for most cases, the loading on the wall can be considered as impulsive. Therefore, in most cases, the peak pressure (which is rather simply obtained) has less importance than the impulse per unit area, the calculation of which requires a knowledge of the pressure as a function of time (which is not so simply obtained).

In order to determine the pressure p (t) at the wall, where t is time after the wave front first hits the wall, all gas properties and velocities must be known throughout the vessel just before impact. For a self-similar pattern with spherical symmetry, the required information is known. More precisely, the relationships are:

$$R(\lambda),\ V(\lambda) \text{ and } P(\lambda)$$

Since, at the first instant of impact, the wave front coincides with the container wall, it is possible to write, for that instant:

$$\lambda = r/R_{wall} \qquad (10)$$

Thus, all gas properties at the first instant of impact can be deduced, and all the subsequent distributions of properties can in principle be calculated from the equations of gas dynamics.

The detailed calculations required to determine the behavior of the reflected wave and the space-time distribution of properties (which must be solved for simultaneously in order to obtain p (t)) are highly involved, and are best carried out with the aid of an electronic computer.

An approximation of the pressure-time variations over the interval during which the major part of the impulse occurs has been derived by assuming linear time variations of the pressure at the wall and of the reflected wave velocity as well as a linear radial variation of the gas properties (p, v, ρ) in the space between the wall and the front of the inward-traveling reflected wave.

The linearized pressure-time variation at the rigid wall is shown in Figure 14.

The resulting impulse on the wall is:

$$\frac{I}{A} = 50.6 R_{wall} \quad \rho_1 \quad \text{lb-sec/ft}^2 \qquad (11)$$

where R_{wall} = distance between ignition point and wall (feet)

ρ_1 = density of undetonated mixture (lb/ft^3)

The duration of the pulse is

$$t = 3.2 \times 10^{-5} \; R_{wall} \text{ sec}$$

where again R_{wall} is in feet.

The interstage volume is not generally spherical in shape and few of the elements of interest (e.g., the outer surface of an engine nozzle) may present concave spherical surfaces to an oncoming wave initiated elsewhere in the interstage. The question then arises as to the significance of the results, based as they are on spherical symmetry. The following discussion is intended to clarify this question.

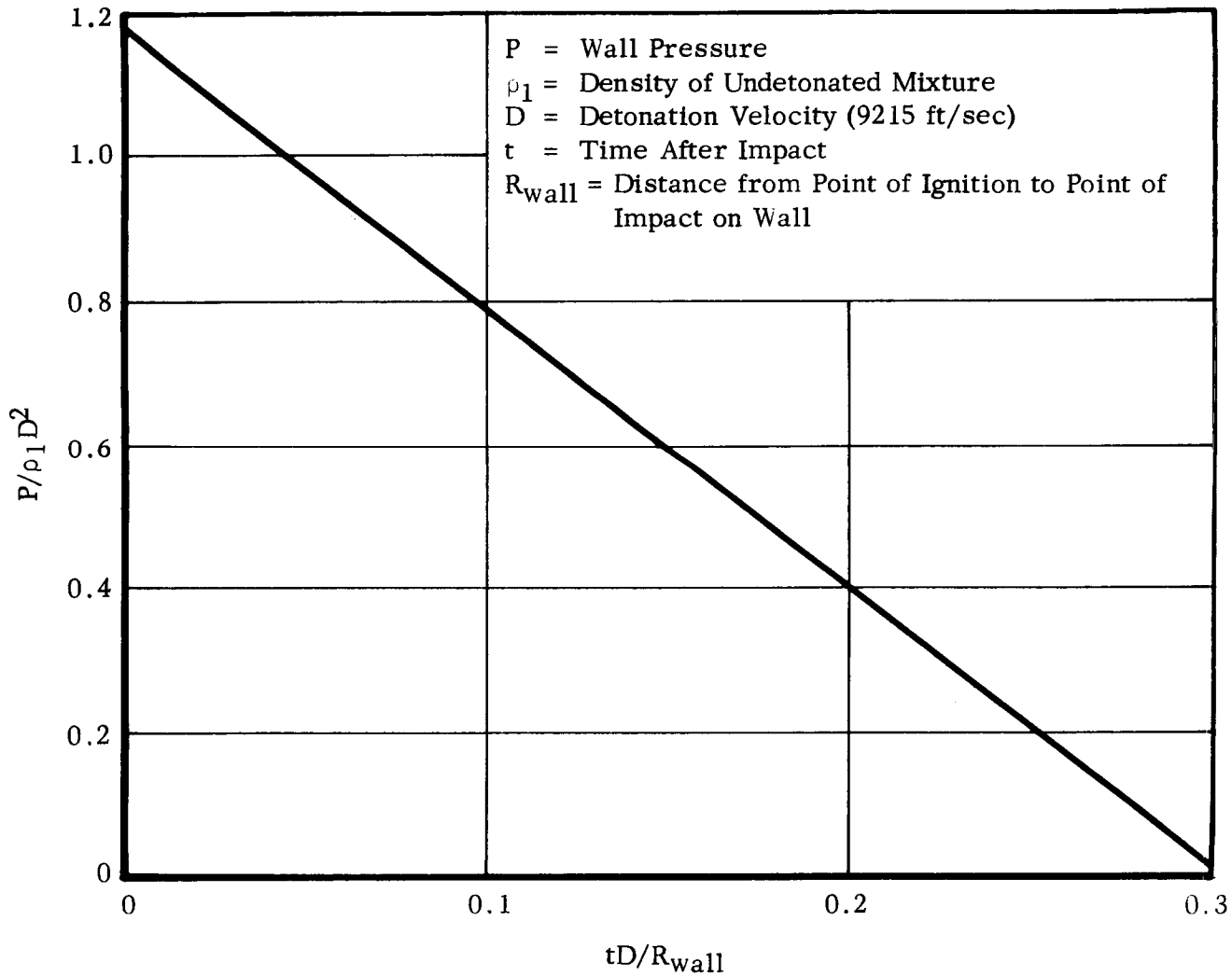

FIGURE 14 APPROXIMATE VARIATION OF WALL PRESSURE WITH TIME AFTER IMPACT OF A SPHERICAL WAVE FRONT WITH A RIGID WALL -- STOICHIOMETRIC H_2-O_2

During the impulsive period, the reflected shock wave travels only a short distance toward the center of symmetry. Thus, the impulse experienced at the wall is the result of gas-dynamical reactions occurring within a relatively thin shell of thickness less than one-tenth the container diameter. Therefore, a local decrease in wall curvature even to zero curvature (i.e., when the wall is locally planar) will not alter these reactions seriously and the impulse will not decrease by a large amount, for a given ignition point-to-wall distance.

Of course, if the change of curvature is continued (the wall now offering a convex surface to the incoming wave), the resulting impulse will decrease, tending toward that found for a small obstruction (see the preceding section).

If, on the other hand, the curvature (concavity) is increased appreciably (e.g., a local distortion seen as a blister from outside the container and as a recess from inside), the impulse per unit area will increase. Eventually, the impulse can become quite large, for instance, in the case where the inner surface of the container has in it wedge-like or cone-like recesses. This case has not been treated in the analysis of the effects of detonation waves on structures. Where an interstage component has a configuration of this type, an allowance must be made for the lack of conservativeness in the analysis.

In summary, the expression given for impulse per unit area applies (at a given distance R_{wall} from the point of initiation) not only to perfectly spherical containers, but also to those having cylindrical surfaces (concave on the side of the detonation) and even to

relatively flat surfaces. In the formula, R_{wall} always represents the distance between the ignition point and the wall--only in the coincidental case of a spherical vessel with ignition at the geometric center does R_{wall} also represent the radius of the container wall.

C. Condensed Phase Explosions

The following mixtures containing condensed phases of either or both hydrogen and oxygen may occur within an interstage during flight:

Gaseous hydrogen--liquid oxygen

Gaseous hydrogen--solid oxygen

Liquid hydrogen--solid oxygen

Solid hydrogen--solid oxygen

Other combinations would be thermally incompatible and cannot be maintained in mixed form except for very short intervals of time.

Until recently, there has been no experimental effort to determine the combustion characteristics of these mixtures. It is understood, however, that this is to be accomplished in a program to be sponsored shortly by George C. Marshall Space Flight Center.

In the first two cases where particles of oxygen are dispersed in gaseous hydrogen, the propagation of the chemical reaction will be similar to gas phase reactions. Thermal and diffusion transport will govern the propagation of the flame. When the particles are small, the propagation rates will approach those of the gas phase condition. When they are large, the rate of heat release may be effected by the rate of evaporation of the particles.

In general, it is expected that the composition limits for deflagration will be reduced and the quenching distance increased over that of a gas phase mixture at the same initial temperature and pressure. Since some of the oxygen must be evaporated in order to initiate the reaction, minimum ignition energy requirements would be much greater.

The propagation of detonation will require that the oxygen particles be sufficiently small so that their evaporation, mixing and reaction with the hydrogen gas can take place in a short enough interval to sustain the fast moving shock wave. The detonation pressures and velocities will be only slightly higher than the gas phase case when the concentration of oxygen is low. With higher concentrations of oxygen, the detonation pressures will be higher because of the increased density of the mixture.

The deflagration and detonation of the other two combinations listed (LH_2 - SO_2, SH_2 - SO_2) will require relatively small particles and be more difficult to ignite. Since detonation pressure and impulse are a function of initial density, much higher values can occur when both reactants are in the condensed phase and particularly when the particles are closely packed as they may be when they collect at the bottom or at some other point in the interstage. It has been estimated that detonation pressures in the order of hundreds of thousands of pounds per square inch may result from the condensed phase detonation of hydrogen and oxygen. Here, again, it is understood that there is an experimental program sponsored by George C. Marshall Space Flight Center to obtain this information.

IV. OCCURRENCE OF EXPLOSIONS IN AN INTERSTAGE

A. Leakage of Hydrogen, Oxygen and Air

Since all vehicles will be designed with great care to prevent accidental leakage of hydrogen, oxygen and/or air, the probability of these fluids entering the interstage is difficult, if not impossible, to define. With the current practice of providing an inert atmosphere in the interstage at launch, the leakage of any single component (H_2, O_2, or air) in itself, will not be sufficient to create an explosive hazard. Both hydrogen and oxygen (or air) must enter the interstage and mix before an explosion could occur.

If all of the hydrogen were contained entirely in the vehicle storage tanks with no transfer or containment in the interstage piping, pumps and valves prior to stage separation, the probability of a hydrogen explosion in the interstage would be remote. However, because satisfactory engine performance requires that the engine feed lines and pumps be at, or close to, the appropriate cryogenic liquid temperatures at start up, all systems require the circulation of both liquid hydrogen and oxygen through interstage components prior to stage separation. The circulation of the propellants for inflight chill down purposes provides the basic potential source of leakage into the interstage. With the RL-10 engine, the propellant transfer rate for chill down is of the order of 1.2 lb/sec and 1.5 lb/sec for liquid hydrogen and oxygen respectively. This takes place during the final 10-40 seconds before stage separation. The propellants are circulated for temperature control in the J-2 engine continually from time of propellant filling until engine start-up. The

rate for liquid hydrogen is approximately 1.2 pound per second. The range of possible rates of accidental leakage of propellants into the interstage, then, is from essentially no leakage at all to a level equal to or greater than the chill down transfer rate.

The influx of air into the interstage is even more difficult to define. With the proper design of the venting system which incorporates a positive pressure of inert gas within the interstage, the probability of air entering would be expected to be small. The loss of (or a severe reduction in) positive pressure through accidental removal of sections of the interstage skirt could result in failure of a mission without the occurrence of a hydrogen-oxygen explosion.

For the purposes of this study, the primary hazard has been assumed to be the simultaneous leakage of both propellants. Maximum allowable leakage rates are defined on this basis and then reviewed in terms of air leakage into the system.

If the propellant leakage rates are small, the relatively warm surfaces of the engine components and interstage structure will, along with other convective processes, be sufficient to evaporate all of the fluids, and only gas phase mixtures will form. With good design, the rate of leakage, if it occurs at all, will tend to be small. Since low rates of escapement will then be more probable and explosions in gaseous mixtures are more readily initiated and propagated, gas phase reactions appear to produce the more severe hazard. In this work, maximum allowable leakage rates have been estimated for gaseous mixtures and then compared with those for mixed and condensed phase reactions.

B. Mixing of Hydrogen, Oxygen and Air

The mixing of the fluids upon entering the interstage is difficult, if not impossible, to predict since the influence of interstage geometry and the relevant thermal and diffusion processes are inordinately complex. The extreme conditions of mixing, however, can be defined and used to provide a conservative basis for predicting the explosive hazard that may occur. For the purposes of this study, the following three mixing processes were considered.

Condition 1--The hydrogen and oxygen leaking into the interstage mix uniformly and instantaneously. They do not mix with the nitrogen blanket. No hydrogen and oxygen escapes from the interstage until all the nitrogen has been vented.

Condition 2--The hydrogen, oxygen and nitrogen mix instantaneously and uniformly. Hydrogen and oxygen as well as the nitrogen are lost from the interstage as the pressure drops with altitude.

Condition 3--The hydrogen, oxygen and nitrogen only become uniformly mixed at the time in flight where the explosion hazard is of interest. Prior to this time, the mixing has been carried out in such a manner that no hydrogen and oxygen has been lost from the interstage.

If the leakage points of each fluid are in close proximity or if the densities of the fluids cause them to fall and mix at the bottom of the interstage, the conditions of item 1 above are approached. It is understood that purging experiments conducted by the Douglas Aircraft Company with a simulated S-IV stage have established that injected fluids do not necessarily mix well with the inert gas in the container.

If the leakage points are far apart and if there is considerable turbulence, the hydrogen and oxygen may mix well with the nitrogen before they mix with each other and conditions approaching items 2 or 3 may be achieved. Condition 2 has not been utilized in this study since it would provide a less conservative estimate of maximum leakage rate than Condition 3.

C. Ignition Sources

There should be no sources of ignition for explosive mixtures in a well designed vehicle interstage. Electrical components such as junction boxes, controls, motors, inverters, etc., that may be capable of producing sparks should be explosion proof. Adequate grounding should be provided so that electrostatic discharges will not occur. No hot wires or surfaces should come in contact with the atmosphere in the interstage.

In spite of precautions of this type, it has been demonstrated at various hydrogen storage and handling facilities that, on occasion, explosive hydrogen mixtures have been ignited. Because, at present, it appears impossible to predict the likelihood of an ignition source occurring within an interstage, it is assumed, in this study, that a source will be present at the worst time relative to the explosive hazard.

Since the strength of the source can have an influence on the severity of the hazard, the levels of ignition energy or source temperature used in the experiments made by Convair[2] were selected for this study. It is assumed that a well designed interstage will be incapable of producing ignition effects more severe than these.

D. Maximum Allowable Leakage Rates

Expressions for maximum allowable propellant leakage rates for different explosion hazards have been developed utilizing the assumptions given in the preceding discussion. It has been further assumed that the leak rates will be constant and, in most cases, the leakage will commence at lift-off since it is impossible to predict when leakage will occur and how it may vary. The general expressions for maximum allowable leakage rate have, however, been derived on the basis of total quantity leaked at a given time. By suitable application, it is believed that they may also be used to judge the severity of variable leak rates.

It is expected that leak detection systems will be used as a basis to prevent or postpone launch if propellants are escaping into the interstage prior to lift-off. The utilization of an active nitrogen purge up to launch should also reduce the concentration of propellants to insignificant values when the leaks are small.

Quantitative values of maximum allowable leakage rates for the S-IC/S-II interstage are given later as an example.

1. Maximum Allowable Rates Based on Deflagration

a. Gas Phase Mixtures

The maximum leakage rate of hydrogen and oxygen into an interstage that can be allowed without a destructive explosion occurring as a result of a deflagration process is evaluated on the basis of case 3 of the mixing conditions previously discussed. The hydrogen, oxygen and nitrogen mixture is assumed to be uniform at any time and no hydrogen

and oxygen that escapes into the interstage is lost by venting.

The most conservative limit appears to be a leakage rate that would result in a concentration of hydrogen and oxygen that is just below the flammable limit at the time when the ambient pressure is so low that the probability of initiating deflagration (of a stoichiometric mixture of hydrogen and oxygen) would be remote. A flammability limit of 90 percent nitrogen and a limiting pressure for ignition of 0.15 psia were used as a basis for this estimate.

The maximum allowable leakage rate is then defined by the total quantity that has escaped at the time that a pressure of 0.15 psia is achieved in flight. From the equation of state, the above values, and an initial temperature of 530°R the maximum allowable combined ($H_2 + O_2$) leakage is

$$W_{H_2 + O_2} = 32 \times 10^{-6} \, V_o / \Delta t \quad \text{lb/sec} \qquad (12)$$

where V_o = free volume of the interstage, ft^3

Δt = time after start of leak to the time at which ambient pressure = 0.15 psia, sec.

It is assumed that this is a stoichiometric mixture so that the individual maximum allowable propellant leakage rates would be:

$$W_{H_2} = 3.5 \times 10^{-6} \, V_o / \Delta t \quad \text{lb/sec} \qquad (13)$$

$$W_{O_2} = 28.5 \times 10^{-6} \, V_o / \Delta t \quad \text{lb/sec} \qquad (14)$$

At some altitude, generally less than that corresponding to the lower pressure limit (0.15 psia), the pressure increase caused by the deflagration process will not be sufficient to damage the interstage structure. The pressure caused by the deflagration of a stoichiometric mixture of hydrogen and oxygen is approximately eight times the initial pressures of the unreacted gas. If the stoichiometric mixture is diluted with nitrogen, the pressure caused by deflagration will also be about eight times ambient since a smaller fraction of the available chemical energy is tied up in dissociation reactions when the mixture is diluted.

For a pressure ratio of eight the initial pressure at which deflagration can no longer cause an increase in pressure that would result in failure of the interstage structure is

$$p_o = \frac{P_m}{7} \tag{15}$$

where p_o = pressure of the unreacted gas, psia

P_m = maximum allowable increase in pressure resulting from the reaction, psi.

The maximum allowable leakage rate is then defined as that which will cause the total quantity of reactants, at a time in flight when the pressure is equal to p_o, to result in a mixture that is just below the flammability limit.

Again using the equation of state, a flammability limit of 10 percent ($H_2 + O_2$) and a temperature of 530°R the maximum allowable

combined leakage rate is

$$W_{H_2 + O_2} = 30 \times 10^{-6} V_o P_m / \Delta t \quad \text{lb/sec} \quad (16)$$

and for the individual propellants

$$W_{H_2} = 3 \times 10^{-6} V_o P_m / \Delta t \quad \text{lb/sec} \quad (17)$$

$$W_{O_2} = 27 \times 10^{-6} V_o P_m / \Delta t \quad \text{lb/sec} \quad (18)$$

If the mixing condition listed as case 1 in the previous discussion prevailed, similar results would be obtained. The deflagration of the stoichiometric mixture would again result in a pressure approximately eight times ambient throughout the interstage. This would result in the same limit as above.

If air as well as oxygen leaked into the interstage, the leakage rate for hydrogen, as defined above, would still apply. If higher rates of leakage of hydrogen were allowed and the rate of leakage of oxygen and/or air were controlling, the allowable rate of oxygen accumulation would be defined by the necessity to keep its concentration below 5 percent at the time when the limiting ambient pressure (p_o = 0.15 psia or P_m /7) is achieved.

b. Condensed Phase

Although condensed phase mixtures generally occur when the ambient pressure is too low for them to be initiated with sources of the strength that are probable in the interstage, the maximum allowable leak rate is defined here as a matter of interest. It is assumed that the ambient

pressure is insignificant and that the total allowable quantity leaked must be less than that which will produce a pressure that would damage the interstage structure. Using the equation of state and a flame temperature of 4500°R, the maximum combined leak rate would be

$$\dot{W}_{H_2 + O_2} = 249 \times 10^{-6} P_m V_o / \Delta t \quad \text{lb/sec} \quad (19)$$

This is much higher than the gas phase case. The periods of time over which leakage may occur can be much greater, however.

2. Maximum Rates Based on Detonation

a. Gas Phase Mixtures

In the case of deflagrations, it was assumed that the maximum pressures produced were achieved and sustained over a sufficiently long period to allow the use of static loading as the criterion for structural effects. With detonation a very rapidly applied short duration, impulsive loading is followed by the longer duration static loading. The effect of the impulsive loading is discussed later in the report. It is applied here to establish maximum allowable leakage rates. In this analysis, it is found that the dynamic loading defines the maximum allowable leakage rates early in flight whereas the static loading is predominant later on. This requires that both criteria be examined in determining the overall maximum allowable rates.

The dynamic effects have been evaluated using the mixing process listed previously as Condition 1. With the assumption that the interstage skirt is the weakest structure (see Section V-D) and that the S-II skirt is typical, the radius of a "bubble" of a stoichiometric mixture

of hydrogen and oxygen that will cause failure at a given ambient pressure can be estimated.

This has been carried out in Section V-D where it is shown that the mass, M, of the stoichiometric mixture is

$$M = \frac{2.76}{p_o^2} \qquad (20)$$

where M is in pounds and p_o is the ambient pressure in psi.

Using a typical trajectory as in Figure 20 for p_o, M may be calculated as a function of flight time. The maximum allowable leakage rate is then defined by the minimum value of the ratio of total allowable leakage (from equation 20) divided by the time. It is later shown that in the case of the S-IC/S-II interstage, this maximum allowable leakage rate is less than that defined by deflagration.

If the hydrogen and oxygen were assumed to mix with the nitrogen, more severe conditions might be imposed since, as in the case of deflagrations, dilution with nitrogen may not significantly reduce the pressures (and in this case, impulse) produced. Lower initial temperatures would also produce more severe loadings for an equivalent amount leaked.

On the other hand, only a portion of the detonable mixture will actually detonate since the ignition sources in the interstage would only be expected to be of sufficient intensity to initiate a deflagration. The flame will travel some distance before the transition to detonation takes place. The initial deflagration would not be expected to contribute significantly to the strength of the detonation wave.

Without more explicit knowledge of induction distances, it is believed that the maximum allowable leakage rates established here are adequate for design purposes.

b. Condensed Phase

The initiation of detonation in a dispersed mixture of condensed phase particles of hydrogen and oxygen, as in the case of deflagration, is improbable at pressures lower than 0.15 psia. Furthermore, unless the particle size is very small, a detonation wave may not propagate through the mixture.

If the reactants collect in the form of a relatively homogeneous mixture on a cold surface, there is some danger of initiation by impact. It is quite likely that the pressures resulting from a detonation of a deposit of the two materials will be sufficient to cause failure of the object on which they have collected. A deposit of the condensed phase, however, requires that the surface on which it collects be precooled to a low temperature. This requires that the fluids impinge upon the surface at some minimum rate for a given period of time. For maximum interstage flight times of the order of 500 seconds (e.g. Saturn), the maximum allowable leakage rates established on the basis of gas phase deflagrations would not appear to allow sufficient cooling of individual surfaces to the extent that they would allow the collection of condensed phase mixtures.

3. Maximum Allowable Leakage Rates for S-IC/S-II Interstage

The maximum allowable leakage rates have been estimated for the Saturn S-IC/S-II interstage to provide an example of the application of the conclusions drawn in the preceding discussion. The free volume of the interstage is assumed to be 15,000 feet^3 and the variation in pressure with time of flight is that given in Figures 2 and 20. From the analysis of the effects of explosions on interstage structures (see Section V), it has been concluded that the interstage skirt is the most critical component both in terms of static and dynamic loads.

For the deflagration case, it is assumed that the explosion pressure produces a static load on the structure. The limiting static pressure differential allowed across a panel of the skirt was estimated to be 2 psi using equation (25) in Section V-B-2. This was based on the panel being a plate 30 x 20 x 0.07 inches made of 7075-T6 aluminum with an ultimate stress of 76,000 psi.

The maximum leakage rates were calculated using the value of 2 psi for P_m in equation (16). The time for leakage was assumed to be from launch until the ambient pressure was reduced to $p_o = P_m/7$ or 0.3 psi (110 seconds). The application of these values in equations (17) and (18) results in the leakage rates given in Table V.

For the case of detonation equation (20) is plotted in Figure 23 using the data for ambient pressure as a function of time as given in Figure 20. From this curve, the maximum allowable rate is defined by drawing a line that passes through the origin and tangent to the curve. At the point of tangency, the leak rate is defined simply as the total quantity divided by the time. The resulting values are also given in Table V.

TABLE V

MAXIMUM ALLOWABLE LEAKAGE RATES S-IC/S-II INTERSTAGE

Basis	Critical Period After Launch sec.	Allowable Combined Leakage (H_2+O_2) lb/sec.	Allowable H_2 Leakage lb/sec.	Allowable H_2 Leakage liquid cc/min	Allowable O_2 Leakage lb/sec.	Allowable O_2 Leakage liquid cc/min.
Gas phase deflagration	0 - 110	81.8×10^{-4}	8.2×10^{-4}	320	73.6×10^{-4}	175
Gas phase detonation	0 - 110	5.7×10^{-4}	$.6 \times 10^{-4}$	23.2	5.1×10^{-4}	12.12
Condensed phase deflagration and detonation	100 - 500	81.8×10^{-4}	8.2×10^{-4}	320	73.6×10^{-4}	175

From the preceding discussion, it is assumed that the leak rate established for the gas phase deflagration case will also serve as a limit for the occurrence of destructive condensed phase deflagrations. This is also shown in Table V.

V. STRUCTURAL CONSIDERATIONS

A. Aerodynamic Loadings Due to a Detonation

In this section we deal with two general types of loading of structures by a detonation wave: "wind drag" and "surface impact." The former will be experienced by a slender beamlike structure, the latter by a wall.

These loadings have been calculated in Section III-B, taking for the detonable gas a stoichiometric H_2-O_2 mixture. The results show that the wind drag is roughly a triangular pulse with a vertical leading edge. To calculate the surface impact loading, we considered a spherical container completely filled with the mixture and with the detonation started at the center. It was found that the pressure experienced by the wall is a triangular pulse with a vertical leading edge followed by a constant pressure equal to about eight times the pressure of the undetonated mixture. The results show that the duration of the wind drag and surface impact pulses are of the order of 3×10^{-5} R sec., where R is the distance in feet from the point of initiation of the detonation. For the interstage of a launch vehicle having the configuration specified for this study, R is of the order of 20 feet. Therefore, the duration of heavy transient loading of various structures in the interstage by a detonation wave will be less than one millisecond. Preliminary

estimates show that the fundamental natural period of vibration of various beamlike and platelike structures in a typical interstage are much greater than one millisecond. Therefore, for all practical purposes the loading of a detonation wave on these structures is impulsive. The strength of the pressure impulse P (psi-sec) is given by the following expressions: for wind drag

$$P = 0.0317 \frac{p_o R C_D}{T_o} \tag{21}$$

and for surface impact

$$P = 0.393 \frac{p_o R}{T_o} \tag{22}$$

where p_o = the pressure of the undetonated mixture (psi)

T_o = the temperature of the undetonated mixture (^oR)

R = the distance from the point of initiation of the detonation (feet)

C_D = the drag coefficient of a beamlike structure

These equations can be easily derived from equations (9) and (11) by expressing the density of the mixture in terms of its temperature and pressure through the equation of state. It should be emphasized that equation (22) gives the pressure impulse on the wall of a spherical enclosure completely filled with the detonable mixture and with the detonation started at the center. We believe that this formula is a good approximation to the pressure impulse experienced by a platelike structure placed normal to the direction of travel of the detonation wave, provided that the radius of curvature of the structure is comparable to R. This is not a very restrictive condition for various structures

of a typical interstage. However, this formula is not applicable to conelike or wedgelike concave structures which exist in an interstage. The present analysis is, therefore, confined to beamlike and almost-flat structures. The detonation wave is assumed normal to the structure.

B. Stresses in Interstage Structural Elements

1. Dynamic Maximum Bending Stress in Beams and Plates

The typical interstage structures considered here are beams and plates under the uniform impulsive loadings given in the preceding Section. The response of the structures can, in principle, be expressed as an infinite series of their natural modes of vibration with time-dependent coefficients. For beams these coefficients can always be computed exactly. For plates this cannot be done except for certain edge conditions. In addition to this difficulty, the computation of the maximum bending stress from such a series is an extremely tedious task (since the loading is impulsive, more than just the first mode of vibration must be considered). Therefore, we have developed the following approximate and very simple analysis.

When a uniform impulsive load acts on a structure of given mass initially at rest, the structure acquires instantaneously a certain amount of kinetic energy. From then on, the structure vibrates converting kinetic energy into strain energy and vice versa. If there are no losses, the structure will vibrate continuously. Our approximate analysis is based on the following three assumptions:

1. The bending moment (and bending stress) is maximum when the strain energy is maximum.

2. When the strain energy is maximum, the kinetic energy is equal to zero.

3. When the strain energy is maximum, the response of the structure is the same as that due to a uniform static load which produces the same amount of strain energy.

The procedure is demonstrated step by step in Appendix C. The results for uniform beams and rectangular plates are given below. In Appendix D the results are compared with those of some possible exact solutions, and it is shown that they are fairly acceptable.

Beams -- For uniform beams of steel or aluminum, the uniform impulsive wind drag loading given by equation (21) produces the following maximum bending stress σ_{max} (psi):

$$\sigma_{max} = 2240\,\gamma\,\frac{bhp_oRC_D}{T_o\sqrt{SI}} \qquad (23)$$

where γ is a constant equal to 1.94 for simply supported beams and 3.16 for clamped or cantilever beams, and

b = the width of the cross-section of the beam (in)

h = the depth of the cross-section of the beam (in)

S = the cross-sectional area of the beam (in^2)

I = the area moment of inertia of the cross-section of the beam (in^4).

The units of the variables p_o, R and T_o are psia, feet, and ^oR, respectively. For beams with circular cross-section the drag coefficient C_D is equal to 1.4 (supersonic flow).

Plates -- For uniform rectangular plates of steel or aluminum, the uniform impulsive surface impact loading given by equation (22) produces a maximum bending stress σ_{max} (psi) given by:

$$\sigma_{max} = 2.48 \times 10^5 \frac{\beta \, p_o \, R}{\sqrt{\alpha} \, h \, T_o} \qquad (24)$$

where h is the thickness of the plate in inches, and α, β are functions of the ratio of the sides (taken always greater than 1) and of the edge conditions. Values of α and β can be taken directly from tables in reference[34]. Two such tables, pertaining to rectangular plates with all four edges either simply supported or clamped, are reproduced in Table VI.

2. Static Maximum Bending Stress in Plates

In a container completely filled with a stoichiometric mixture of hydrogen and oxygen, the static pressure after detonation may be as great as eight times the pressure before detonation. Hence, a portion of the enclosure, which can be considered as a rectangular, flat plate, will be loaded with a uniform static pressure equal to 7 p_o where p_o is the pressure before detonation. The pressure outside the container has been taken equal to p_o. The maximum bending stress σ_{max} (psi) due to this loading is given by:

$$\sigma_{max} = 42 \; \beta \, p_o \; \frac{a^2}{h^2} \qquad (25)$$

where a and h are the smaller side and thickness of the plate in inches. The units of p_o are psi. The variable β is a function of the ratio of the sides and of the edge conditions as defined in Section V-B-1.

TABLE VI

VALUES OF THE PARAMETERS α AND β FOR RECTANGULAR PLATES WITH ALL EDGES EITHER SIMPLY SUPPORTED OR CLAMPED, POISSON's RATIO EQUAL TO 0.3 Ref. (34)

Ratio of Sides	Simply Supported		Clamped	
	α	β	α	β
1.0	0.00406	0.0479	0.00126	0.0513
1.1	0.00485	0.0554	0.00150	0.0581
1.2	0.00564	0.0627	0.00172	0.0639
1.3	0.00638	0.0694	0.00191	0.0687
1.4	0.00705	0.0755	0.00207	0.0726
1.5	0.00772	0.0812	0.00220	0.0757
1.6	0.00830	0.0862	0.00230	0.0780
1.7	0.00883	0.0908	0.00238	0.0799
1.8	0.00931	0.0948	0.00245	0.0812
1.9	0.00974	0.0985	0.00249	0.0822
2.0	0.01013	0.1017	0.00254	0.0829
3.0	0.01223	0.1189		
4.0	0.01282	0.1235		
5.0	0.01297	0.1246		
∞	0.01302	0.1250	0.00260	0.0833

C. Typical Interstage Components

1. Loads on the Interstage

Major components within the interstage are subjected to severe thrust, aerodynamic, and acoustic loadings during the boost phase. A gas-phase detonation within the interstage during the boost phase will be superimposed on the three major loads and structural failure may result at a level which is much lower than would be expected of an unloaded structure. A load factor must be determined for each structure which is based on the ultimate strength of the structure and the load environment. On the other hand, some structural elements can be considered unloaded, for all practical purposes, when detonation effects are examined.

a. Design Load Factors

George Marshall Space Flight Center's specifications for boosters have a factor of safety[35] of 1.1 based on yield and 1.4 based on ultimate strength. For most tempered materials (7075-T6 aluminum), the factor of safety based on the ultimate strength is commonly used.

b. The Load Environment

For a typical manned space vehicle with one or more interstages, a typical launch profile would be composed as follows:

Lift-off	1.25 g
Maximum aerodynamic load (Max Q)	2.08 g
First stage burnout	4.68 g
Second stage ignition	0.726 g
Second stage burnout	2.24 g

The sustained thrust loads on the interstages will be maximum at first stage burnout. However, at Max Q the combination of the sustained acceleration and the aerodynamic excitation may create the worst vibratory stress condition. The aerodynamic loads may be applied locally as the result of boundary layer or near acoustic field effects. They also may take the form of gross bending of the missile as a free beam as the result of wind shear. Bending loads are also applied as a reaction to the engine control system. Realistic design practice limits the possibility of two "worst case" loads occurring simultaneously. Therefore, the stress state of a structure when a detonation occurs may be determined from one load condition (we suggest axial acceleration). The possibility that a detonation will occur, for instance, when a maximum wind shear is encountered is negligible.

c. Stress Required to Failure

For the purpose of this analysis, we shall assume that the interstage thrust structure is fully stressed to 71.5% of the ultimate stress (factor of safety of 1.4) during the period between Max Q and first stage burnout. (See Figure 15). This premise is generally checked by reference [36]. The stress which will cause failure is the difference between the ultimate and the developed stress under load. This "failure" stress state is taken as the difference between the design factor of safety (1.4) and the stress factor (Figure 15) times the allowable stress. This relationship has been plotted on Figure 16 for Aluminum 7075-T6, which has an ultimate stress of 76,000 psi[37].

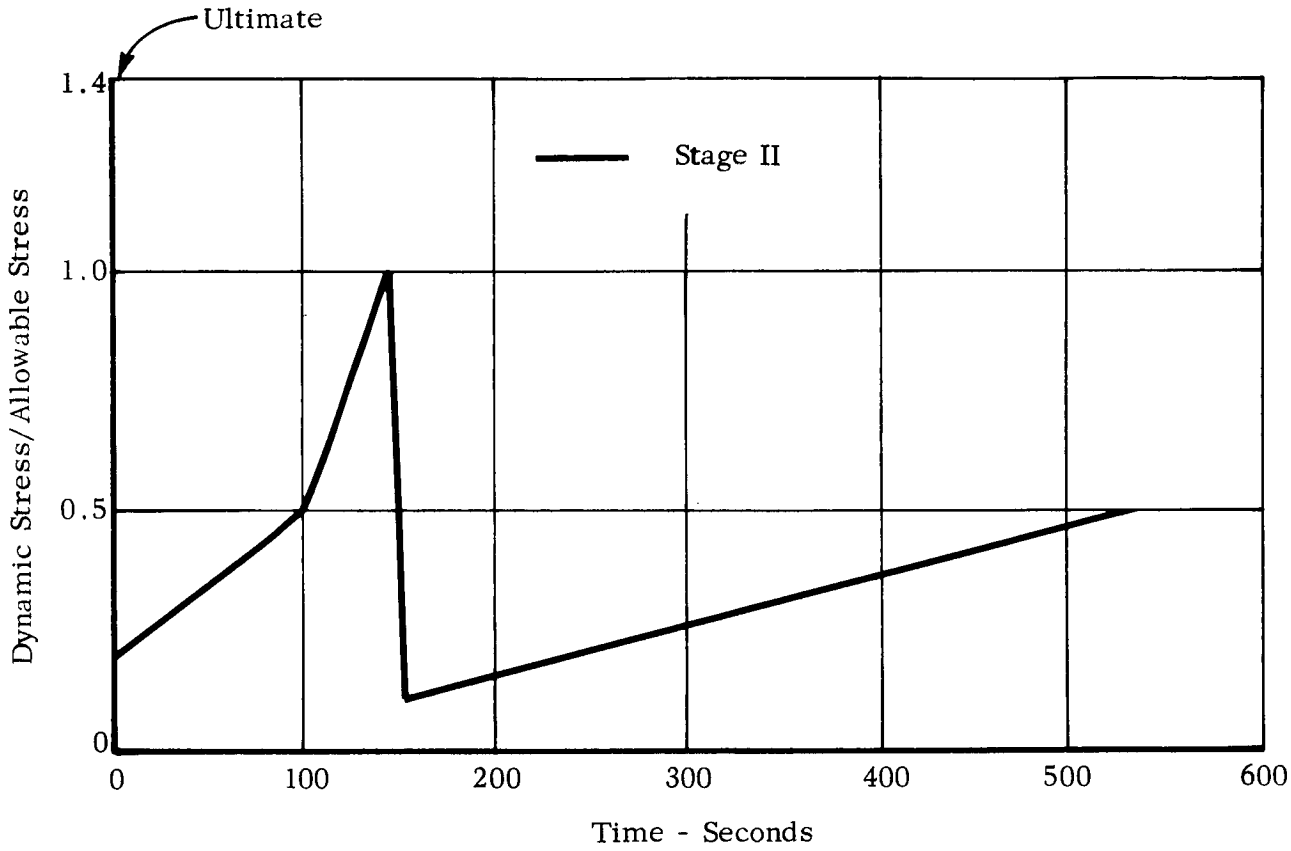

FIGURE 15 DYNAMIC STRESSES DUE TO SUSTAINED LAUNCH ACCELERATION - SATURN-V

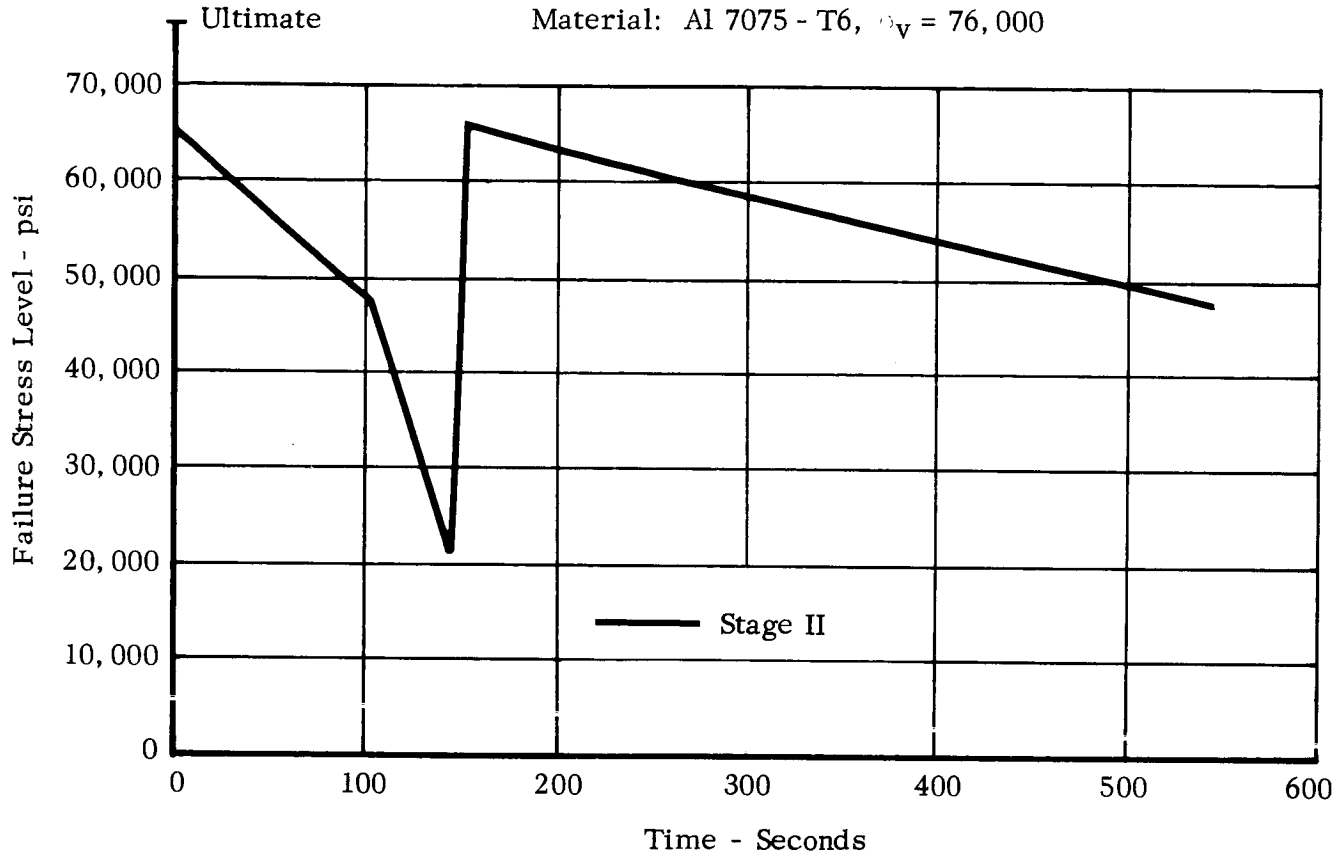

FIGURE 16 STRESS REQUIRED TO CAUSE FAILURE DURING LAUNCH

We acknowledge that this "failure" stress is only an approximate method of determining the loads which will cause structural failure in an interstage. We believe that this failure criterion is consistent with the accuracy of existing linear dynamic stress analysis techniques, however.

2. Arrangement of Components

In a typical hydrogen fueled upper stage of a launch vehicle, the much larger liquid hydrogen storage tank is placed above the tank for liquid oxygen. The interstage necessarily has a diameter as large as that of the tanks of the upper stage and will be tapered to match the diameter of the lower stage if it is larger. The length of the interstage is defined by the length of the engine nozzle and its associated thrust structure. In many present designs, doubled jacketed, flexibly supported hydrogen feed lines do not penetrate the oxidizer tank but are taken outside of the liquid oxygen tank and re-enter the interstage at the thrust structure-skirt intersection.

Two typical interstage sections (a "middle stage" and an "upper stage") are shown on Figures 17 and 18. These interstages are general models of the North American Saturn S-II stage and the Douglas Aircraft Company Saturn SIVB stage. Both interstages are representative of a wide variety of structural components, skirt geometries, engine mountings, even though the stages are integral parts of the Saturn V system. The stages are of different diameter, have different volume surface areas, yet us a semi-monocoque thrust structure and the NAA Rocketdyne J-2 engine. General resemblance ends with the latter two components.

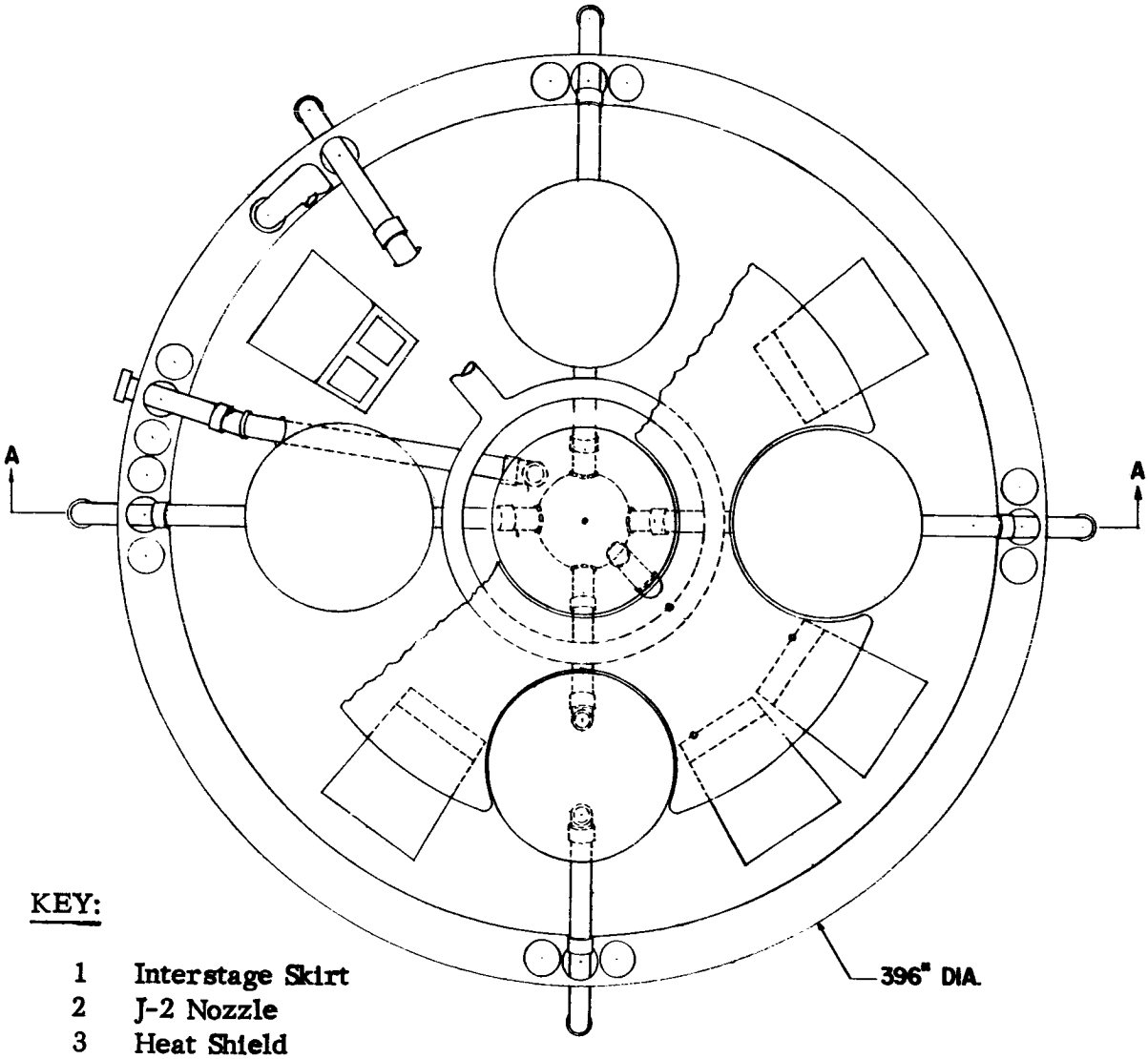

KEY:

1 Interstage Skirt
2 J-2 Nozzle
3 Heat Shield
4 Engine Thrust Structure
5 LH_2 Feed Line
6 Lox Feed Line
7 Center Engine Spider Beam
8 Interstage Ventilation Duct
9 Lox Tank Bulkhead

FIGURE 17 MIDDLE INTERSTAGE

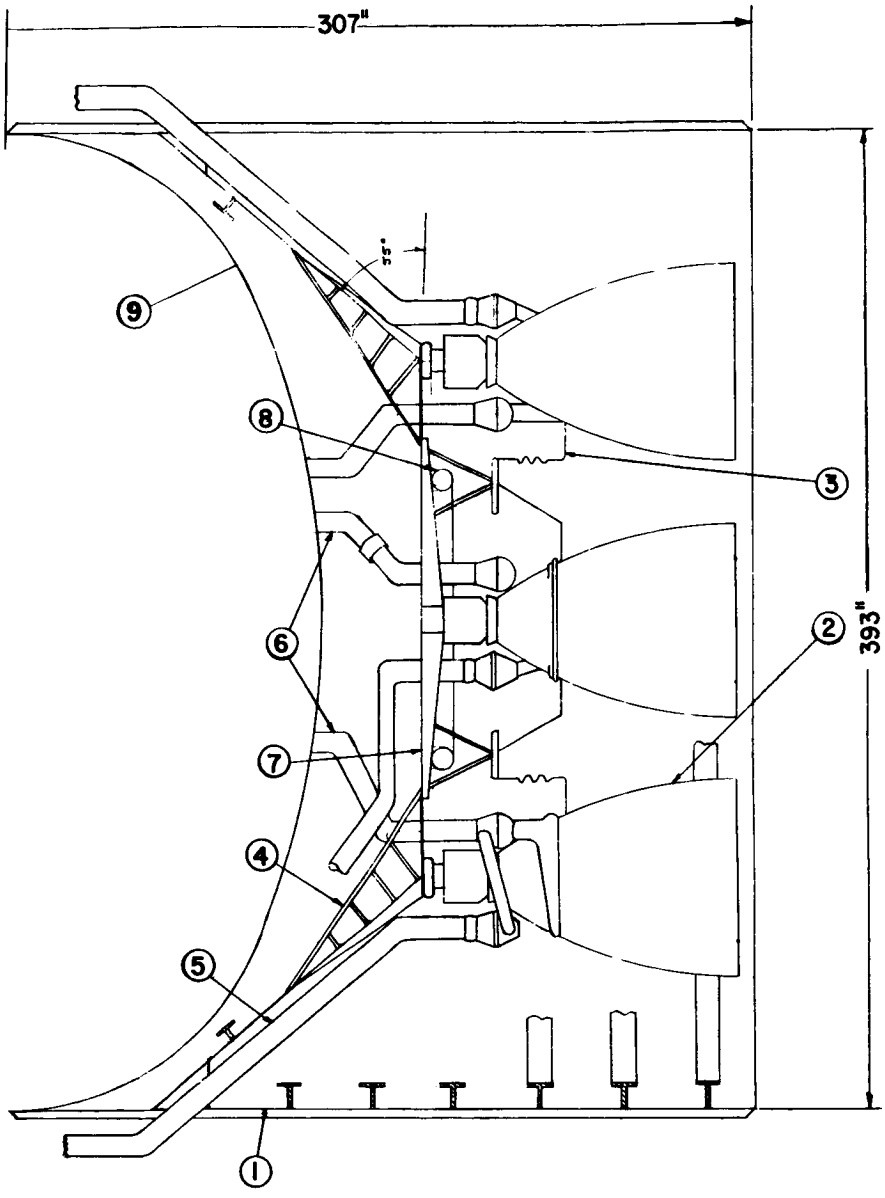

SECTION A-A

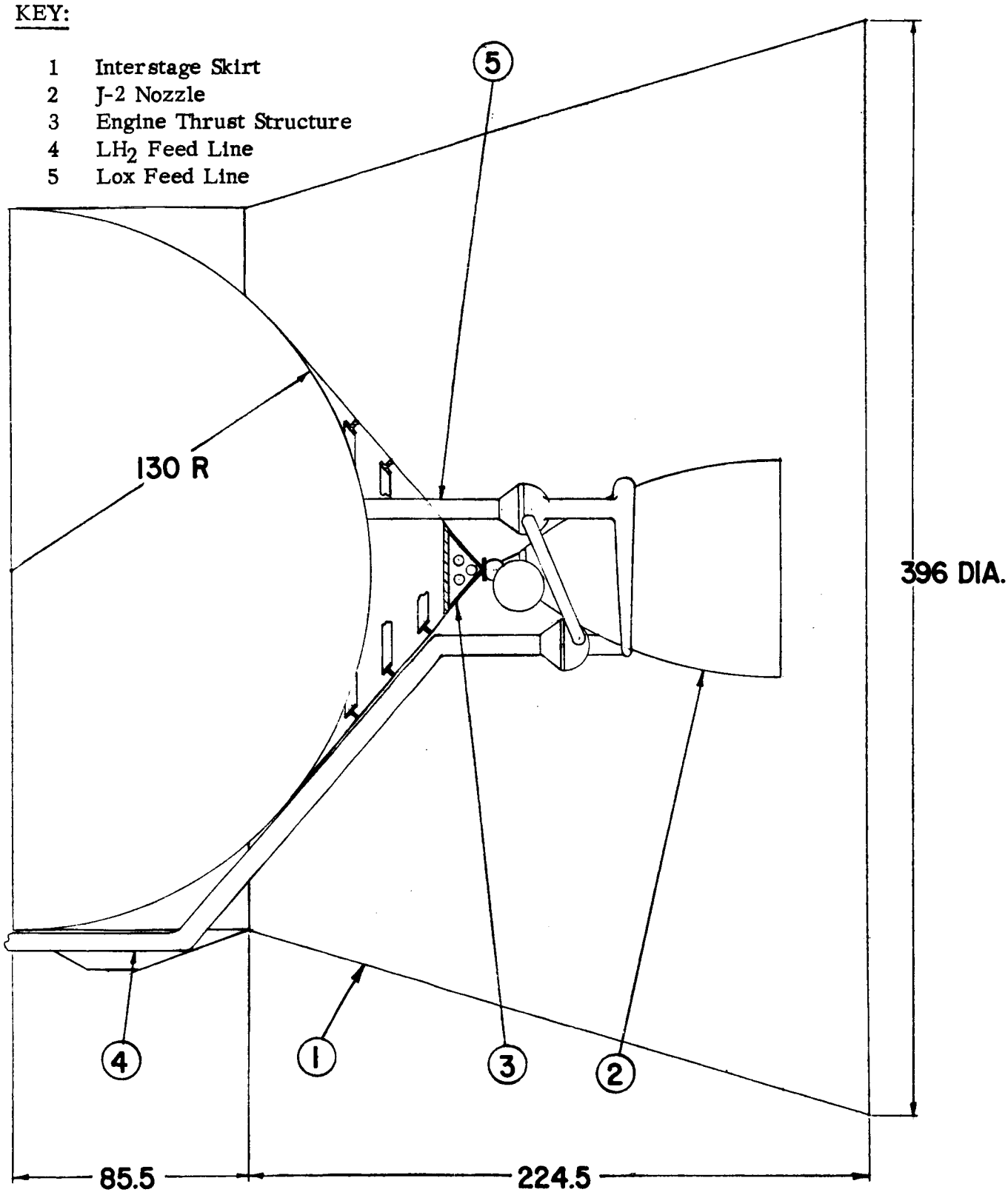

FIGURE 18 UPPER INTERSTAGE

3. Structural Elements of the Interstage

The structural components or elements within the interstage which are most susceptible to damage by a gas-phase detonation wave are noted numerically on Figures 17 and 18.

a. Interstage Skirt

The interstage skirt must carry the axial acceleration loads during lower stage boost and must withstand bending loads generated by aerodynamic forces (usually wind shear) and the resultant engine control system reaction. These bending moments may be noted generally in the first few modes of the missile which acts as a free-free beam. To carry these loads, skirts are generally composed of longitudinal stringers, hoop frames, and a thin skin.

The skin will be subjected to the most damage by an interstage detonation as its dimensions normal to the shock front are large (see Figure 19). The detonation loading will be a diffraction shock uniformly distributed over the surface of an equivalent flat plate.

Prior to detonation, the hoop forces are small, sufficient only to prevent the heavily loaded longitudinal stringers from buckling. The skin does not carry thrust or bending loads--only the acoustic and aerodynamic loads--the magnitude of which is most difficult to define. For this analysis, we shall consider the frames and stringers to carry the load during launch and the skin is unstressed.

For skirt designs which have no hoop frames, the skin will have small hoop forces to restrain the stringers. For this analysis, we consider the hoop forces to be small in comparison with the pressure stresses.

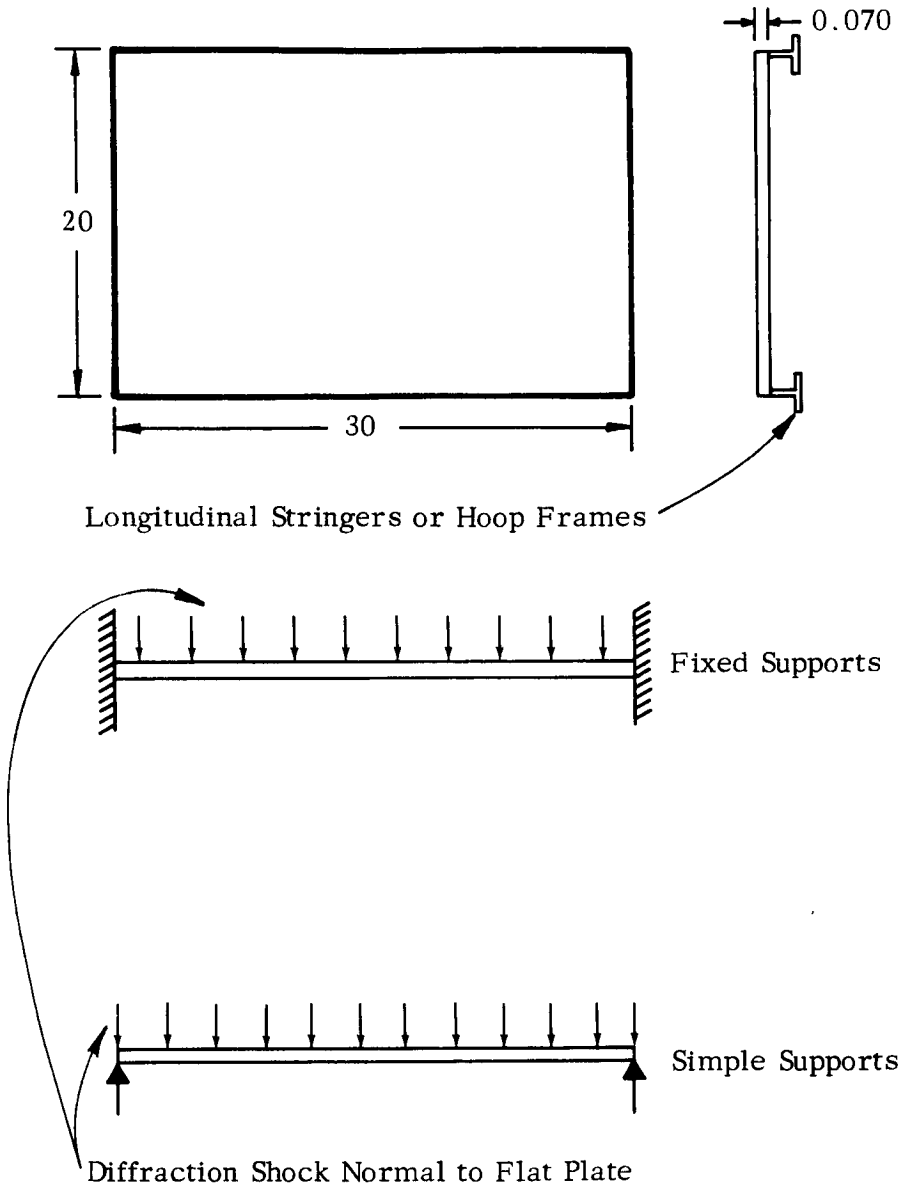

FIGURE 19 AFTER SKIRT PANEL SII INTERSTAGE

The cylindrical skirt in the middle stage is subjected to external pressures caused by gusts and wind shear. To reduce the buckling under these loads, the interstage is semi-sealed and the expanding air (or inert purge gas) is programmed to have a 1 or 2 psi pressure drop across the skin.

The loss of a portion of the conical skirt will abort the mission as the skirt will collapse if the internal pressure falls below a safe level. The cylindrical stage is less susceptible to damage if the interstage pressure is lost. Damage could occur due to high drag effects or the thrust structure could be buckled by high wind shears or gusts.

The unstressed skin of the middle stage skirt can be represented by a flat plate with the edges fixed. Fixing the edges of the plate will cause high bending stresses at the boundaries and yielding will occur. Thus, a stress condition within the flat plate model will result which is between that of a simply supported plate and a fixed edge restraint. Substituting in equation (24)--see Appendix E for details--we can obtain the relationship (for $T_o = 500^oR$)

$$R = 6.65/p_o \qquad (26)$$

where R is the distance in feet over which a spherical detonation wave must travel to be of sufficient intensity to cause a tensile rupture in the flat plate. p_o is the pressure in psi at a given time or altitude during the launch. The dimensions for the plate are taken from Figure 19. Figure 20 shows a typical ambient pressure history.

Referring to Figure 20, note that, about 120 sec after lift-off, R exceeds the maximum 2nd stage diameter of 33 ft (Saturn V). Therefore, beyond that time, the interstage skirt can withstand the detonation blast load--even if the interstage is completely filled with a detonable gaseous hydrogen-oxygen mixture.

b. The Rocket Engine

The combustion chamber and the nozzle throat are designed to withstand internal pressure loads. The expansion cone of the nozzle is also designed to withstand a pressure differential that is close to atmospheric since this will occur during sea level static firings. It appears that the engine and nozzle will be damaged by diffraction loading only when the strong detonation waves resulting from a large leakage occur near ground level. The reaction of the drag loading on the expansion cone caused by a detonation wave would not be expected to be damaging since the engines are designed to withstand large overturning moments.

Because of the relative fragility of other components within the interstage, and the central location of the nozzle (which may result in a higher probability of being close to the source of the detonation), we believe that the engine is not a critical component.

c. The Base Heat Shield

The heat shield in multi-engine installations prevents gas circulation and radiant heating of the liquid oxygen and liquid hydrogen feed lines and other temperature sensitive components in the pump section of the rocket engine. The heat shield is a light structure of laminated construction (aluminum or fiberglass covered honeycomb)

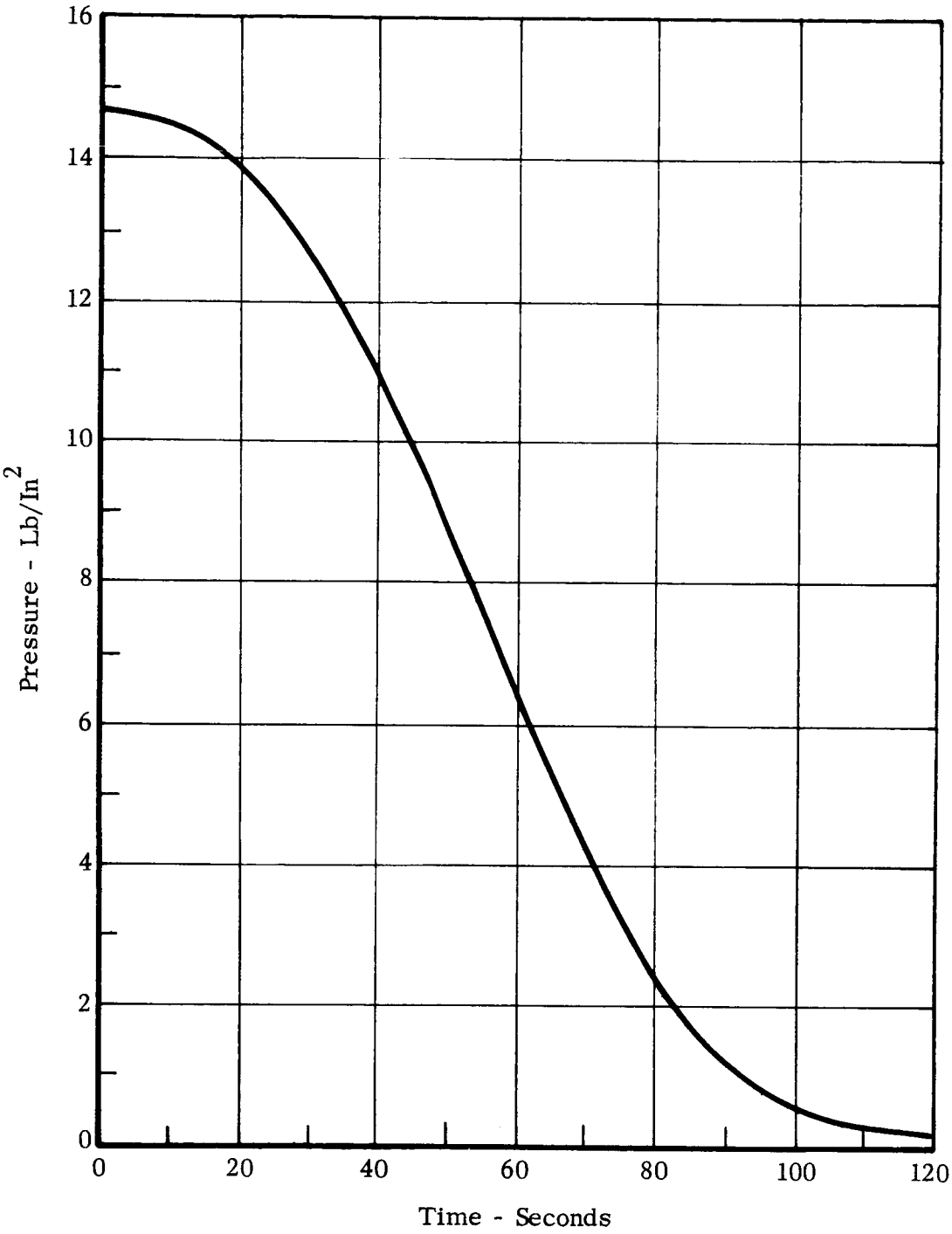

FIGURE 20 AMBIENT PRESSURE HISTORY FOR S-IVB/S-II INTERSTAGE

which is simply supported from the thrust ring. Since the outer engines are movable, flexible boots are required between the engine nozzles and the main section of the heat shield.

As the design loads on the heat shield are minimal (i.e. a relatively low distributed stagnation pressure and small inertia loads), the structure and the support system are comparatively weak. The shield, therefore, is susceptible to damage from the detonation wave. The shield can be modeled as a simply supported flat plate (Figure 21) and is subjected to a normal diffraction shock. Because the plate is of laminated construction, an effective uniform plate thickness must be used in equation (24). When this is done, the following result is obtained:

$$R = 14.9 \sqrt{p_o} \qquad (27)$$

R and p_o are as defined in Section V-C-3-a.

Conversely, as the loadings on the structure are normally small, the heat shield can be easily strengthened to have the same blast resistance as the next weak link in the interstage structural chain. The flexible boots, of course, will be carried away by the mass movement of the combustion products. It is understood that the mission may be aborted if these membrane-like boots are ruptured.

d. Engine Thrust Structure

Engine thrust loads during stage ignition and operation are transferrred to the outer tank wall and ultimately to the upper stages by a conical frame-stringer structure below the oxidizer tank. For multiple engine installations, the conical section is truncated near the

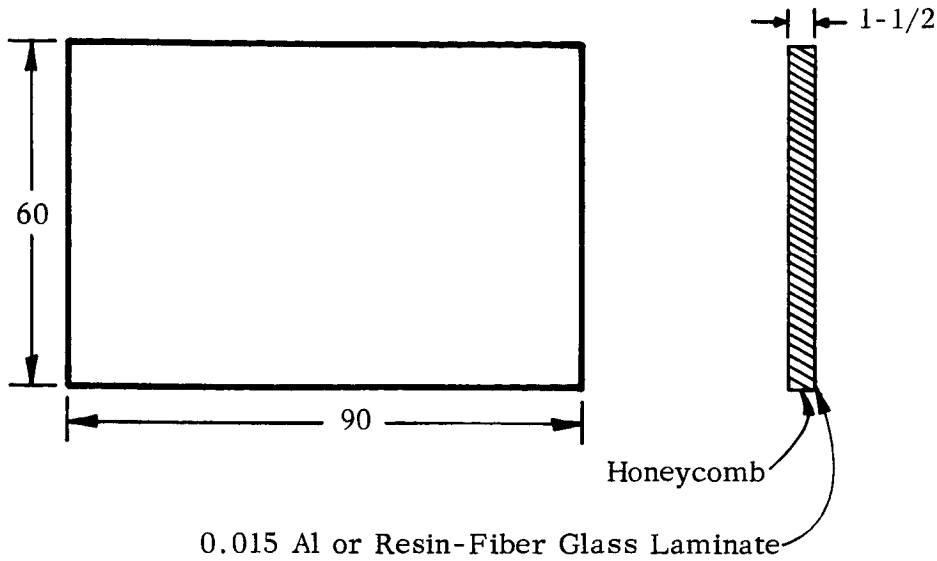

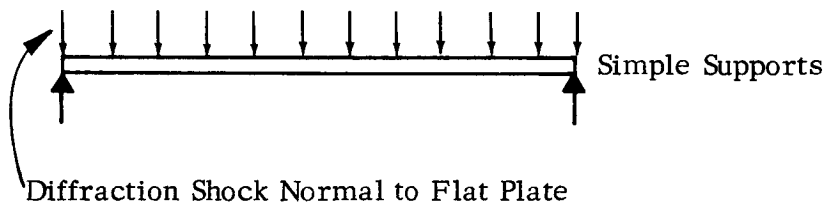

Material: 7075 - T6 Aluminum

FIGURE 21 BASE HEAT SHIELD PANEL

apex and a circular thrust ring distributes the individual engine thrust loads. Usually a spider thrust beam is used to transfer the center engine thrust to the thrust ring. Single engine stages mount the engine near the apex. The thrust cone usually is covered with a skin which may be stressed during engine firing but will be unstressed when gas phase detonations are a hazard.

If such a detonation occurs on either side of the thrust cone, the skin will be damaged. For low frontal area components such as the center engine thrust beam, the primary load will be a gust-like drag load.

Prior to stage separation, the tensile inertia loads of the engine will be the principle load on the structure. However, if blast loads were severe enough to permanently deform the center engine thrust beam or a portion of the conical structure, then buckling might occur during stage ignition. The dynamic stress analysis considers the cone to be impulsive loaded and to be represented by a fixed plate. The center engine thrust beam experiences drag loads.

Calculations show that the center engine thrust beam will be unaffected by detonations that would cause severe damage to the skin. The dimensions of a flat plate representing the skin are similar to the skirt panel and therefore the relationship that defines the loading caused by a detonation wave is similar.

e. Propellant Feed Lines

The hydrogen feed lines (nine inch OD for Saturn V) are double jacketed and simply supported due to the flexibility of the bellows joints that are necessary to accommodate thermal strains. The fuel lines extend into the interstage structure and are supported by the conical thrust structure. The lines are subjected to intense, airborne vibration loads during engine firing; however, the excitation is at high frequencies and therefore the overpressures are small. The lines whose frontal area dimensions are small will be loaded as beams exposed to gust loads.

The liquid oxygen lines are of the same general diameter as the liquid hydrogen lines except that the doubling jackets are omitted. The lines will be flexible due to the expansion joints; however, the length of the lines are small due to the proximity of the liquid oxygen tank. In estimating the stresses caused by a detonation wave, sections of the hydrogen and oxygen feed lines were considered as simply supported beams 150 inches long (see Figure 22). The diameter and thickness of these circular pipes are 8 and 0.025 inches, respectively. The stress allowed for detonation effects is taken equal to 25,000 psi (one-fourth the ultimate strength of stainless steel). With $T_o = 500^oR$, the following relationship between R and p_o is computed in Appendix E.

$$R = \frac{56.8}{p_o} \qquad (28)$$

where R and p_o are as defined in Section V-C-3-a.

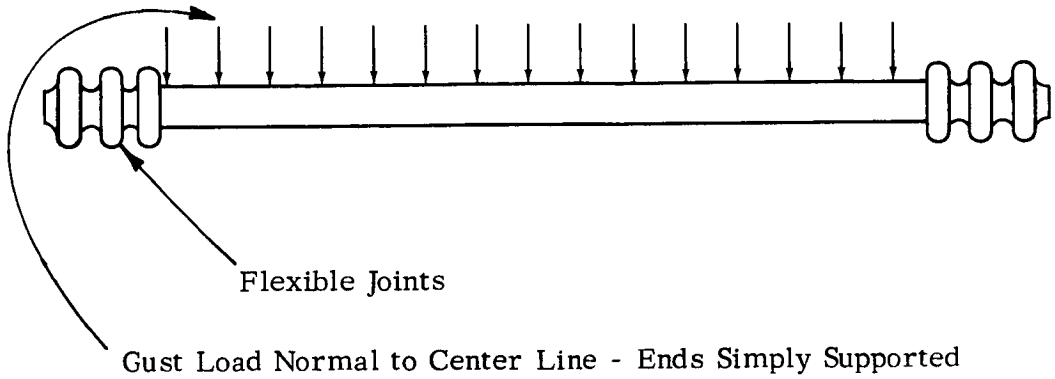

FIGURE 22 LH_2 OR LOX FUEL LINES

f. Interstage Conditioning Manifold

The purge system has a plastic manifold which distributes the purge flow (gaseous nitrogen or air) during prelaunch operations. The plastic is designed to sublimate at 600°F in the S-II interstage and will evaporate during stage burning. The loss of the air-conditioning manifold due to a detonation or a deflagration will not in itself abort the launch--the manifold is not considered a critical component.

g. The Liquid Oxygen Tank Head

The bottom of the liquid oxygen tank (spheroid head) comprises the upper boundary of the interstage compartment. The head will be subjected to internal pressures which are equal to the dynamic head of the oxidizer during boost plus any ullage pressurization. Normally the tank design pressure is between 20 and 40 psi. The head, therefore, is pressure stiffened and an intense diffraction shock of slightly greater magnitude will be necessary to rupture the head. The oxidizer tank wall will withstand impulsive loadings far greater than other components within the interstage and is not considered critical.

D. Minimum Mass of Detonable Mixture

Comparing equations (26) to (28), we see that the most critical structure of the S-IC/S-II interstage of Saturn V is the interstage skirt (the skirt of the engine thrust structure is almost as critical). Equation (26) gives the minimum radius of a "bubble" of a stoichiometric mixture of hydrogen and oxygen which will fail the skirt, when it is placed next to the skirt and is detonated. The maximum allowable weight of stoichiometric mixture was then estimated as follows.

From the equation of state, the pressure of the mixture before detonation is:

$$p_o = 1545 \frac{\rho_o T_o}{M.\ W.} \qquad (29)$$

where p_o = pressure, psf

ρ_o = density, lbs/ft^3

T_o = temperature, ^oR

The mean molecular weight (M.W.) of a H_2 - O_2 stoichiometric mixture is equal to 12.

The total mass M of the stoichiometric mixture before detonation in a spherical bubble of radius R is given by:

$$M = \frac{4\pi}{3} \rho_o R^3 \qquad (30)$$

Substituting for ρ from equation (29) and for R from equation (26) and assuming a temperature of 500°R, the following expression for M is obtained:

$$M = \frac{2.76}{p_o^2} \qquad (20)$$

where M = weight of stoichiometric mixture, lbs

p_o = pressure, psi

With p_o as given in the typical flight of Figure 20, M versus flight-time has been plotted in Figure 23. This curve gives an estimate of the maximum mass of detonable H_2 - O_2 stoichiometric mixture versus flight-time, which can be tolerated in this interstage.

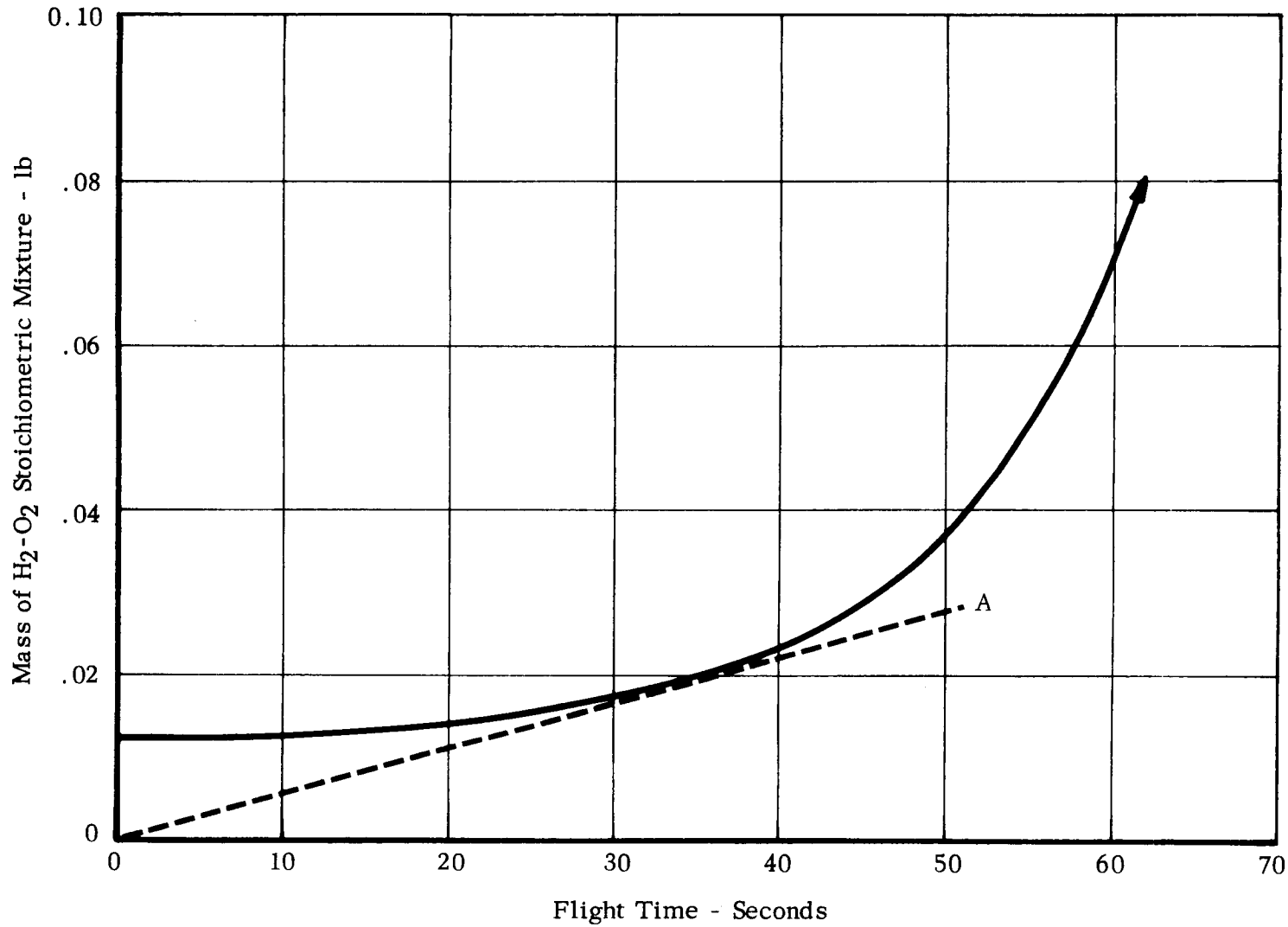

FIGURE 23 MASS OF DETONABLE MIXTURE ALLOWED AS A FUNCTION OF FLIGHT TIME

VI. METHODS OF PREVENTION AND CONTROL OF EXPLOSIONS

A. System-Requirements for Inert Gas Purging

1. Discussion

The formation of combustible mixtures of propellant gases within the interstage compartment of a rocket vehicle can be prevented or minimized by continuous purging of the compartment with an inert gas. The mechanism by which combustible mixtures are eliminated differs with the flow rate of the purge gas and the manner in which it is injected. Three distinct flow conditions within the compartment can be considered:

1. Well-Stirred Condition
2. Streaming Condition
3. Natural Convection Condition

The well-stirred condition results from injection of the purge gas in a manner which promotes mixing so that a nearly uniform mixture is obtained throughout the compartment. The rate of injection must be sufficient to insure that the mixture is not combustible. If this condition can be achieved, it will be very effective in eliminating hazards. However, the required purge gas flow rates may be excessive.

The streaming condition results from injection of the purge gas in a manner which minimizes mixing, but establishes a smooth flow of gas between the injection point and the vent location. The objective of this type of system would be to create a sweeping action throughout the compartment to remove propellant vapors before any substantial degree of mixing could occur.

The natural convection condition is established by providing either a low or high density atmosphere within the compartment so that leaking propellant vapors are carried to the vent location by the effects of gravity and vehicle acceleration. With this approach, the need for purging during flight would be eliminated. However, it is unlikely that combustible mixtures can be avoided completely under this condition.

2. Purging Fluids

a. Properties

The effectiveness of a purge gas in eliminating hazards is related to a number of its physical properties. The property of primary interest is its density or molecular weight. In most of the purging methods, a low density is desirable, though the reasons for desiring a low density vary among the methods.

A second property of importance is the vapor pressure of the purge gas. Its vapor pressure must be sufficiently high so that the gas does not condense on cold surfaces within the compartment. Potential condensation sites include the propellant feed lines and the compartment walls at high altitudes.

b. Suitable Fluids

(1) Gas or Liquid Storage

Materials which could be employed as purging fluids are listed in Table VII with values of pertinent physical properties. Two categories of fluids are indicated--those stored as compressed gases and those

TABLE VII

PHYSICAL PROPERTIES OF PURGING FLUIDS

Gaseous Storage

Material	Mol. Wt.
H_e	4
H_2	2
N_2	28
CH_4	16

Liquid Storage (20C)

Material	Mol. Wt.	Liquid Density (lb/ft^3)	N.B.P. (^oC)	Storage Pressure (atm)
CO_2	44	48	-78.5	60
N_2O	44	50	-88.5	50
C_2H_6	30	35	-88.6	40
CH_3F	34	55	-78.2	40
NH_3	17	38	-33.4	10

stored as liquids. Liquid storage offers the advantage of reduced tank volume and weight. However, a distinct disadvantage in the use of a liquid is the necessity of an energy source to supply the heat of vaporization of the liquid. Unless an existing source of energy were utilized, this requirement could negate the saving in tank weight accompanying liquid storage.

Materials listed in Table VII have been limited to low molecular weight fluids which will not condense at -55°C and a pressure of 1/4 atmosphere. This condition is encountered at approximately 35,000 feet altitude in a standard atmosphere and is the worst condition encountered from the standpoint of condensation on the external panels of the vehicle. A similar criterion cannot be established for condensation on propellant passages unless the degree of precooling of the engines is known. If the engines are to be precooled to propellant storage temperatures, consideration of purging fluids will be limited to light gases.

(2) Gas Generator Systems

As an alternative to a gas or liquid storage system, a gas generator could be utilized as a source of gas for purging interstage compartments. A wide variety of either solid or liquid generating materials could be used, depending upon the desired properties of the purge gas. It would be expected, however, that the combined weight of the propellant storage vessel and combustor would be of the order of 20 to 30 per cent of the propellant weight. Solid propellant gas

generators available commercially reportedly[38] produce gaseous products with an average molecular weight as low as 22 and temperatures approaching 100C.

3. Storage Vessels

In analyzing the requirements of vessels for storage of gas for purging interstage compartments, it is assumed that spherical shapes can be employed and that construction materials can be utilized at their maximum practical working stresses. The required thickness of a spherical tank can be expressed as:

$$t = \frac{Pd}{4S} \tag{31}$$

where P = internal pressure

d = diameter

S = stress

The weight and volume of the tank are as follows:

$$W_T = \pi \rho_T t d^2 \tag{32}$$

$$V_T = \frac{\pi}{6} d^3 \tag{33}$$

where ρ_T = tank density

By combining Equations (31), (32), and (33) an expression is obtained for the ratio of tank weight to fluid weight where ρ_F = fluid density:

$$\frac{W_T}{W_F} = \frac{W_T}{\rho_F V_T} = \frac{3}{2} \frac{\rho_T}{S} \frac{P}{\rho_F} \tag{34}$$

In the case of liquid storage, P becomes the vapor pressure of the liquid and ρ_F the liquid density, both of which remain constant if the temperature is fixed. In the case of a compressed gas which can be treated as a perfect gas, Equation (34) can be written:

$$\frac{W_T}{W_F} = \frac{3}{2} \frac{\rho_T}{S} \frac{RT}{M} \tag{35}$$

where R = universal gas constant

T = temperature

M = molecular weight of gas

Thus, in either case, it is observed that the ratio of tank weight to fluid weight is independent of the tank size, quantity of fluid, or in the case of a compressed gas, the tank pressure. Consequently, the tank weight can be related directly to the fluid weight and this relationship is independent of total quantity of fluid. Similar relations can be written for cylindrical or toroidal tanks. In these cases, the tank weight is increased by a factor of 4/3.

The critical tank property affecting its weight is the ratio S/ρ_T, sometimes referred to as "specific strength." Values of specific strength, based on ultimate tensile strength, are listed in Table VIII for materials currently used in high pressure storage vessels. For purposes of this analysis, a specific strength of 0.8×10^6 lbf in/lbm is assumed which provides a safety factor of 1.5 with titanium or 2.4 with fiberglass reinforced plastic. Using this value in Equations (34) and (35), ratios of tank weight to fluid

TABLE VIII

SPECIFIC STRENGTH OF TANK MATERIALS

Material	Ultimate Strength (psi)	Density (lbm/in^3)	Specific Strength (S/ρ) (lbf in/lbm)
Glass Fiber and Binder	150,000	.079	1.9×10^6
Titanium	200,000	.162	1.2×10^6
Steel	250,000	.278	0.9×10^6
Aluminum	75,000	.097	0.8×10^6

weight for typical fluids have been determined and are listed in Table IX.

In the case of light gases, such as hydrogen and helium, the tank weight is considerably greater than that of the gas. Whereas, with heavier gases such as nitrogen, the tank and fluid weights are comparable, and with liquid storage system, the tank weight is an insignificant portion of the system weight.

4. Purging Techniques

a. Well-Stirred System

The operation of a well-stirred purging system is based upon the rapid mixing of the purging fluid with other gases in the compartment so that combustible mixtures cannot accumulate in any appreciable volume. The effectiveness of the system is dependent upon the rate of mixing and the degree of mixing which is achieved. In addition to the rate of injection of purging fluid, mixing effectiveness will be influenced by the relative locations of injection points, leak points, and vents, and by the velocity and orientation of the streams of purging fluid.

With regard to relative positioning, the location of the vents often is dictated by considerations other than combustion hazards. The locations of leaks cannot be controlled, but the most likely leak sites can be designated. Therefore, only the purging fluid injection points can be located independently. These injection points should be located in the vicinity of the potential leak points so that contact

TABLE IX

RATIO OF TANK WEIGHT TO FLUID WEIGHT

Fluid	W_T/W_F	
	Spherical Tank	Cylindrical Tank
Hydrogen	9.0	12.0
Helium	4.5	6.0
Nitrogen	0.65	0.87
Carbon Dioxide (Liquid)	0.06	0.08

Specific strength (S/ρ) of tank material = 0.8×10^6 lbf/in/lbm

between the leaking propellants and the purging fluid is established quickly.

Orientation of purging fluid jets should be such that no ordered flow pattern is produced within the compartment. Instead, the initial energy of the jets should be allowed to dissipate through turbulence, resulting in a random flow pattern in which mixing is enhanced. In order to obtain the maximum amount of turbulent mixing, the fluid injection velocity should be as high as possible without creating damaging impingement loads on structures within the compartment.

If reasonably complete mixing is achieved, the concentration of propellant vapor within the compartment will be uniform, except in the immediate vicinity of the leak point. Early in the launch period, the concentration will vary according to the following relationship, assuming that the volumetric flow rates of propellant and diluent (purging fluid) are constant:

$$v_p = v_{po} e^{\frac{-t}{A}} + (1 - e^{\frac{-t}{A}}) \frac{\dot{V}_p}{\dot{V}_d + \dot{V}_p} \qquad (36)$$

where $A = V/(\dot{V}_d + \dot{V}_p)$

v_p = volume fraction of propellant vapor

v_{po} = initial volume fraction of propellant

$\dot{V}_d$ = volumetric flow rate of diluent

$\dot{V}_p$ = volumetric flow rate of propellant

V = compartment volume

t = time

If the time constant A is small compared to the time period during which combustion hazards are apt to occur, the propellant concentration will approach a steady value quickly which can be described simply:

$$v_p = \frac{\dot{V}_p}{\dot{V}_d + \dot{V}_p} \tag{37}$$

If the well-stirred purging method is employed, this condition will prevail since the flow rate of diluent will be large in order to avoid combustible mixtures. The diluent flow rate will be much greater than the propellant leak rate and can be written as:

$$\dot{V}_d = \frac{\dot{V}_p}{v_{pm}} \tag{38}$$

where v_{pm} = maximum propellant concentration (volumetric).

In terms of mass flow rates, the rate of diluent injection can be written as follows, assuming that the temperature of the propellant vapor is raised to that of the diluent during mixing:

$$\dot{w}_d = \frac{\dot{w}_p}{v_{pm}} \frac{M_d}{M_p} \tag{39}$$

where M_d = molecular weight of diluent

M_p = molecular weight of propellant

In the case of hydrogen, v_{pm} is equal to 0.04 which is the lower

flammability limit for this material. In the case of oxygen, the maximum concentration is 0.05 in the presence of hydrogen. The volumetric flow rate of diluent required is shown in Figure 24 as a function of propellant leak rate for dilution with helium or nitrogen. The tank weights for compressed gas storage as a function of volumetric flow rate of diluent (for a period of 100 seconds) is given in Figure 25. The combined weight of the purging fluid and storage tank is shown in Figure 26. For comparison purposes, it is estimated that the weight of a solid propellant gas generator would approach that required by the nitrogen purge system.

If the maximum propellant leak rate can be estimated, the purging system weight can be determined from Figure 26, assuming that the weight of incidental equipment (valves, controls, etc.) is negligible. It may be concluded that the well-stirred purging approach involves a weight penalty which may be high. If it is intolerably high, then the information presented here will form a reference in order to evaluate the effectiveness of other approaches to the problem.

b. Streaming System

In contrast to a well-stirred purging system, the operation of a streaming system is based upon the minimization of mixing of a leaking propellant with either the diluent or other propellants, and the rapid transport of propellant vapors to the vent locations. To be effective, the system requires an ordered flow pattern within the

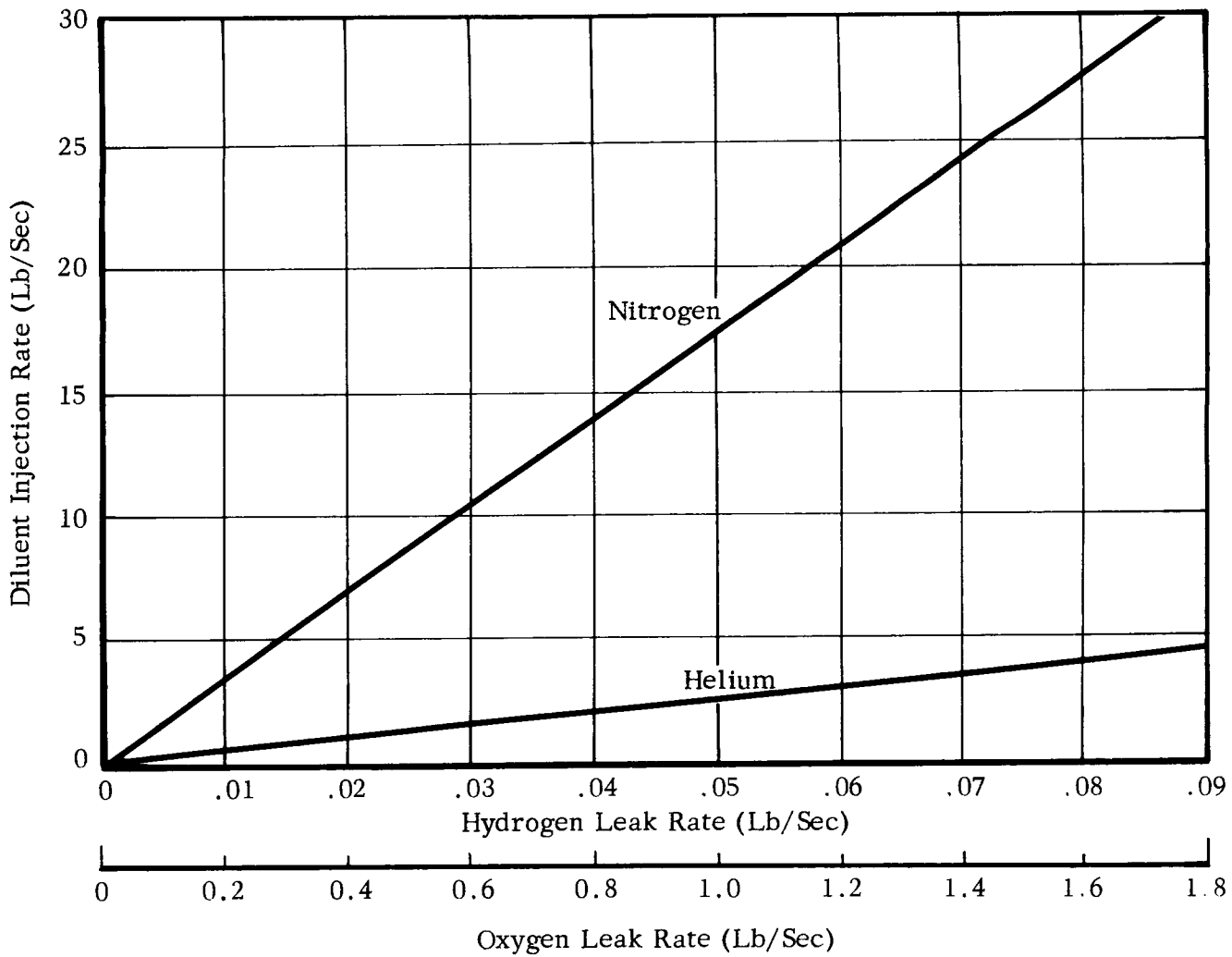

FIGURE 24 DILUENT INJECTION RATES REQUIRED IN WELL-STIRRED CASE

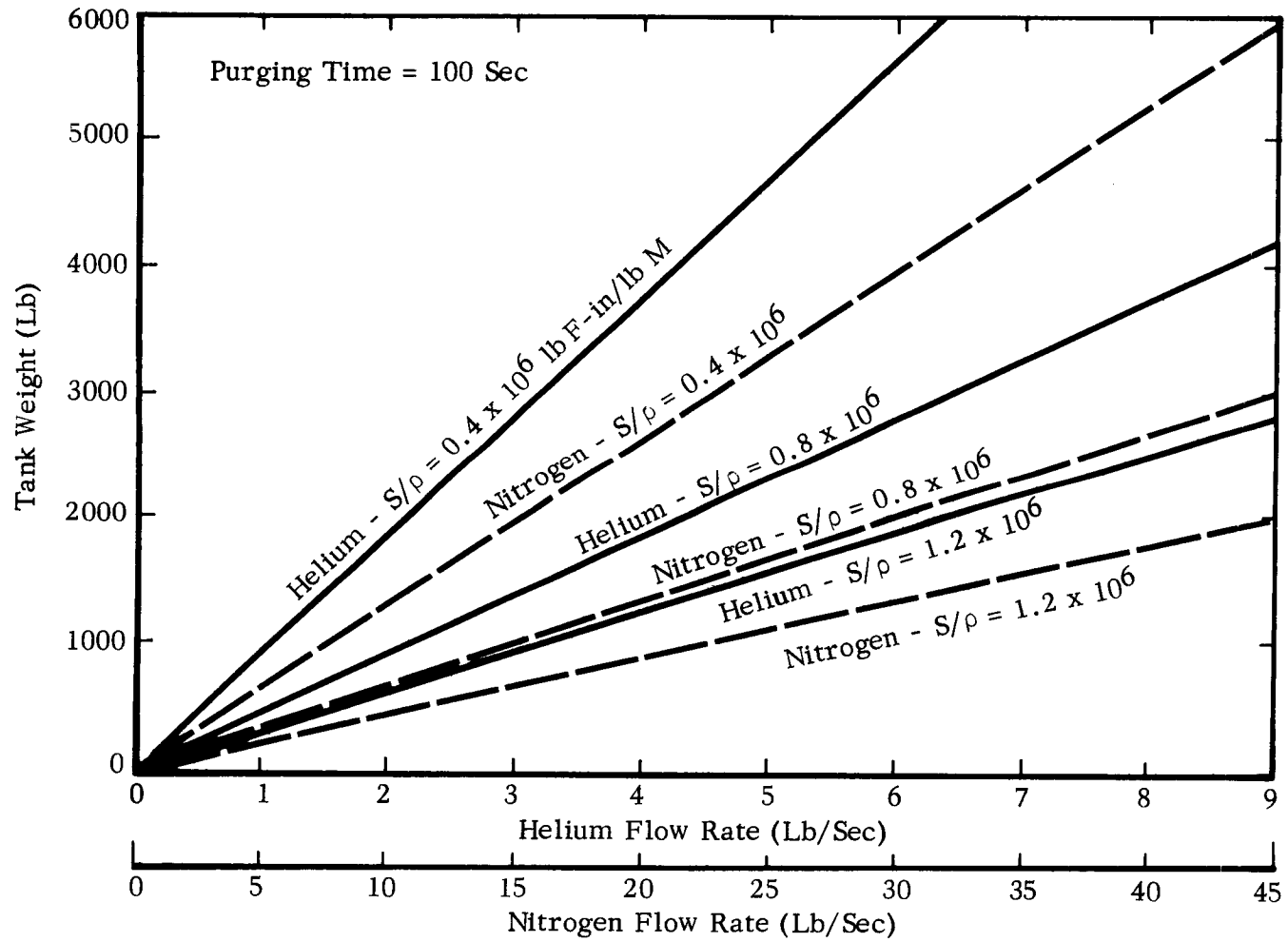

FIGURE 25 TANK WEIGHTS FOR COMPRESSED GAS STORAGE

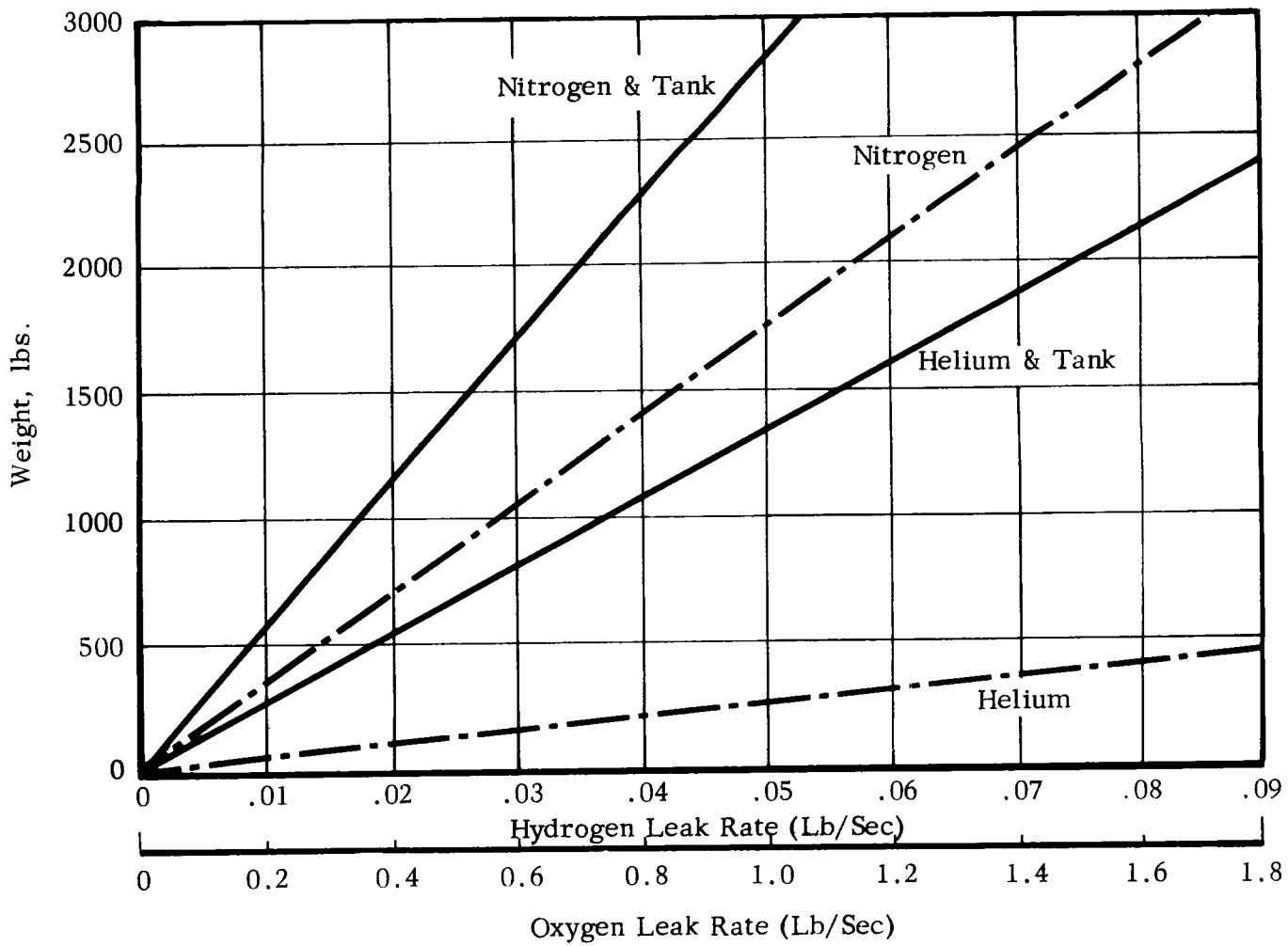

FIGURE 26 WEIGHT OF GAS STORAGE SYSTEM FOR PURGING HYDROGEN OR OXYGEN-- CONSTANT MASS FLOW OF DILUENT, WELL-STIRRED (100 SEC DURATION)

compartment and a low level of turbulence. If full advantage is taken of the relative positions of leak points and vent locations, and of buoyancy effects, the system should be more economical in terms of purging fluid requirements than the well-stirred approach.

The design of a streaming system must be based on the particular compartment configuration and the location of potential leaks. Only a few general remarks can be stated concerning the principles involved. In general, the diluent should be injected at low velocity, and possibly at a large number of points to establish the desired flow pattern. Buoyancy effects will differ depending upon the purging fluid used, and their analysis is complicated by differences in temperature. For example, if helium is used as a purging fluid, leaking hydrogen will be negatively buoyant initially and will become positively buoyant as its temperature rises. In this situation, it probably would be best to ignore hydrogen leakage and concentrate upon oxygen removal since the buoyancy of oxygen will be strongly negative at all times. This approach would require the vents to be located near the lower end of the compartment.

It would be difficult to estimate the quantity of purging fluid required with this type of system. The most reliable approach to determining the effectiveness of streaming in preventing combustible mixtures would be through the use of an experimental program. A model of the interstage compartment with appropriate gas-sampling devices could be used to establish the purging system design.

c. Convection System

The convection purging system is simply an extension of the streaming system where buoyancy effects alone are relied upon to remove propellant vapors. The approach is based upon flushing the compartment with a diluent prior to launching so that the initial propellant concentration is low. Through proper diluent selection and vent location, at least one of the propellants can be removed from the compartment. The primary mechanism of removal would be the differential effects of gravity and vehicle acceleration. However, the effect of decreasing pressure with altitude also would provide some sweeping action due to removal of diluent.

If helium were used as the diluent, oxygen would drop rapidly to the bottom of the compartment where it could be vented outboard. However, the accumulation of hydrogen at the top of the compartment might progress to the point where oxygen was leaking directly into a hydrogen atmosphere. This condition would be undesirable.

Alternatively, a heavy diluent fluid could be employed which would cause hydrogen to leave the top of the compartment. In this case, oxygen might accumulate near the bottom, but, in this position, it would not be in the vicinity of potential hydrogen leak points. In addition, the volumetric leak rate of oxygen is likely to be less than that of hydrogen.

The convective approach obviously would involve less of a weight penalty than purging techniques involving the use of storage fluids.

However, its effectiveness is questionable and could be established only by experiment. It would appear desirable to rely on convective purging only in instances where no additional weight can be tolerated.

B. Analysis of Aerodynamic Purging of Rocket Engine Components

1. Discussion

Aerodynamic purging of an engine compartment of a multistage rocket vehicle can be utilized to reduce explosion hazards due to propellant leakage. The mechanism by which hazards are reduced is the dilution of fuel vapors to concentrations below the lower or lean limit of flammability. With this mechanism, the leakage of oxidizer vapors contributes to the dilution process and does not create an additional hazard.

The analysis of the effectiveness of aerodynamic purging is difficult except under certain simplified conditions. The simplest condition to evaluate is the well-stirred case wherein the purging air is distributed throughout the compartment and the concentration of fuel vapor is uniform. This case is idealized but not unrealistic. If aerodynamic purging were utilized, the well-stirred condition would be desirable and effort should be directed toward achieving this condition. Otherwise, the accumulation of fuel vapor and the development of hazards would be dependent upon location of leaks and local flow conditions. If the location of a fuel leak is uncertain, aerodynamic purging cannot be depended upon to eliminate a hazard in an unstirred condition.

Therefore, it appears that a brief analysis of aerodynamic purging of a well-stirred compartment would be useful to establish the requirements and limitations of this approach to hazard reduction. In the analysis which follows, the following assumptions are made:

a. The volumetric influx of air is sufficient to replace the fluid in the compartment in a time which is short compared to the operating time of the rocket.

b. Incoming air is distributed such that the concentration of fuel vapor is uniform throughout the compartment.

c. The volumetric rate of fuel leakage is small compared to the volumetric influx of air.

d. The temperature of the fuel vapor is equal to that of the incoming air.

2. Analysis of Well-Stirred Case

Under the conditions stated above, the fuel concentration in the compartment will vary with time as follows:

$$\frac{d\nu_f}{dt} = \frac{1}{V}(\dot{V}_f - \dot{V}_e) \qquad (40)$$

where ν_f = volumetric fraction of fuel concentration

$\dot{V}_f$ = volumetric fuel leakage rate

$\dot{V}_e$ = volumetric exhaust rate

V = volume of engine compartment

t = time

The volumetric exhaust rate can be expressed as:

$$\dot{V}_e = \dot{V}_a + \dot{V}_f - \rho V \frac{d}{dt} \frac{1}{\rho} \tag{41}$$

where $\dot{V}_a$ = volumetric air intake rate

ρ = density

Under the assumption of a high purging rate, the last term of equation (41), which results from the change of pressure with altitude, is small compared with other terms of the equation.

Equation (40) then can be written as:

$$\frac{d\nu_f}{dt} + \frac{1}{V}(\dot{V}_a + \dot{V}_f)\ \nu_f = \frac{\dot{V}_f}{V} \tag{42}$$

and the solution of this equation is:

$$\nu_f \exp\int \frac{1}{V}(\dot{V}_a + \dot{V}_f)\, dt = \int \frac{\dot{V}_f}{V}\left\{\exp\left[\frac{1}{V}\int(\dot{V}_a + \dot{V}_f)\, dt\right]\right\} + C \tag{43}$$

Equation (43) can be simplified if the air and fuel flow rates can be expressed as functions of time. For this purpose, it is assumed that air is introduced into the compartment through scoops and the volumetric flow rate can be described as:

$$\dot{V}_a = aAU \tag{44}$$

where a = scoop effectiveness

A = scoop frontal area

U = flight velocity

where "a" is a constant accounting for failure of the scoop to capture an air stream equivalent to AU, and for reduction of the air velocity

in the boundary layer of the vehicle.

The programmed flight velocity of a typical vehicle is plotted in Figure 27 and can be expressed approximately as:

$$U = C_1 \, t^{1.5} \tag{45}$$

where $C_1 = 1.8 \text{ ft/sec}^{2.5}$

Therefore, the air flow rate can be written:

$$\dot{V}_a = C_1 \, a \, A \, t^{1.5} = C_2 \, t^{1.5} \tag{46}$$

where $C_2 = C_1 \, aA$

The fuel flow rate, on the other hand, cannot be represented by a simple expression. Assuming that the mass rate of fuel leakage remains constant, the volumetric flow rate will increase with altitude. However, during the initial period of flight, the rate of change of density of fuel vapor will be low, and, as will be shown below, the time dependent terms in equation (43) are important only during the initial period. Therefore, for purposes of this analysis it is justifiable to assume that both the mass and volumetric fuel flow rates are constant.

Making use of equation (45), equation (43) can be reduced to the following:

$$\nu_f = \nu_{fo} \exp\left[-\left(\frac{\dot{V}_a}{2.5} + \dot{V}_f\right) \frac{t}{V}\right] + \dot{V}_f \left\{1 - \exp\left[-\left(\frac{\dot{V}_a}{2.5} + \dot{V}_f\right) \frac{t}{V}\right]\right\} \tag{47}$$

where ν_{fo} = initial fuel concentration (volume fraction)

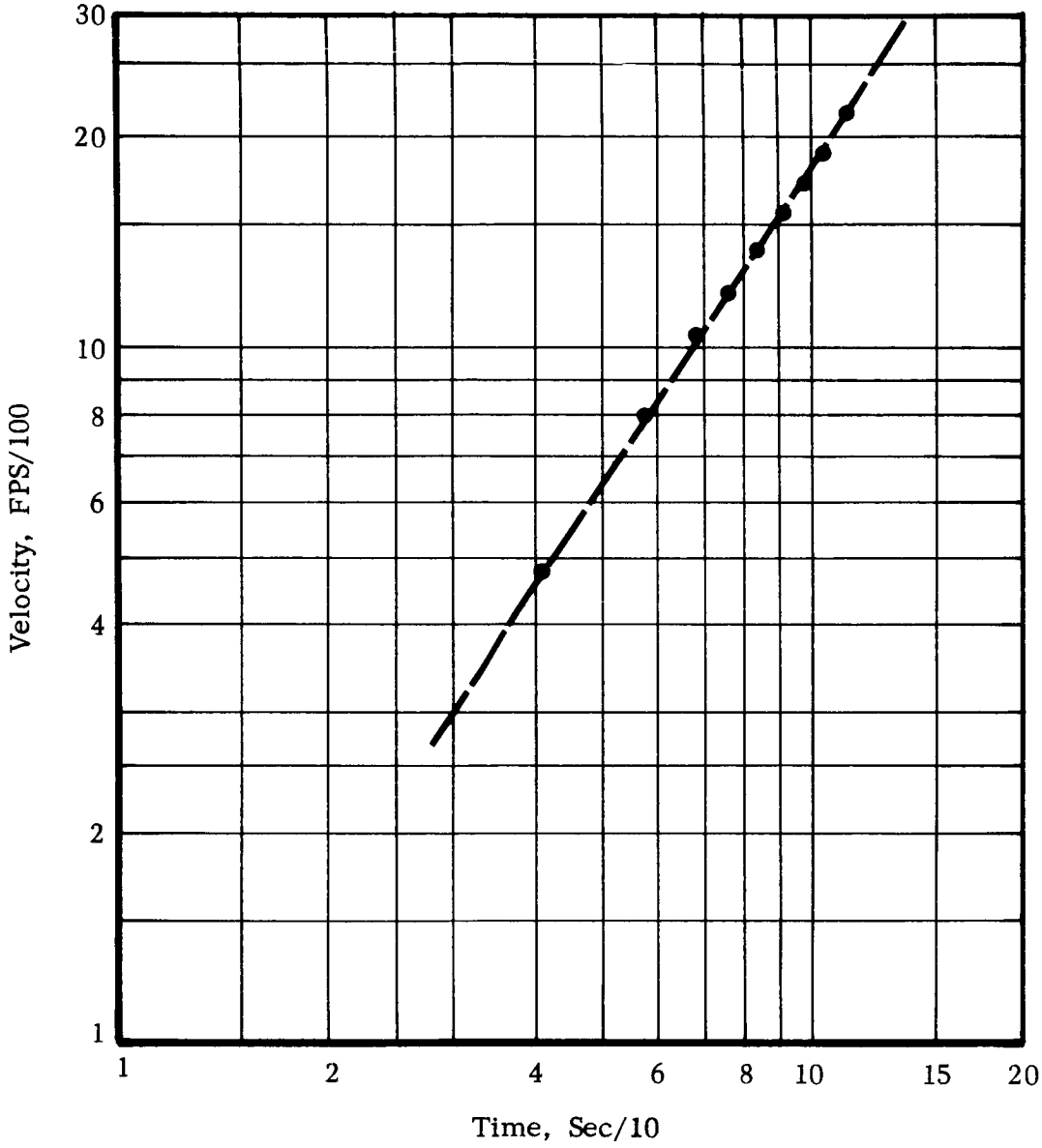

FIGURE 27 FLIGHT VELOCITY OF TYPICAL VEHICLE

The first term on the right of equation (47) represents the sweeping away of the fuel vapor present at time zero. If the fuel leakage rate is zero, this term indicates the decay of fuel concentration with time. However, if a finite fuel leakage rate exists, the second term dominates after a short period of time. In fact, as soon as the air flow rate becomes substantial, that is:

$$\dot{V}_a >> \dot{V}_f \tag{48}$$

and

$$\frac{\dot{V}_a t}{V} > 2.5$$

then the fuel concentration reduces simply to the ratio of the flow rates of fuel to air, as might be expected intuitively:

$$\nu_f \cong \frac{\dot{V}_f}{\dot{V}_a} \tag{49}$$

The volumetric fuel flow rate can be expressed in terms of the mass leakage rate as follows:

$$\dot{V}_f = \frac{\dot{W}_f \; R \; T}{P \; M_f} \tag{50}$$

where M_f = molecular weight of fuel

$\dot{W}_f$ = weight rate of fuel leakage

R = gas constant

T = temperature

P = pressure

so that by combining equations (44), (49), and (50), the following expression is obtained for fuel concentration during flight:

$$\nu_f \cong \frac{R \ \dot{W}_f}{a \ A \ M_f} \ \frac{T}{PU} \tag{57}$$

With a constant mass rate of fuel leakage, it is observed that fuel concentration varies with the factor T/PU. The variation of this factor for a typical vehicle launched through a standard atmosphere is indicated in Figure 28, which shows the variation of fuel concentration with altitude. The concentration remains relatively constant at altitudes between 10,000 and 30,000 feet. At lower altitudes, the concentration may be higher or lower, depending upon the concentration at time zero. At higher altitudes, the concentration rises rapidly, indicating a reduction in effectiveness of aerodynamic purging.

The scoop area required to achieve adequate purging can be calculated by rearranging equation (51) as follows:

$$\frac{A}{\dot{W}_f} \cong \frac{R \ T}{a \nu_f \ M_f \ P \ U} \tag{52}$$

If the scoop effectiveness "a" is assumed to be unity and the desired fuel concentration is 0.04 (lower flammability limit of hydrogen in air), the scoop area required for altitudes up to 30,000 feet is approximately 10 square feet for a leak rate of 1 lb/sec of hydrogen vapor. The volumetric flow rate of air through the compartment, calculated by means of equation (44), would be approximately 5000 ft^3/sec at an altitude of 10,000 feet. The addition of a scoop

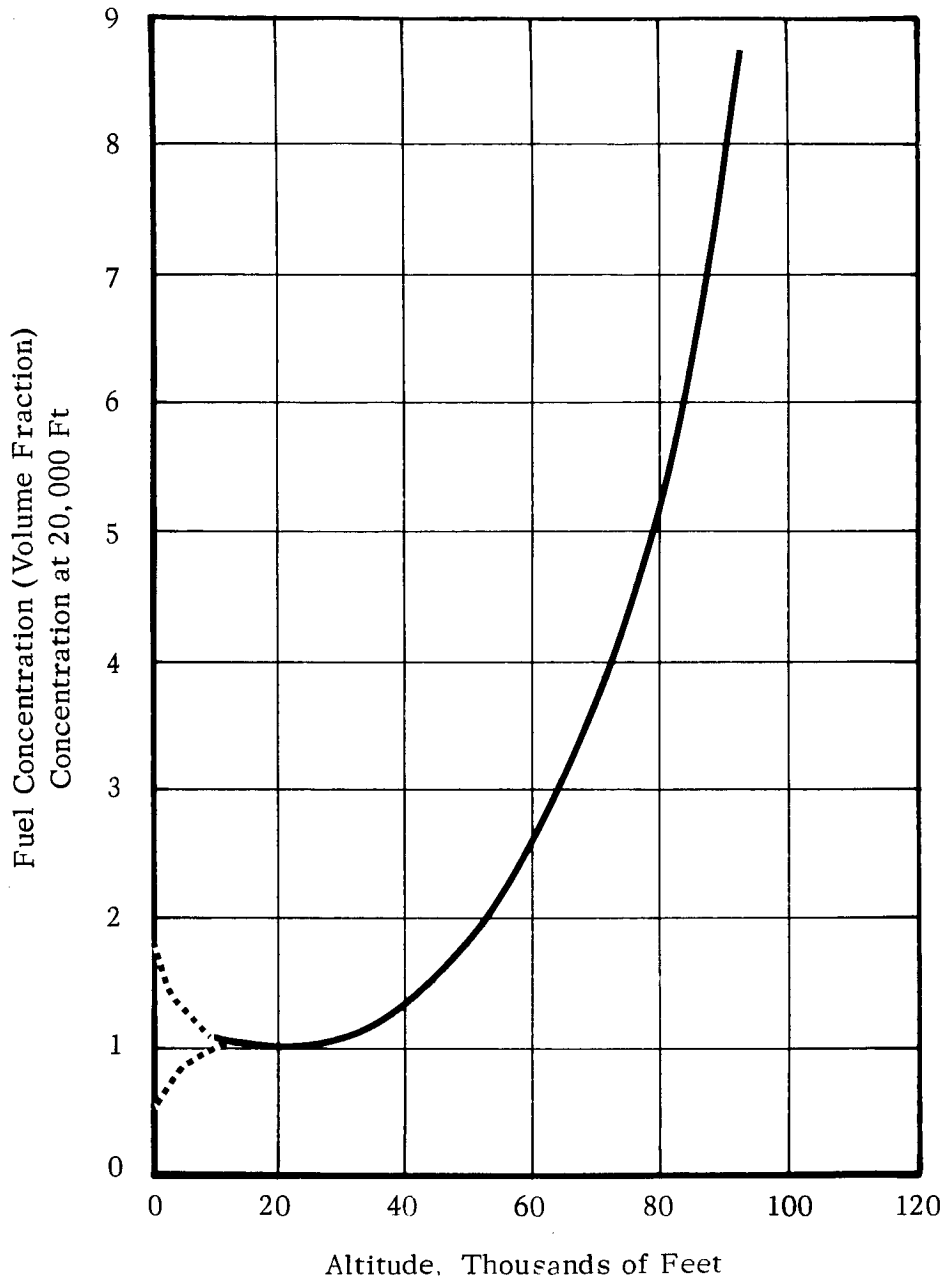

FIGURE 28 TYPICAL VEHICLE FUEL CONCENTRATION IN INTERSTAGE WITH AERODYNAMIC PURGING

with a 10 square foot frontal area to a typically large vehicle should not increase the aerodynamic drag significantly. This area is small compared to the total frontal area of the vehicle, and, if the scoop effectiveness "a" is near unity, the drag force created will be small.

3. Effects of Non-Uniform Fuel Distribution

In the previous section, a brief analysis was carried out of the effects of aerodynamic venting in a well-stirred compartment. However, it is obvious that a uniform fuel concentration cannot be maintained throughout the compartment, no matter what means are used to promote mixing. In particular, high fuel concentrations will exist at the site of each leak from the system. The concentration will be highest at the leak and will fall off with distance in all directions due to diffusion of fuel into the surrounding medium. Thus a certain volume surrounding the leak will contain a combustible mixture, if air is used as the venting fluid. The magnitude of this volume will be determined by the rate of fuel leakage and the rate of diffusion into the surrounding air.

In attempting to determine the extent of the volume of combustible mixture formed, the air velocity past the leak must be taken into account, since it will affect the diffusion process. Sources of thermal energy moving through a conducting medium have been analyzed [39] and a relation has been established for the temperature distribution in the medium:

$$T = \frac{\dot{q}}{4\pi Kr} \exp\left[-\frac{U_s}{2\alpha}(r - x)\right] \tag{53}$$

where $\dot{q}$ = thermal energy source strength

K = thermal conductivity

U_s = velocity of source through fluid

α = thermal diffusivity

r = radius from source

x = distance in downstream direction from source

Analagously, an expression can be written for the diffusion of mass from a source moving through a fluid (or for a fixed source in a moving fluid):

$$\rho_f = \frac{\dot{W}_f}{4\pi Dr} \exp\left[-\frac{U_s}{2D}(r - x)\right] \tag{54}$$

where ρ_f = partial density of fuel

D = mass diffusivity

In the present case, it would be difficult to utilize this relation to predict fuel concentration profiles since the true value of the diffusion coefficient D is unknown. Coefficients have been established for purely molecular diffusion in non-moving fluids. However, in moving fluids, the existence of turbulence can increase the rate of diffusion by a large factor. The use of a molecular diffusion coefficient would be overly conservative. Results from mixing experiments could be used to estimate diffusion coefficients. However, the accuracy of results obtained in this manner would be poor since the flow conditions at the leak location cannot be predicted.

On the other hand, it is possible to draw useful qualitative conclusions from relationships for mass diffusion. From equation (53) it is observed that, if the fluid velocity is zero, a surface of constant concentration is a sphere. If the concentration of interest is the lowest flammability limit, then the combustible mixture produced by a leak will occupy a spherical volume with the leak site at the center.

If the surrounding fluid is in motion, it is observed from equation (54) that the distance r from the source to the concentration boundary is reduced in all directions, except the downstream direction x. In the direction of flow x, the distance r does not change with velocity. If, in addition, the velocity of the fluid is accompanied by turbulence, the diffusion coefficient will be increased. The increased rate of diffusion will cause the concentration boundary to move closer to the source. Therefore, it can be concluded that the effect of fluid velocity, in general, is to reduce the volume of the combustible mixture.

4. Conclusions

It is concluded from this analysis that aerodynamic venting can be used to reduce the hazards associated with fuel leakage in engine compartments of multistage rocket vehicles. It is unlikely, however, that such hazards can be eliminated completely by aerodynamic venting alone.

The effectiveness of aerodynamic venting is dependent upon the

rate of mixing of the incoming air with the fuel vapor. It appears that the greatest effectiveness will be achieved by maintaining high flow velocities through the compartment so that large volumes of combustible mixtures cannot accumulate near the site of the leakage. High velocities might be achieved by using a small number of large scoops with the incoming streams directed toward the fuel feed system, rather than using a finely divided distribution system.

It appears that the addition of air scoops of the required size would have a negligible effect on the flight performance of the vehicle.

C. Interstage Venting Requirements

1. General

Vents are incorporated in all current launch vehicle interstages to maintain a small pressure differential across the interstage skirt. In most cases, gas is relieved through the vents as ambient pressure is reduced with altitude at a rate that will provide a small positive pressure of the inert gas within the interstage. In general, the vents have not been designed on the basis of reducing the effects of explosions that might occur.

In some instances, careful control of the venting of the inert gas must be maintained so that the pressure in the interior balances the aerodynamic forces acting on the outer surfaces of the interstage (e.g., S-II/S-IV interstage). In all cases, if the vent area is very large, aerodynamic effects may be detrimental to the performance of the vehicle during the early phases of flight.

Venting to reduce the effects of explosions must then operate

within the confines of the required pressure balance across the interstage skirt and the maintenance of positive pressure of the inert gas to prevent air from entering the system. These limits will vary with interstage design and flight regime.

Venting to reduce the effects of explosions on interstage structures is only effective when deflagrations rather than detonation occur. Since detonation wave velocities are many times the speed of sound in the unreacted mixture, there will be no gas vented as the result of a pressure increase caused by detonation until the wave front reaches the vent. By this time, the major structures may have received the full force of the detonation wave. Vents may reduce the intensity of the detonation, in some instances, however, through the relief provided during the interval of time that combustion takes place prior to the transition to detonation. The severity of the wave will be reduced by the fact that the unreacted gas will be at a lower pressure during the propagation of the wave. By keeping the pressure low, the probability of transition to detonation will also be reduced.

2. Venting Requirements--Deflagrations

The venting requirements for reducing the effects of explosions produced by a deflagration process are difficult to define since the inability to predict flame propagation rates and the pressure and temperature distribution within the interstage during the combustion process limits the effectiveness of analytical techniques. No useful experimental data on the effect of venting on the characteristics of

explosions produced by hydrogen and oxygen reactions could be found in the literature. However, in order to provide some insight as to the effectiveness of venting, a simplified analysis has been made for the relatively severe case where the interstage is completely filled with a stoichiometric gas phase mixture.

By suitable use of the ideal gas law (applied to the reactants and products) it can be shown that the rate of outflow of gas, dm/dt required to limit the pressure to some specified value, P_e at time t is:

$$\frac{dm}{dt} = \left[\frac{T_e}{T_i}\,\frac{P_i}{P_e}\,\frac{M_e}{M_i} - 1\right]\frac{P_e}{P_i}\,\frac{dm_i}{dt} \qquad (55)$$

where T_e = temperature of the product gases

P_i = pressure of the reactants

M_e = number of moles of products

M_i = number of moles of reactants

$\frac{dm_i}{dt}$ = number of moles of reactants, reacting per unit time

This relationship assumes that the pressure is uniform throughout the interstage at any given time and that the temperature of the unreacted gas is maintained at its initial value. Only unreacted gas is vented.

It also may be shown that the rate at which the gas reacts is

$$\frac{dm_i}{dt} = \frac{S_u\,A_b\,\rho_i}{\bar{M}_i} \qquad (56)$$

where S_u = flame velocity

A_b = area of the flame front

ρ_i = density of the reactants

$\bar{M}_i$ = mean molecular weight of the reactants

The required rate of relief may then be expressed as

$$\frac{dm}{dt} = \left[\frac{T_e}{T_i} \frac{P_i}{P_e} \frac{M_e}{M_i} - 1\right] \frac{P_e}{P_i} \frac{S_u A_b \rho_i}{M_i} \tag{57}$$

When the initial pressure is relatively high (i.e., near sea level conditions), the pressure in the interstage may reach the limiting pressure shortly after the deflagration is initiated and P_e may be set equal to P_i. Also, since at the lower altitudes, the ratio of the pressure in the interstage, P_e, to ambient pressure will be low, the flow through the vent will be subsonic and the realtionships for incompressible flow may be used. That is

$$\frac{dm}{dt} = \frac{C_c A_v}{M} (2 \rho_i \Delta P)^{\frac{1}{2}} \tag{58}$$

where A_v = cross-sectional area of the vent

$\Delta P = P_e - P_i$

C_c = contraction coefficient

Substituting this expression in equation (57), the ratio of vent area to flame area for a given limiting interstage pressure is as follows:

$$\frac{A_v}{A_b} = \left[2/3 \frac{T_e}{T_i} - 1\right] \frac{S_u}{C_c} \left(\frac{\rho_i}{2 \Delta P}\right)^{\frac{1}{2}} \tag{59}$$

When the initial pressure is low (at higher altitudes), a large portion of the gas may burn before P_e is reached; hence $P_e \neq P_i$. Also, the ratio of internal to external pressure will be high and sonic flow will occur. Using the expressions for choked flow and equation (57), it can be shown that the ratio of vent area to flame area required for a pressure P_e is

$$\frac{A_v}{A_b} = 0.0227 \left[2/3 \frac{T_e}{T_i} \frac{P_i}{P_e} - 1 \right] \left[\frac{T_e}{T_i} \right]^{\frac{1}{2}} \frac{S_u}{\sqrt{T_i}} \qquad (60)$$

Vent areas that will provide the degree of effectiveness implied by these relationships may be derived for specific launch vehicles by setting a maximum value for the flame area equal to the interior surfaces of the interstage.

On setting a value for the maximum allowable pressure differential across the interstage skirt equal to $P_e - P_i$, a value for the flame temperature, and by assuming values for the initial temperature and pressure of the unburned gas, estimates of the vent area ratios may be made. This has been done for the S-IC/S-II interstage, as an example, using the following values:

$P_e - P_i = 2$ psia

$T = 530^{\circ}R$

$P_i \begin{cases} = 1 \text{ atm.} \\ \quad 1 \text{ psia} \end{cases}$

$T_e = 4500^{\circ}R$

For the sea level case ($P_i = 1$ atm) using equation (59), the ratio of $\frac{A_v}{A_b}$ turns out to be 0.3, whereas at low pressures

(P_i = 1 psia) utilizing equation (60) the ratio is 0.16. Taking A_b equal to the surface area described by the maximum diameter and length of the interstage, the vent area for a ratio (for the worst case) of 0.3 would be of the order of 1000 ft^2. This may be compared with the vent area of 3 ft^2 that is currently employed in the vehicle.

An increase in the vent area by the proportion indicated for the S-IC/S-II interstage could add to the explosive hazard by markedly increasing the likelihood that air would enter the system. Also, since this vent area would occupy more than 40 per cent of the skirt area, adverse effects resulting from aerodynamic loadings may be unduly severe.

Blowout panels that would be forced from the vehicle as a result of the increased pressure applied during the early phases of the explosion would help to avoid these problems. However, they will recur after the panels have been removed unless this action takes place at altitudes well above the point where the maximum aerodynamic forces (maximum Q) on the vehicle are created.

Since there will be some benefit achieved through an increase in vent area at the higher altitudes, it would appear desirable to provide a means of automatically increasing the vent size at a point in flight where the aerodynamic effects no longer play a major role. At altitudes less than this, the utilization of blowout panels, or increased vent area, would not appear to be good practice.

D. Compartmenting

The severity of both deflagrations and detonations is dependent

upon the quantity of explosive mixture that reacts. This suggests that improvements may be derived by using compartments within the interstage to limit the quantity of reactants that may accumulate as the result of a leak. One approach would be to fill the entire space with an easily removable low density material. An example of this technique would be the incorporation of nonporous plastic spheres of a few inches in diameter. Spaces between the spheres would allow the leaked gases to vent.

The weight introduced by the filling material will be much greater than can be allowed in most launch vehicles. If a very light-weight material such as double free expanded polystyrene beads were used, the lowest density achievable would be of the order of 1/2 to 1 pound per ft^3. For a free volume of 15,000 ft^3, as in the S-IC/S-II interstage, this would represent some 8 to 15 thousand pounds.

If, on the other hand, the interstage were divided into individually vented but separate compartments through the use of light-weight membranes, for example, the added weight might be significantly reduced. A large fraction of the free volume where there is no source of hydrogen nor oxygen leakage would not have to be compartmented. A membrane separating this space from areas where leakage may occur would suffice. In those spaces where leakage can occur, the compartment volumes would have to be similar to or smaller than the volumes of gas defined by the establishment of minimum leakage rates for detonation. This turns out to be a volume represented by a sphere of less

than one foot in diameter. This is so small that it would not be very different than providing separate enclosures around each potential source of leakage. This would essentially involve leakage control which is considered to be beyond the scope of this work.

In conclusion, it appears that the addition of compartments to the interstage to reduce the effects of an explosion is not practical. Either the system will weigh too much or the compartments will approach the dimensions of systems that would be better considered as leak control devices.

E. Hardening of Interstage Structures

The interstage skirt will be the component which is most susceptible to blast damage from a hydrogen-oxygen gas phase detonation. The dimensions of the skirt are large and therefore its weight is not negligible. Thickening the panel would represent a large additional mass to the missile system which would constitute a severe operational penalty. Therefore, the conclusion is drawn that hardening of major components is not recommended. Conversely, smaller components, even if they represent structures such as the heat shield, could be brought up in strength without great weight penalties. Honeycomb structures with stronger restraints might easily be incorporated. However, this hardening procedure would provide little benefit to the over-all ability of the interstage to survive detonation.

F. Prevention of Accumulated Condensed Phase Mixtures

If escaping liquid hydrogen and oxygen impinge upon a concave

surface at a sufficient rate and duration, the surface may be cooled to the extent that a condensed phase mixture would collect. The accumulation of the condensed phase mixture could present a destructive hazard.

This hazard may be reduced by the elimination of small concave surfaces that are capable of being cooled rapidly and that would tend to collect the condensed fluids. Larger surfaces with more heat capacity would, in general, require higher leakage rates before sufficient cooling was achieved for the deposit of the liquids or solids. It is recommended, however, that consideration be given to the addition of heat to those critical surfaces in the interstage where the condensed phase may collect.

G. Intentional Ignition Sources

It has been shown that the severity of an explosion of hydrogen and oxygen (or air) is highly dependent upon the quantity of reactive mixture that is present when ignition occurs. The quantity of material that could accumulate at the time of ignition could theoretically be reduced by the use of an ever present ignition source such as pilot flames, hot wires, etc.

To be effective these ignition sources must be placed in a manner that will insure early ignition. If not, the sources may increase the explosion hazard by providing an ignition source after a considerable quantity of combustible material has accumulated when no other ignition source is present.

Because of the difficulty of predicting the location where flammable mixtures may occur, it has been concluded that with present knowledge the design of an intentional ignition system cannot be achieved with sufficient probability that it will not cause a delayed (and destructive) ignition. The use of intentional ignition sources is not recommended.

H. Weight Comparison of Control Techniques

Of the various techniques for the elimination and control of explosions in an interstage the well-stirred, inert purging case is the only method amenable to a weight analysis that is applicable to interstagesin general. The comparative weights as a function of leakage rate are given in Figure 26.

Other purging techniques involving aerodynamic and inert with other types of mixing require either experimental effort or involve factors related to a specific vehicle design in order to establish weight as a function of effectiveness. This is also true of venting techniques. Other control methods are either not recommended or have a relatively small influence on weight.

VII. RECOMMENDATIONS FOR ADDITIONAL WORK

It has become evident in this study that additional experimental and analytical data would add significantly to the evaluation of explosive hazards in vehicle interstages and would form the basis for better decisions as to the optimum means of prevention and control of explosions. As knowledge is increased, the precautionary measures that have to be taken should impose less severe penalties and provide a lighter, less complex system.

Additional effort in the following areas is recommended.

A. The Impulsive Loading of Detonation Waves--Analytical

It is recommended that the calculation of impulse due to the reflection of a detonation wave on surfaces of various geometries be refined. In particular, the effects of walls of various curvatures and converging passages need further study for, in some cases, they may result in more severe loadings than those evaluated in this study.

The effect of diluents on the state and flow properties at the detonation front for a reflected wave also requires further evaluation.

Calculations using the methods presented in this report would be applied. However, it is recommended that a computer be used to provide a means of obtaining a network of information that would incorporate, in parametric form, all of the major factors that govern the loading effects of detonations within an interstage.

B. The Impulsive Loading of Detonation Waves-- Experimental

Estimates of pressure loading on structures by detonation waves has been primarily determined by analytical means. An experimental program is recommended for verifying and supplementing these efforts. This program would involve the initiation of detonations in various mixtures of interest contained in vessels of various configurations. Careful measurement of pressure and velocity would provide basic data that would be necessary for the verification of the analytical estimates.

C. Response of Structures to Detonations

A hydrogen-oxygen (diluent) gas phase detonation imposes a diffraction or drag load on a structure that is quite different in nature than that from the more thoroughly analyzed free air blasts. In this program analytical predictions of the blast effects occurring as the result of direct impingement of the detonation wave on the structure have been made. Dynamic structural analyses based on theoretical load inputs have been carried out.

It is believed that an experimental correlation is in order for the verification of these analyses. Elementary structural components, beams and supported plates should be exposed to laboratory controlled gas phase detonations. The response of the structures would be measured and compared to the predicted dynamic stress levels.

D. Transition from Deflagration to Detonation

Theory and experimental data that has been generated to date are insufficient to allow a prediction to be made as to whether a detonation will occur when a detonable mixture is formed in an interstage. It is known that there will be a distance of travel of the deflagration wave before transition to detonation takes place. This distance has been defined experimentally for relatively simple configurations. It is impossible to relate the results of these experiments to the complex geometry of an interstage. Furthermore, induction distances at reduced temperatures and pressures have not been well established.

It is realized that complete simulation of the various conditions that may prevail in an interstage would be extremely difficult. Tests with simplified models that produce more severe conditions for transition would aid immeasurably in defining the real hazards of detonation.

E. Venting

The use of enlarged vents or blow out panels appear to offer some utility particularly after the vehicle has passed through the regime of severe aerodynamic loading. There is little or no experimental data on the effect of vents on gas phase explosions. It has been pointed out that vents offer the possibility of reducing the probability of occurrence of detonations and would reduce the pressures produced by deflagrations. It is expected that an experimental program to establish the benefits of venting (or blow out panels) would provide the impetus necessary for the design of a system that would allow the use of enlarged vents through the entire flight regime. This program would again entail the initiation

of explosive mixtures at various temperatures and pressures. The effect of various vents and blow out panels would be evaluated in terms of the pressures produced.

F. Purging

The benefits of purging either with inert gases or aerodynamically have been pointed out in this study. Experimental effort is required, however, to further refine the estimates of the mixing that can be achieved. Flow experiments in simulated scale models of portions of typical interstages are recommended.

G. Condensed Phase Reactions

There is a severe lack of basic information on the formation of condensed phase mixtures in an interstage and on the explosive hazards that they may create. Experimental effort related to the formation of condensed phase mixtures, their ignition and propagation and the pressure loadings that would be produced is badly needed. It is understood that a program of this type is currently being implemented and is under the sponsorship of the George Marshall Space Flight Center.

REFERENCES

1. Lewis, Bernard and vonElbe, Guenther, "Combustion Flames and Explosions of Gases," Second Edition, Academic Press, New York, 1961.

2. Jensen, C.L. and Berlin, E.D., "Hydrogen-Oxygen Combustion Tests in a Large Chamber - Interim Report No. 1," Convair/Astronautics, 8 March 1962, Contract AF 18(600)-1775.

3. Skinner, G.B., "Survey of Chemical Aspects of Flame Extinguishment," Monsanto Research Corp., ASD Technical Report 61-408.

4. Taylor, G.I. and Tankin, R.S., "Gas Dynamical Aspects of Detonation - High Speed Aerodynamics and Jet Propulsion," H.W. Emmons, Editor, Princeton University Press, Princeton, N. J.

5. Lewis, B., Pease, R.N., Taylor, H.S., "Combustion Processes, High Speed Aerodynamics and Jet Propulsion, Vol. II," Princeton University Press, 1956.

6. Grass, R.A., Oppenheim, A.K., "Recent Advances in Gaseous Detonation," ARS Journal, 29, 173-179, (1959).

7. Bollinger, L.E., Edse, R., "Thermodynamic Calculations of Hydrogen-Oxygen Detonation Parameters for Various Initial Pressures," ARS Journal, 31, 251-256, (1961).

8. Jost, W., Just, Th. and Wagner, H. Gg., "Investigation of the Reaction Zone of Gaseous Detonations," Eighth Symposium on Combustion, Williams and Wilkins Company, Baltimore, Maryland, 1962, pp 582-588.

9. Zeleznik, F.J., Gordon, S., "Calculation of Detonation Properties and Effect of Independent Parameters on Gaseous Detonations," ARS Journal, 32, 606-615, (1962).

10. Zel'dovich, Ia.B., Kogarko, S.M., and Simonov, N.N., "An Experimental Investigation of Spherical Detonation of Gases," Zhurnal Tekhnicheskoi Fiziki, Vol. 26, No. 8, 1956, 1744-1768. Translated in Sov. Phys. - Tech. Phys. Vol. 1, No. 8, August 1953, pp 1689-1713.

11. Fay, J.A., "Some Experiments on the Initiation of Detonation in $2H_2$-O_2 Mixtures by Uniform Shock Waves," Fourth Symposium on Combustion, Williams and Wilkins Company, Baltimore, Maryland, 1953, pp 501-507.

12. Berets, D.J., Greene, E.F., and Kistiakowsky, G.B., "Gaseous Detonations II Initiation by Shock Waves,: Journal of American Chemical Society, Vol. 72, 1950, pp 1086-1091.

13. Steinberg, M., Kaskan, W.E., "The Ignition of Combustible Mixtures by Shock Waves,: Fifth Symposium on Combustion, Rheinhold Pub. Co., New York, 1955, pp 664-672.

14. Richmond, K.H., "Spectrophotometric Analysis of Detonation Wave Structure," Detonation and Two-Phase Flow - Academic Press, New York, 1962.

15. Arthur D. Little, Inc., "Final Report on an Investigation of Hazards Associated with the Storage and Handling of Liquid Hydrogen," Contract No. AF 18(600)-1687, March 22, 1960. (C)

16. Arthur D. Little, Inc., "Final Report on an Investigation of Hazards Associated with the Storage of Liquid Hydrogen in Close Proximity to Liquid Oxygen and RP-1," Contract No. AF 18(600)-1687, July 15, 1960. (C)

17. Markels, M., Jr., "A Program to Advance the Technology of Fire Extinguishment (Hydrogen-Oxygen)," Atlantic Research Corporation ASD Technical Documentary Report ASD-TDR-62-526, Part II, March 1, 1963.

18. Litchfield, E.L., Hay, M.H., and Forshey, D.R., "Direct Electrical Initiation of Freely Expanding Gaseous Detonation Waves," Ninth Symposium on Combustion, Academic Press, New York, 1963, pp 282-286.

19. Laffitte, P., and Bouchet, R., "Suppression of Explosion Waves in Gaseous Mixtures by Means of Fine Powders," Seventh Symposium on Combustion, Buttersworth Sci. Pub., London, 1959, pp 504-508.

20. Laderman, A.J., Urtuw, P.A., and Oppenheim, A.K., "On the Generation of a Shock Wave by Flame in an Explosive Gas," Ninth Symposium, pp 265-273.

21. Laderman, A.J., and Oppenheim, A.K., "Initial Flame Acceleration in an Explosive Gas," Proceedings of the Royal Society, Vol. 268, pp 153-180, 10 July 1962.

22. Brinkley, S.R., and Lewis, R., "On the Transition from Deflagration to Detonation," Seventh Symposium on Combustion, Buttersworth Sci. Pub., London, 1959, pp 807-811.

23. Salamandra, G.D., Bazhenova, T.V., and Naboko, I.M., "Formation of Detonation Wave During Combustion of Gas in Combustion Tube," Seventh Symposium on Combustion, Buttersworth Sci. Pub., London, 1959, pp 851-855.

24. Laderman, A.J., and Oppenheim, A.K.,"Influence of Wave Reflections on the Development of Detonation," The Physics of Fluids, Vol. 4, pp 778-782 (1961).

25. Bollinger, L.E., Fong, M.C., and Edse, R., "Experimental Measurements and Theoretical Analysis of Detonation Induction Distances," ARS Journal 31, pp 588-594 (1961).

26. Evans, M.W., Given, F.I., and Richeson, W.E., "Effect of Attenuating Materials on Detonation Induction Distances in Gases," J. Appl. Phys., Vol. 26, No. 9, September 1955, pp 1111-1113.

27. Bollinger, L.E., Fong, M.C., Laughrey, J.A., and Edse, R., "Experimental and Theoretical Studies on the Formation of Detonation Waves in Variable Geometry Tubes," National Aeronautics and Space Administration, Technical Note D-1983, June 1963.

28. Seamans, T.F., and Wolfhard, H.G., "Detonation and Suppression of Detonation in Fuel-Air Mixtures at Elevated Pressures," Fire Research Abstracts and Reviews, 4, January and May 1962, pp 92-105.

29. Belles, F.E., "Detonability and Chemical Kinetics: Prediction of Limits of Detonability of Hydrogen," Seventh Symposium on Combustion," Buttersworth Sci. Pub., London, 1959, pp 745-751.

30. Gordon, W.E., Mooradian, A.J., and Harper, I.A., "Limit and Spin Effects in Hydrogen-Oxygen Detonations," Seventh Symposium on Combustion, Buttersworth Sci. Pub., London, 1959, pp 752-759.

31. Patch, Richard W., "Prediction of Composition Limits for Detonation of Hydrogen-Oxygen-Diluent Mixtures," ARS Journal, 31, pp 46-51 (1961).

32. Laderman, A.J., Jako, C., and Williams, G.T., "Study of Detonation of Mixtures of Gaseous Hydrogen and Gaseous Oxygen," Space Science Laboratory, University of California, Annual Progress Report, August 8, 1963, Contract NAS8-2634.

33. Taylor, G.I., "The Dynamics of the Combustion Products Behind Plane and Spherical Detonation Fronts in Explosives," Proc. Roy. Soc. A, 200 (1949-1950), pp 235-247.

34. Timoshenko, S., Woinowsky-Krieger, S., "Theory of Plates and Shells," McGraw-Hill Book Co., Inc., Second Edition, 1959.

35. Correspondence from G.A. Kroll, George Marshall Space Flight Center, Letter dated August 27, 1963.

36. Internal Memorandum, M-AERO-A-89-63, George Marshall Space Flight Center, August 28, 1963.

37. MIL-HDBK-5, "Metallic Materials and Elements for Flight Vehicle Structures."

38. Rocket Research Corp., "Sublex Gas Generator," Letter from Rocket Research Corp., Seattle, Washington.

39. Eckert, ER.G., and Drake, R.M., Jr., "Heat and Mass Transfer," McGraw-Hill, New York, 1959, p 113.

APPENDIX A

A. Gas Dynamics of Spherical Detonation

The requirements for initiating a spherical detonation wave are more demanding than for cylindrical or plane detonation. Energy must be supplied to support the radially diverging detonation out to radii which are much larger than the thickness of the reaction zone. When the radius of curvature becomes large compared to the thickness of the reaction zone, the detonation wave can be expected to have essentially the same properties as those of a plane wave. A study of the energy required for initiation was made by Zel'dovich.[1] Besides deriving the energy requirement, he conducted experiments in which he (a) observed spherical detonation waves, (b) measured the energy required for their initiation, and (c) obtained good agreement with theory.

Spherical detonation has been observed in the past, both in gaseous[1,2] and in solid[3] media.

1. Assumptions

In analyzing the behavior of the burnt products of detonation, we make the following assumptions:

1. The reaction zone thickness is negligible.
2. The undetonated mixture is at rest at uniform pressure and density.
3. The burnt product is a perfect gas.
4. The flow of burnt product is adiabatic.
5. The Chapman-Jouguet condition is obeyed.

2. Equations of Motion

The equations of continuity for momentum, mass and energy in the case of spherical symmetry may be written as:

$$\dot{v} + v\, v_r + \frac{1}{\rho}\, p_r = 0 \qquad \text{(A-1)}$$

$$\dot{\rho} + (\rho v)_r + 2\,\frac{\rho v}{r} = 0 \qquad \text{(A-2)}$$

$$(\dot{p/\rho^{\gamma}}) + v\,(p/\rho^{\gamma})_r = 0 \qquad \text{(A-3)}$$

The dot sign and the subscript r represent differentiation with respect to time and radius, respectively.

3. Transformation of Variables

The rules of dimensional analysis may be employed to determine whether there is any similitude in the flow pattern which would allow some simplification in the problem of solving equations (A-1,2,3). Sedov[4] used fundamental similarity laws to show that, when a spherical detonation wave has proceeded out to radii such that the region affected by the initiation appears small (and, of course, such that the reaction zone appears very thin, as we have assumed), there is a similarity of flow pattern which permits great simplification in handling the gas-dynamical equations. Taylor[5] has determined the flow pattern for spherical detonation in T.N.T., based on a remarkable intuition as to how the simplification may proceed.

The simplification shown to be valid by Sedov lies in the possibility of expressing all flow variables as functions of a single parameter $\lambda \equiv r/Dt = r/R_o$, that is, the ratio of the radius of interest to the radius of the detonation front at the time of interest. When this is

done, the partial differential equations (A-1,2,3) reduce to ordinary differential equations.

We define λ, V, R, P and Z as follows:

$$\lambda \equiv \frac{r}{Dt} \tag{A-4}$$

$$v \equiv \frac{r}{t} \; V(\lambda) = D \lambda V \tag{A-5}$$

$$\rho = \rho_1 \; R(\lambda) \tag{A-6}$$

$$p \equiv \rho_1 \; (r^2/t^2) \; P(\lambda) = \rho_1 \; D^2 \lambda^2 P \tag{A-7}$$

$$Z(\lambda) \equiv \gamma P/R \tag{A-8}$$

We substitute into (A-1,2) the expressions for v, ρ and p given in the defining equations (A-5,6,7), and make use of (A-8), to obtain:

$$\frac{dZ}{dV} = 2Z \; \frac{[\gamma(V-1)^2 + (\gamma-1)(V-1) - Z]}{(V-1)^3 + (V-1)^2 - 3Z(V-1) - 3Z} \tag{A-9}$$

$$\frac{d \ln \lambda}{dV} = \frac{Z - (V-1)^2}{(V-1)^3 + (V-1)^2 - 3Z(V-1) - 3Z} \tag{A-10}$$

These equations can be written more simply in terms of $W \equiv V-1$:

$$\frac{dZ}{dW} = 2Z \; \frac{[\gamma W^2 + (\gamma-1) W - Z]}{(W+1)(W^2 - 3Z)} \tag{A-11}$$

$$\frac{d \ln \lambda}{dW} = \frac{Z - W^2}{(W+1)(W^2 - 3Z)} \tag{A-12}$$

Equation (A-3), which represents energy conservation, is replaced by an adiabatic integral, a consequence of the conservation of entropy, which for a perfect gas may be expressed as follows:

$$\frac{\gamma P}{R^{\gamma}} = \frac{Z}{R^{\gamma-1}} = \frac{\text{const}}{\lambda^2} \tag{A-13}$$

Equation (A-13) can be interpreted as a statement that all gas particles suffer the same entropy change due to the passing of the detonation wave; therefore, for adiabatic flow of burnt product, the entropy of that gas, and the ratio p/ρ^{γ} if it is a perfect gas, is constant.

4. Boundary Conditions

Equations (A-11,12,13) are to be solved simultaneously for Z (λ), W (λ) and R (λ), in conjunction with boundary conditions at the detonation front. These are found by specifying conditions just ahead of the shock front (i.e., in the undetonated mixture), and joining them to those just behind the reaction zone through the Rankine-Hugoniot (R-H) relations and the C-J condition. We have

Conditions at 1 (just upstream of the shock)

$$V_1 = 0, \text{ or } W_1 = -1 \tag{A-14}$$

$$P_1 = \frac{P_1}{\rho_1 D^2} = \frac{\mathcal{R}_1 T_1}{D^2} \tag{A-15}$$

$$R_1 = \rho_1/\rho_1 = 1 \tag{A-16}$$

$$\lambda_1 = R_o/R_o = 1 \tag{A-17}$$

$$Z_1 = \frac{\gamma P_1}{R_1} = \gamma_1 \; p_1/\;(\rho_1 D^2)$$

$$= \frac{\gamma_1 \mathcal{R}_1 T_1}{D^2} \tag{A-18}$$

Relations across the shock (R-H)

$$R_2 W_2 = R_1 W_1 \tag{A-19}$$

$$W_2 + \frac{Z_2}{\gamma_2 W_2} = W_1 + \frac{Z_1}{\gamma_1 W_1} \qquad \text{(A-20)}$$

$$\frac{1}{2} W_2^{\ 2} + \frac{Z_2}{W-1} = \frac{1}{2} W_1^{\ 2} + \frac{Z_1}{\gamma_1 - 1} + \frac{Q}{D^2} \qquad \text{(A-21)}$$

<u>Conditions at 2(C-J)</u>

$$Z_2 = W_2^{\ 2} \qquad \text{(A-22)}$$

Instead of solving simultaneously for Q, D, and the properties at 2, we wish to make use of information available in the literature[6] giving Q, D, and γ_2 as functions of conditions at 1. In order to utilize that information directly, we manipulate equations (A-14) to (A-22) (except A-21) into the following form:

$$W_2 = - \frac{\gamma_2}{1+\gamma_2} \left(1 + \frac{R_1 T_1}{D^2}\right) \qquad \text{(A-23)}$$

$$Z_2 = W_2^{\ 2} \qquad \text{(A-24)}$$

$$R_2 = - \frac{1}{W_2} \qquad \text{(A-25)}$$

$$P_2 = - \frac{W_2}{\gamma_2} \qquad \text{(A-26)}$$

Equations (A-23, 24) give boundary values of W and Z for equations (A-11, 12), in terms of the initial temperature, and D and γ calculated elsewhere.[6] Equation (A-25) gives R_2, which is needed, in conjunction with Z_2, to determine the value of the constant in equation (A-13). Finally, the expression for P_2, although not necessary for solving equations (A-11, 12) is shown as a matter of interest. Of course, P (λ)

(with P (1) = P_2) is one of the important results of this analysis; it can be obtained from Z (λ) and R (λ) after equations (A-11, 12) are solved.

From Table 3 in Reference[6], it can be inferred that R_1T_1/D^2 is never greater than 0.03 for cases of interest and may be neglected in Equation (A-23); substitution of the simplified expression into (A-26) gives

$$P_2 = \frac{1}{1 + \gamma_2} \qquad \text{(A-27)}$$

and from the definition of P_2 we obtain an expression for the pressure ratio across the detonation wave:

$$\frac{p_2}{p_1} = \frac{1}{1 + \gamma_2} \frac{D^2}{R_1T_1} \qquad \text{(A-28)}$$

This relationship is followed very closely by the results in Reference [6].

We restrict ourselves to a stoichiometric hydrogen-oxygen mixture. The results of the work in Reference[6] show that D and γ for the products of detonation of a gaseous explosive depend on the initial pressure and temperature. However, for the ranges expected (pressures from 0.1 to 1 atmosphere; temperatures of 300° K or less) D varies by no more than 3% about a mean value of 9150 feet per second. The value of γ affects the form of the relations, V (λ), P (λ), R (λ), since γ appears in the equations whose solutions gives these relations. Upon solving these equations for two extreme values of γ, we find the differences to be unimportant, and in setting boundary conditions in the present context, we use a mean value (γ_2 = 1.123).

5. Solution

Equations (A-11) and (A-12) are non-linear, and their solution requires numerical computation. The equations need not be solved simultaneously, however, since (A-11) contains only Z and W. We, therefore, proceeded as follows:

(i) Solve (A-11), with boundary values (Z_2, W_2) at the detonation front, to obtain Z (W).

(ii) Solve (A-12), which can now be written

$$\frac{d \ln\lambda}{dW} = \frac{W^2 - Z(W)}{(W + 1[3Z(W) - W^2])} \qquad \text{(A-19)}$$

with $\lambda = 1$ at the detonation front, to obtain W (λ).

(iii) Obtain $Z[W(\lambda)] = Z(\lambda)$.

(iv) Use equation (A-13) with the constant evaluated at the detonation front, together with Z (λ), to obtain R (λ).

(v) Obtain P (λ) from Z (λ), R (λ) and the definition of Z.

(vi) Calculate $V(\lambda) \equiv 1 + W(\lambda)$.

(vii) From the respective definitions calculate p/p_2, ρ/ρ_2, v/v_2 as functions of λ; the subscript 2 refers to conditions just behind the detonation front.

The results of these calculations are presented in Figure 13 of the main text.

REFERENCES - APPENDIX A

1. Zel'dovich, Ia.B.; S.M. Kogarko; and N.N. Simonov, "An Experimental Investigation of Spherical Detonation of Gases," Zhurnal Tekhnicheskoi Fiziki, 26, 8, (1956), 1744-1768. Translated in Sov. Phys. - Tech. Phys. 1, 8, (August 1953), 1689-1713.

2. Glass, I.I. and J.G. Hall, "Shock Sphere - An Apparatus for Generating Spherical Flows," J. Appl. Phys. 28, 4, (1957), 424-425.

3. Schardin, H., "Measurement of Spherical Shock Waves," Comm. Pure. & Appl. Math. VII, (1954), 223-243.

4. Sedov, L.I., "Similarity and Dimensional Methods in Mechanics," N.Y., Academic Press, 1959.

5. Taylor, Sir. G.I., "The Dynamics of the Combustion Products Behind Plane and Spherical Detonation Fronts in Explosives," Proc. Roy. Soc. A, 200, (1949-1950), 235-247.

6. Zeleznik, F.J. and S. Gordon, "Calculation of Detonation Properties and Effects of Independent Parameters on Gaseous Detonations," ARS Journal 32, 4 (1962), 606-615.

APPENDIX B

A. Effect of a Detonation Wave at Normal Incidence on a Rigid Wall

1. Characteristics of Wave Reflection

As a detonation wave reflects from a wall, the shape of the wave and the pressure at the wall will be as depicted in Figure B-1. We consider only spherical waves.

Just before impact with the wall (Figure B-1(a)), the pressure varies with distance in the manner discussed in Appendix A. The presence of the wall does not as yet influence the pressure distribution. The pressure at the wall, p_{wall}, is still that of the undisturbed, undetonated mixture, p_1.

An infinitesimal time interval after impact (Figure B-1(b)), p_{wall} has become more than double the pre-impact detonation front pressure. The wave is proceeding away from the wall, into the burnt products (Figures B-1(b, c)). Meanwhile, p_{wall} is decreasing.

Figure B-1-(d) illustrates conditions at the time when p_{wall} has fallen back to its original value, p_1, thus, ending the impulsive loading on the wall. There may be succeeding impulses on the wall, caused by reflection and return from other points, but the first impulse is the most severe and is the one we consider in this Appendix.

2. The Analytical Problem

To determine the impulsive load on the wall, we must determine p_{wall} as a function of time, and integrate it over the impulsive interval. The value of p_{wall} at any time during that interval depends on $p(r, t)$, $\rho(r, t)$ and $v(r, t)$ at all points within the gas volume from

the time of impact until that time. The determination of these functions can begin at the moment of impact ($t = o$), since the functions are known at that time.

To determine the functions requires integrating the equations of motion, with boundary conditions at the origin of initiation and at the wall, and matching at the returning shock front. A detailed solution of this problem requires the use of an electronic computer.

3. Approximate Solution

At the time of impact ($t = o$) the gas properties, p, ρ and v are known everywhere in the region of interest. They are also known at $t > o$, in the region not yet traversed by the reflected shock wave, since the effect of the oncoming (supersonic) shock wave is not yet felt in that region; therefore, the gas there continues to behave as if the wave had not reflected, but had continued radially outward unimpeded. Therefore, the functions $P(\lambda)$, $R(\lambda)$, $V(\lambda)$, where $\lambda = r/Dt$ as discussed in Appendix A, still apply. However, in this case the time, t, equals that required for the wave to reach the wall ($t = R_{wall}/D$) plus the time elapsed since then. Hence, now

$$\lambda = \frac{r}{R_{wall} + Dt} \qquad \text{(B-1)}$$

where t is the time from impact and the denominator equals the distance the wave would have traveled in the absence of the wall. Thus, at a given value of r, λ varies with time after impact.

Consider the time, t, at which the reflected wave just reaches a point at a distance, r, from the initiation point, as in Figure B-1(c).

It is possible to apply the laws of conservation of mass, momentum and energy to the control volume contained between r and R_{wall}, over the interval 0 to t_1. In the case of spherical symmetry, this control volume is a spherical shell of thickness $(R_{wall} - r)$.

To apply the conservation laws, we equate the changes in total mass, momentum and energy within the control volume during the interval t_1, to the time-integrals of the fluxes of these quantities at the boundaries r and R_{wall}.

As previously stated, at t = o all properties are known within the control volume. Therefore, the initial total mass, momentum and energy can be found by integration.

To express the final total mass, momentum and energy, we make a linearized approximation. The pressure distribution, at time t_1, is assumed to be linear (line a, b in Figure B-1(c) is assumed straight). Similar assumptions are made regarding density and particle velocity at time t_1. Thus, the final total mass, etc., can be expressed in an approximate manner in terms of the boundary values at time t_1. These are p_y, ρ_y, v_y just downstream of the shock, and $p_{w1}, \rho_{w1}, v_{b1}$ at the wall (see Figure B-1(c)). The first five quantities are unknown; v_{b1} if of course zero.

The fluxes at r are known at all times up to time, t_1, since during that time all properties can be found through the value of λ evaluated from Equation (B-1). Note that t_1 is unknown, but that the time-integrals of the fluxes can be found as functions of t_1.

Because the velocity is zero at the wall, there is only one non-zero flux there, namely the pressure (flux of momentum). Its initial value p_{wo} is that represented in Figure B-1(b), and is found by applying the Rankine-Hugoniot (R-H) relations across the shock. p_{wo} is therefore not an unknown in the present calculation. We linearize the time-variation in pressure at the wall and approximate the time-integral of pressure by $1/2(p_{wo} + p_{w1})t_1$.

From the R-H relations applied at the wall at t = o, we can also find v_{wo}, the initial velocity of the reflected shock wave. The R-H relations applied at point r, time t_1, give three relationships between p_x, ρ_x, v_x, (all known) and p_y, ρ_y, v_y, V_{w1}. The last quantity is the velocity of the reflected shock wave as it passes point r. We linearize the time variation in V_w and use a mean value, to obtain a relation:

$$t_1 = \frac{R_{wall} - r}{\frac{1}{2}(V_{wo} + V_{w1})} \qquad \text{(B-2)}$$

There are now seven unknowns: $p_y, \rho_y, v_y, p_{w1}, V_{w1}, t_1$. These are related by the same number of equations: three conservation equations for the control volume, three R-H relations applied at r, t_1, and equation (B-2). The set of equations can therefore be solved simultaneously.

We can therefore find an approximate value for the pressure at the wall at the time when the reflected wave reaches a point r, by solving the equations just discussed. The solution can be repeated, for various values of r, until we find a pressure at the wall which is equal to or less than the initial pressure of undetonated gas, such as is represented in Figure B-1(d). When this is done, we have available the initial and

final pressures at the wall, and the time interval t_2 required for the change. This information can be used to obtain an approximate expression for the impulse at the wall:

$$\frac{I}{A} = \frac{1}{2} (p_{wo} + p_{w2}) \; t_2 \qquad \text{(B-3)}$$

which was required. In discussing the solution of the problem, the flow variables were used. These can be normalized with respect to the detonation wave properties and initial explosive properties. Thus, in Figure 14 of the main text which shows the results of our calculations, we have plotted a normalized pressure against a normalized time.

The integral below the curve of Figure 14 is therefore also normalized, and we can express it as (see Figure 14):

$$\frac{I}{A} = \frac{1}{2} \; (1.17 \rho_1 \; D^2) \; (0.3 R_{wall}/D)$$

$$= 0.175 \; D \rho_1 \; R_{wall}$$

$$= 50 \rho_1 \; R_{wall} \; \frac{\text{lb-sec}}{\text{ft}^2} \qquad \text{(B-4)}$$

where ρ_1 = the initial mixture density, in lb/ft^3.

R_{wall} = the distance between the wall and the point of initiation, in feet.

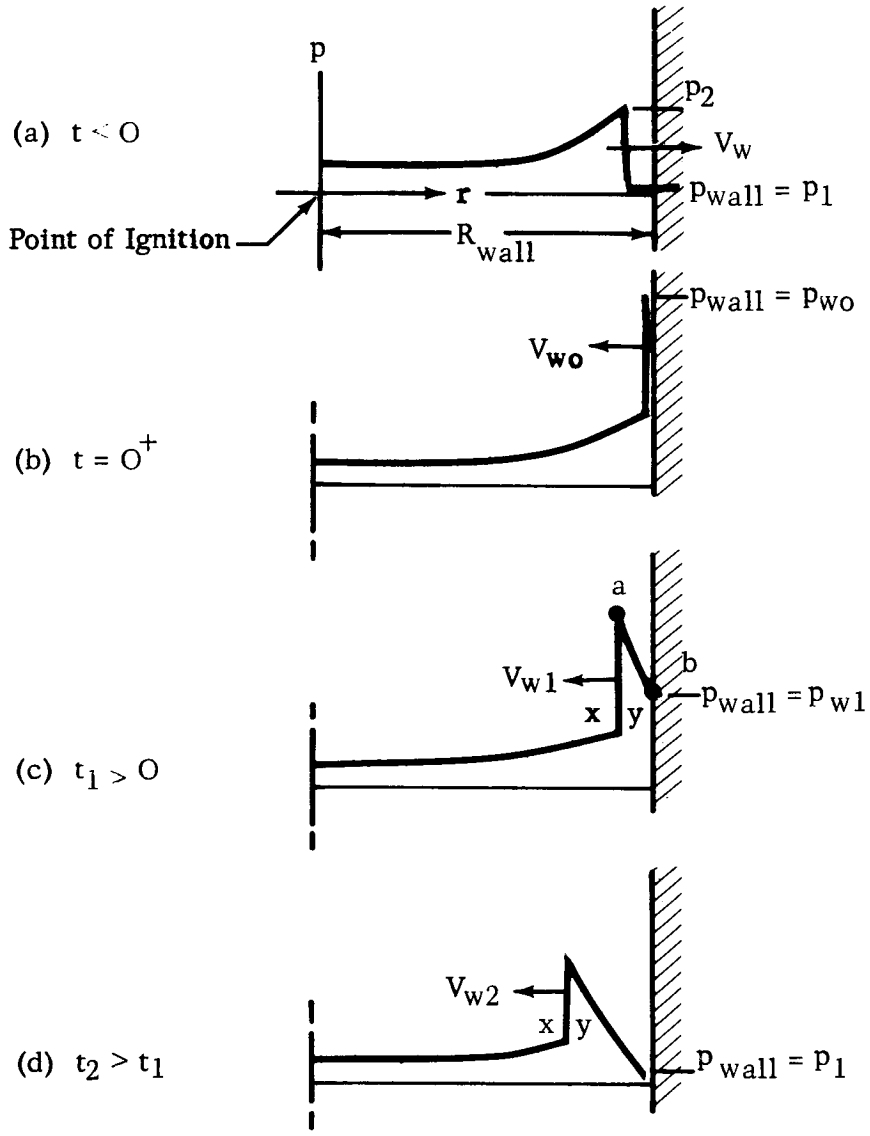

FIGURE B-1 SHAPE OF PRESSURE WAVE AND WALL PRESSURE DURING REFLECTION OF A DETONATION WAVE

APPENDIX C

A. Calculation of Maximum Bending Stress

1. Clamped Uniform Beam

Consider a clamped uniform beam of length ℓ, cross-sectional area S, width b and density ρ. The beam is initially at rest. When the beam is loaded with a uniform impulsive load P (psi-sec), it acquires instantaneously a velocity given by $bP/\rho S$. Therefore, the total kinetic energy of the beam is given by:

$$K.\ E. = \frac{b^2 \ell P^2}{2 \rho S} \qquad \text{(C-1)}$$

When the beam is loaded with a uniform static load q (lb/ft), the deflection of the beam y satisifies the differential equation:

$$EI \frac{d^4 y}{dx^4} = q \qquad \text{(C-2)}$$

where E is Young's modulus of elasticity and I is the area moment of inertia of the cross-section of the beam.

Subject to the boundary conditions that y and its derivative with respect to x must vanish at x = 0 and $x = \ell$, the solution of equation (C-2) is:

$$y = \frac{q}{24EI} (x^4 - 2\ell x^3 + \ell^2 x^2) \qquad \text{(C-3)}$$

Then the total strain energy of the beam is:

$$S.\ E. = \frac{1}{2} \int_0^{\ell} qy dx = \frac{q^2 \ell^5}{1440EI} \qquad \text{(C-4)}$$

Equating this strain energy to the kinetic energy given by equation (C-1), we obtain the following value of the unknown q:

$$q = 26.8 \frac{bP}{\ell^2} \sqrt{\frac{EI}{\rho S}} \qquad \text{(C-5)}$$

Now, the maximum bending stress σ_{max} will occur at the ends of the beam. From equations (C-3) and (C-5), we obtain:

$$\sigma_{max} = 1.12\ bhP \sqrt{\frac{E}{\rho SI}} \qquad \text{(C-6)}$$

where h is the depth of the beam. Finally, substituting for P from equation (21) (of the main text) and using the values of E and ρ for steel or aluminum, we obtain equation (23).

Similarly, we can obtain σ_{max} for beams with other boundary conditions.

2. Rectangular Uniform Plates

Consider a rectangular plate with sides a and b, uniform thickness h and density ρ. When the plate is loaded with a uniform impulsive load P, it acquires instantaneously a velocity equal to $P/\rho h$. Therefore, the total kinetic energy of the plate is given by:

$$K.E. = \frac{abP^2}{2\rho h} \qquad \text{(C-7)}$$

When the plate is loaded with a uniform static load q (psi), the deflection of the plate w satifies the differential equation:

$$\frac{\partial^4 w}{\partial x^4} + 2\frac{\partial^4 w}{\partial x^2 \partial y^2} + \frac{\partial^4 w}{\partial y^4} = \frac{q}{D} \qquad \text{(C-8)}$$

where D is the flexural rigidity of the plate given by:

$$D = \frac{h^3 E}{12(1-\nu^2)} \qquad \text{(C-9)}$$

ν being Poisson's ratio.

After the solution for w, satisfying equation (C-8) and the appropriate boundary conditions, is obtained, the total strain energy of the plate can be computed from:

$$S.\ E. = \frac{q}{2} \int_0^a dx \int_0^b w dy \qquad \text{(C-10)}$$

By equating this strain energy to the kinetic energy given by equation (C-7), the value of the unknown q is determined. Then the maximum bending moments and stresses in the plate are determined.

The calculation of the integral in equation (C-10) involves very long and tedious integrations. A quite accurate value of this volume integral can be obtained by approximating it by the volume of a pyramid with height equal to the maximum deflection w_{max}. This approximation is very convenient because values of w_{max} as well as of the maximum bending moment M_{max} as functions of b/a and of the boundary conditions have been tabulated. In general, one has the following

relations:

$$S.\ E. = \frac{1}{6}\ abqw_{max} \qquad \text{(C-11)}$$

$$w_{max} = \alpha \frac{qa^4}{D} \qquad \text{(C-12)}$$

$$M_{max} = \beta\ qa^2 \qquad \text{(C-13)}$$

$$\sigma_{max} = \frac{6}{h^2}\ M_{max} \qquad \text{(C-14)}$$

where α and β are constants depending on the ratio of the sides b/a and on the boundary conditions. They are well tabulated.

From equations (C-7, C-9, C-11, and C-12), we obtain:

$$q^2 = \frac{h^2\ E\ P^2}{4\alpha\rho a^4(1-\nu^2)} \qquad \text{(C-15)}$$

Then, from equations (C-13 to C-15), we obtain:

$$\sigma_{max} = \frac{3\beta\ P}{h} \sqrt{\frac{E}{\alpha\rho(1-\nu^2)}} \qquad \text{(C-16)}$$

Finally, using the values of E, p and ν for steel or aluminum and the value of P from equation (22), we obtain equation (24)--in the main text.

APPENDIX D

A. Comparison of Results with some Possible Exact Solutions

1. Uniform Beams

Exact solutions can always be obtained by superposition of the natural modes of vibration with time-dependent coefficients. For example, the bending moment M at the middle of a simply supported beam

loaded impulsively by a uniform load P (psi-sec) is given by:

$$M = \frac{4}{\pi} \; bP\sqrt{\frac{EI}{\rho S}} \sum_{n=1,3\ldots}^{\infty} \frac{(-1)^{\frac{n-1}{2}}}{n} \sin\omega_n t \qquad \text{(D-1)}$$

where the natural frequencies of vibration ω_n are given by:

$$\omega_n = \frac{\pi^2 n^2}{\rho^2} \sqrt{\frac{EI}{\rho S}} \qquad \text{(D-2)}$$

Now, to find the maximum bending moment M_{max}, equation (D-1) must be plotted as a function of t. Such a plot will give the value of M_{max} as well as the times at which it occurs. On the other hand, if we take only the first term of the series, then:

$$M_{max} = 1.27 \; bP \sqrt{\frac{EI}{\rho S}} \qquad \text{(D-3)}$$

The second term of the series has a frequency nine times higher and an amplitude as given by equation (D-3) with 1.27 replaced by -0.423. The maximum total bending moment computed by the present approximate theory is the same as that given by equation (D-3) with 1.27 replaced by 1.37.

A similar comparison can be carried out for a clamped beam. The numerical constants of the fundamental and first harmonic of the bending moment at the ends of beam are 1.70 and 0.728. The present approximate theory gives a value of 2.24 for the numerical constant of the maximum total bending moment.

2. Simply Supported Rectangular Uniform Plate

The rectangular uniform plate loaded impulsively with a uniform load p is one of few cases for which an exact solution is possible. For simplicity, we will consider a square plate. It can be shown that the bending moment at the middle of the plate is given by:

$$M = 0.492\ Ph\sqrt{\frac{E}{\rho}} \sum_{n=1,3..}^{\infty} \sum_{m=1,3..}^{\infty} \frac{m^2+0.3n^2}{mn(m^2+n^2)} (-1)^{\frac{m-1}{2}} (-1)^{\frac{n-1}{2}} \sin\omega_{mn} t \qquad \text{(D-4)}$$

Poisson's ratio has been taken equal to 0.3. The natural frequencies of vibration ω_{mn} are given by:

$$\omega_{mn} = \frac{\pi^2}{a^2} (m^2 + n^2) \sqrt{\frac{D}{\rho h}} \qquad \text{(D-5)}$$

Thus, we see that the numerical constant of the first, second and third components of the bending moment is 0.32, -0.153, and -0.0607, respectively. According to the present approximate theory, the numerical constant of the maximum total bending moment is 0.394.

APPENDIX E

A. Numerical Derivation of Maximum Allowable Radius of Stoichiometric Mixture

1. The Effect of a Detonation on the S-IC/S-II Interstage Skirt

A panel of the interstage skirt is considered as a rectangular plate with clamped edges and with dimensions as shown in Figure 19. The ratio of the sides is equal to 1.5. Hence, from Table VI, the values of the constants α and β are 0.0022 and 0.0757, respectively. The thickness of the plate h is equal to 0.070 inches. Using a value for σ_{max} equal to 76,000 psi (for 7075-T6 aluminum) and an average value of T_o equal

to $500^{o}R$, we obtain from equation (24) the following relationship between R and p_o:

$$R = \frac{\sqrt{\alpha}\ h\ T_o \sigma_{max}}{2.48 \times 10^5 \beta\ p_o} = \frac{(0.0022)^{\frac{1}{2}}\ (0.07)\ (500)\ (76{,}000)}{(2.48 \times 10^5)\ (0.0757)\ p_o} = \frac{6.65}{p_o} \quad (26)$$

where R is in feet and p_o in psi.

2. The Effect of a Detonation on the Propellant Feed Lines

Sections of the H_2 and O_2 feed lines can be considered as simply supported beams 150 inches in length and with an annular cross-section 8 inches in diameter and 0.025 inches thick. The area moment of inertia I and the area S of the cross-section are:

$$I = (3.14)\ (0.025)\ (4)^3 = 5.02\ in^4$$

$$S = (3.14)\ (0.025)\ (8) = 0.628\ in^2$$

The width b and depth h of the cross-section are equal to the diameter, i.e., 8 inches. The drag coefficient C_D of a cylinder in supersonic flow is equal to 1.4. Taking the average temperature T_o equal to $500^{o}R$ and a value of σ_{max} equal to 25,000 psi (one-fourth the ultimate strength of stainless steel), the following relationship between R and p_o can be computed from equation (23)--with γ equal to 1.94 for a simply supported beam--

$$R = \frac{\sigma_{max} T_o \sqrt{SI}}{2{,}240\ \gamma\ bhp_o C_D} = \frac{(25{,}000)\ (500)\ (0.628 \times 5.02)^{\frac{1}{2}}}{(2{,}240)\ (1.94)\ (8)\ (8)\ (1.4) p_o} = \frac{56.8}{p_o} \quad (28)$$

where R is in feet and p_o in psi. Note that the result is independent of the length of the pipe.

APPENDIX F

A. Sample Calculations

The examples given in this appendix are intended to illustrate the manner in which some of the derivations presented in this report may be used in considering the prevention and control of explosions in an interstage.

Problem 1: If the ambient pressure in the interstage is one atmosphere (sea level) what is the maximum allowable quantity of hydrogen that could be detonated in the S-IC/S-II interstage without causing failure of a propellant feed line?

Solution: It was estimated in the text that the maximum radius (R) of a detonable mixture of hydrogen and oxygen that could occur without causing failure of a propellant feed line can be expressed as:

$$R = \frac{56.8}{p_o^2} \qquad (28)$$

The weight of hydrogen and oxygen encompassed by this radius can be estimated as on page 94 of the text as follows:

$$M = 4\pi/3 \quad (144) \quad \frac{MW}{RT_o} \quad \frac{(56.8)^3}{p_o^2}$$

substituting the following values:

$MW = 12$

$R = 1545$

$T_o = 500$

$p_o = 14.7$

M becomes approximately 8 lbs.

Hence, approximately (8/9) (8) or 0.7 lb of hydrogen is the maximum that could be detonated at sea level pressure without causing damage to the feed lines from a detonation.

Problem 2: If the interstage skirt panel used as an example on page 157 were doubled in thickness how would this effect the maximum allowable leakage rate based on a detonation? What would be the approximate weight increase?

Solution: From equation (26) as expressed in Appendix E, it may be seen that the maximum allowable radius (R) of a detonable mixture is proportional to the thickness of the panel. Since the quantity of detonable is proportional to R^3 equation (20) then may be modified as follows:

$$M = \frac{2.76}{P_o^2} \times 2^3 = \frac{22.1}{P_o^2}$$

By plotting M vs. flight time as in Figure 23, the maximum allowable rate of leakage is estimated to be 48.5×10^{-4} lbs of hydrogen and oxygen or 5.4×10^{-4} lbs and 43.1×10^{-4} lbs of hydrogen and oxygen respectively. This is roughly eight times the leakage rate allowed with the standard panel. The time in flight where the most critical detonation hazard would occur at this leakage rate would be of the order of 35 seconds (from the plot as in Figure 23). The radius of the detonable mixture would be 1.1 feet.

If it is assumed that the skirt panels have a surface area of the order of 2600 feet^2, doubling the thickness will result in a weight increase of the order of 2500 lbs.

Problem 3: In problem 2, it was estimated that the maximum allowable leakage rate of liquid hydrogen would be of the order of 5.4×10^{-4} lbs if the skirt paneling were doubled in thickness. What rate of helium purge gas would be required to prevent a detonation occurring if hydrogen leaked at the above rate (assuming that both the leakage and purge started at lift-off and instantaneous mixing occurs)?

Solution: From Figure 24, it can be seen that the rate of helium purge required would be less than 0.1 lb/sec and the weight of the purge system from Figure 26 would be very small. Since the radius of detonable mixture necessary to cause damage when no purge is added is of the order of 1 foot, it may be difficult to achieve sufficient mixing to insure that the detonation does not occur, however. Higher rates of purge injection would, in general, aid in the mixing and reduce the probability of a destructive detonation occurring.

Problem 4: The maximum allowable quantity of hydrogen and oxygen that may be allowed in order not to create a hazardous deflagration in the S-IC/S-II interstage can be estimated from equation (16) of the text by multiplying the maximum allowable leakage rate by the time after launch (beyond which a hazard would no longer exist). For hydrogen this would be $8.2 \times 10^{-4} \times 110$ or 0.09 lbs (see Table V). If a larger quantity than this (and the corresponding amount of oxygen necessary for a stoichiometric mixture) reacted at some period of time prior to 110 seconds, would there be some periods of time when the pressures produced

would not be destructive?

Solution: From the equation of state, it can be shown that the increase in pressure in the interstage caused by the reaction of a pocket ("gas bubble") of a flammable mixture can be approximated by:

$$P_e - P_i = \frac{R}{V_T} (N_p T_p - N_r T_r)$$

where P_e = pressure when reaction is completed

P_i = pressure in interstage immediately prior to reaction

R = gas constant

V_T = free volume of the interstage

N_p = number of moles of the products of the reaction

T_p = temperature of the products

N_r = number of moles of reactants

T_r = temperature of the reactants

This equation shows that the value of $P_e - P_i$ does not depend on the initial pressure. For a hydrogen and oxygen mixture (and nitrogen as the inert gas in the interstage), the pressure difference is primarily dependent on the quantity of reactable mixture (N_r) available at the time of reaction. Since the difference $P_e - P_i$ is used as the criterion for destructive damage, a deflagration involving more than 0.09 lbs of hydrogen (and the necessary oxygen for the reaction) in the interstage any time up to and beyond 110 seconds in flight would produce destructive pressures.

By the same reasoning, a deflagration involving less than this quantity would not be destructive at any period in flight.